UNIVERSITA' DEGLI STUDI DI UDINE

Dottorato di Ricerca in Scienze e Biotecnologie Agrarie

Ciclo XXIX

Coordinatore: prof. Giuseppe Firrao

TESI DI DOTTORATO DI RICERCA

On the role of phloem protein in plant-pathogen interaction

Dottorando: dott.ssa Laura Pagliari

Supervisore: prof.ssa Rita Musetti

ANNO ACCADEMICO 2016/2017

Table of contents

Abstract

Diseases caused by phytoplasmas, prokaryotic plant pathogens restricted to phloem tissue, result in a huge impact on agriculture and, at the present day, no effective control strategy has been developed. The individuation of resistance or tolerance sources, need to understand the mechanisms existing at the basis of plant responses to phytoplasma infection.

Investigations in natural plant hosts are limited by the impossibility to control the numerous environmental conditions that could affect plant-pathogen relationship. The reliability of *Arabidopsis thaliana* as model plant for studying phytoplasma-plant interaction was proved in this work, comparing macroscopic, histological and ultrastructural modifications induced by phytoplasma infection in *A. thaliana* with those reported in natural host plants.

The agglutination of phloem protein filaments in the sieve elements following phytoplasma infection has been hypothesised to limit phloem mass flow and, consequently, to prevent pathogen spread. To elucidate the interaction between phytoplasmas and SE-protein filaments, Arabidopsis mutant lines lacking genes related to SE-protein filament (*AtSEOR1, AtSEOR2 AtPP2-A1*) were used both in healthy and in infected conditions. Various microscopic techniques were used, in order to combine fresh and embedded tissue observations, gaining information on both ultrastructural and physiological sieve element modifications. The analysis of healthy and infected plants suggested that SE-protein filaments affect phloem flow only even if agglutinated SE-protein masses are present in the sieve elements, and this occurs only in infected tissues. Moreover, even if filament presence was observed in mutant lines (indicating that in case of stressful condition SE-protein filament formation can overcome *AtSEOR1* and *AtSEOR2* absence), only filaments proper of wild-type plants are able to block the phloem mass flow in case of phytoplasma infection. No correlation between phloem impairment and pathogen concertation was found, but the low phytoplasma titre in *AtSEOR1ko* lines could indicate the involvement of this gene in plant defence mechanism, probably related to jasmonic acid and *cis*-12-oxo-phytodienoic acid pathway.

Keywords

Arabidopsis thaliana; phloem proteins; phytoplasma; sieve element occlusions; combined microscopy

1. Introduction.

1.1. The pathogen: the phytoplasmas.

Phytoplasmas are prokaryotic plant pathogens belonging to the class *Mollicutes* (order *Acholeplasmatales*, family Acholeplasmataceae), a group of wall-less microorganisms phylogenetically related to low G/C % molar content Gram-positive bacteria (Weisburg *et al.*, 1989). Phytoplasmas were discovered by Doi and collaborators in 1967 and were named mycoplasma-like organisms (MLOs), due to their morphological and ultrastructural similarity to mycoplasmas, already known as etiologic agents in animal and human diseases. Following the application of molecular technologies MLOs were designed as a coherent, genus-level taxon, named '*Candidatus* Phytoplasma' (IRPCM, 2004). In this new clade, groups and subgroups have been defined and many of them are now considered species (Bertaccini and Duduk, 2009). The most comprehensive and widely accepted phytoplasma classification system relies on restriction fragment length polymorphism (RFLP) analysis of polymerase chain reaction (PCR)-amplified 16S rDNA (Lee *et al.*, 2004a, b; Marcone *et al.*, 2000; Zhao and Davis, 2016).

Phytoplasmas are procariotes of small dimensions, varying from 200 nm to 800 nm in diameter, delimited by a plasma membrane, but devoid of the cell wall (Lee *et al.*, 2000). The absence of a rigid cell wall allows them to be highly pleomorphic and to change shape adapting to the environment. The trilaminar plasma membrane encloses ribosomes and DNA. Plasma membrane predominantly consists of immunodominant proteins (Berg *et al.*, 1999), categorized in three different nonhomologous types: Imp (Immunodominant Membrane Protein), IdpA (immunodominant membrane protein A) and Amp (antigenic membrane protein) (Kakizawa *et al.*, 2006; Morton *et al.*, 2003). Although recent results indicate that Amp is involved in vector specificity interacting with insect proteins such as actin, the specific functions of these proteins are still unknown (Galetto *et al.*, 2011).

Phytoplasmas are obligate parasites, living inside the cells of plants and vector insects and replicating intracellularly in both (Hogenhout *et al.*, 2008). Phytoplasmas are transmitted by phloem-feeding insect species within the Order *Hemiptera*, such as *Cicadellidea* (leafhoppers), *Fulgoridea* (cicada) and *Psyllidae* (psyllids) (Weintraub and Beanland, 2006). Phytoplasma transmission is persistent and propagative. Through insect nutrition activity on infected plants, phytoplasmas enter the vector (Fig. 1). The insects must feed for an extended period of time (called acquisition access period, AAP) to acquire a sufficient titre of phytoplasmas to establish infection. During a latent period (LP) in the vector, phytoplasmas pass from the alimentary canal through the midgut into the

haemolymph, they invade salivary gland cells, multiply and are incorporated into saliva. Then they are transmitted to a new host plant by injection into phloem tissue during insect feeding (inoculation access period - IAP) (Bosco *et al.*, 2007; Christensen *et al.*, 2005; Hogenhout *et al.*, 2008; Oshima *et al.*, 2011).

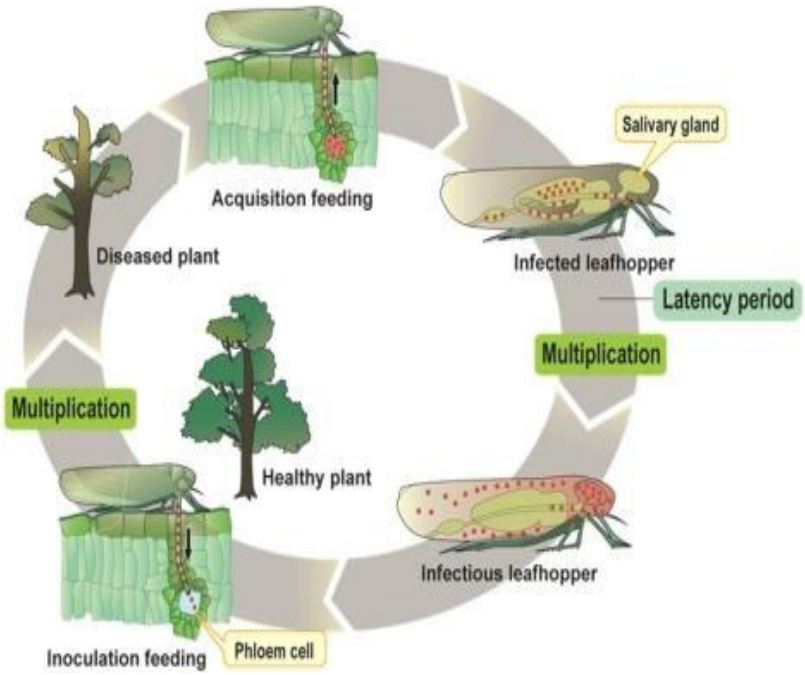

Figure 1. Life cycle of phytoplasmas. Phytoplasmas (here represented as red dots) are *Mollicutes* that infect the phloem of many host plants and several organs of phloem-feeding insect vectors and actively multiply in both hosts. Insects can acquire phytoplasmas during nutrition activity on infected plants. In the vector, phytoplasmas reach salivary glands and multiply. After the latency period, the phytoplasmas can be inoculated through saliva in the phloem of healthy plants.
Picture from Oshima *et al.* (2011)

Inside the sieve elements the phytoplasmas moved systemically through the plant. Phytoplasma spread into the plant cannot be explained solely by assimilate flow (Garcia-Chapa *et al.*, 2003; Marcone *et al.*, 2009; Wei *et al.*, 2004). On the other hand, considering the fact that phytoplasmas have no gene coding for cytoskeleton elements or flagella, their active movement seems unlikely (Christensen *et al.*, 2005). Even if their way to move in plant tissue is poorly understood, in a variable period of time (Hogeout *et al.*, 2008), phytoplasmas reach every plant organ (Cordova *et al.*, 2003).

Phytoplasma-infected plants exhibit symptoms suggesting a profound disturbance in the normal balance of growth regulators and interference in mass phloem flow (Lee *et al.*, 2000; Osler *et al.*, 1996) (Fig. 2). Hormone unbalance deals to virescence, phyllody, big bud, flower sterility or abnormalities, witches'-brooms, rosetting, internode elongation and off-season growth (Lee *et al.*, 1997; Lee *et al.*, 2000; Bertaccini and Duduk, 2009). Symptoms attributable to the impairment of the phloem transport are: leaf yellowing or reddening, alteration of leaf blades that appear thick and folded on the petiole, rolling and leaf curls, dwarfism and general decay (Bertaccini and Duduk, 2009; Himeno *et al.*, 2014; Loebenstein *et al.*, 2009; Osler *et al.*, 1996).

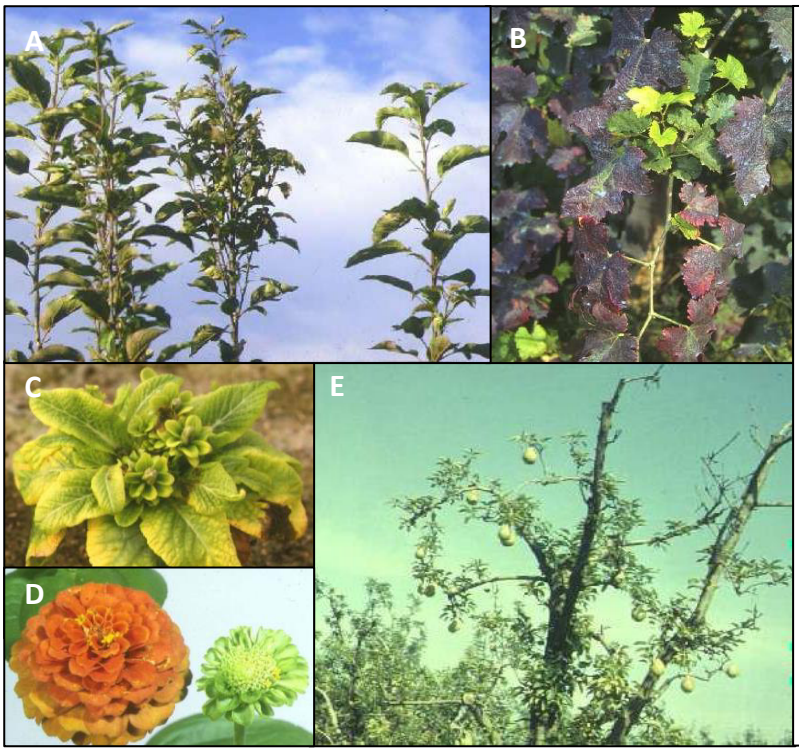

Figure 2. Symptoms associated with phytoplasma presence. Typical symptoms include: a bushy or "witches' broom" appearance due to changes in plant normal growth patterns (A -*Malus domestica*-), the yellowing and reddening of the leaf tissue (B -*Vitis vinifera*- and C -*Primula vulgaris*-), the abnormal transformation of a floral structure into a foliage leaf (phyllody) and the green coloration of non-green flower parts (C -*Primula vulgaris*- and D -*Zinnia elegans*-). The great majority of phytoplasma disease causes stunted growth, general decline and, in some cases, plant death (E -*Pyrus communis*-).

Images from www.fitoplasmi.it

Although not all infections are necessarily deleterious, the great majority of phytoplasma diseases causes stunting of overall plant growth, general decline, loss of productivity and, in some cases, plant death (Seemüller *et al.*, 2002). Phytoplasmas are reported to be associated with plant diseases in several hundred plant species, including many important vegetable and fruit crops, ornamental and woody plants, causing an impressive impact on agriculture (Bertaccini *et al.*, 2014; Valiunas *et al.*, 2015). Moreover, their impact is intended to grow by accidental introduction, by globalized human activities, of insect vectors and infected plants and by global warming, which will advantage the cold-sensitive phytoplasma vectors (Hogenhout *et al.*, 2008).

Despite the economic importance of phytoplasma diseases, progress on the understanding the plant-phytoplasma interactions has been slow as compared to other plant bacterial pathogens (Bertaccini and Duduk, 2009). Since their discovery, the study of phytoplasmas has been inherited by the extreme difficulty to culture them *in vitro* (Contaldo *et al.*, 2012). In fact, they exhibit a strong host-specific and a tissue-specific correlation, highlighting a durable adaptation to life as obligated parasite. They lack several pathways for the synthesis of compounds considered to be necessary for the cell metabolism (Marcone *et al.*, 1999) and thus probably they can survive by means the absorption of host cell substances (Bai *et al.*, 2006). The absence of a clear comprehension of the phytoplasma physiology entails ineffective ways of disease management. Phytoplasma outbreak and spread can be controlled only by the eradication of infective plants and the use of insecticides to

reduce insect vector populations. However, this approach results burdensome both for its economic impact and for health implications to human and environment (Desneux *et al.*, 2007; Bertaccini *et al.*, 2014). Mitigation of disease is slowly shifting from chemical vector control to habitat management and the use of genetic methods to produce naturally disease-resistant plants (Osler *et al.*, 2014; 2016). The understanding of the fine mechanisms at the basis of plant responses to phytoplasma infection represents the necessary background for the development of these new strategies.

1.2. The plant: the phloem tissue.

For the plants, the transition from an aquatic life to a terrestrial one occurred roughly 470 million years ago and involved the evolution of a number of specialized cells, tissues and organs required for land survival and reproduction (Bowman, 2013; Delwiche and Cooper, 2015). Among them, a vascular transport system evolved into two effective microfluidics systems with different roles: the xylem, which translocates, through the apoplast, water and minerals gathered by the roots, and the phloem, which transports assimilates in the symplasm. While xylem is a network of channels that consists of dead cells, phloem consists primarily of living cells (Lucas *et al.*, 2013).

Functional phloem consists of sieve elements (SEs) and companion cells (CCs). While SEs are enucleated conducting cells, CCs are cells with intact cellular components and are known to support the functioning of SEs. The strong relationship between SEs and CCs has induced to consider them and unique complex, called SE/CC complex (van Bel, 2003), and originates from a common ontogeny (Fig. 3) (Esau, 1969; van Bel, 2003). Originated from unequal division of a mother cell, the two cells develop different function and morphology. While one daughter cell develops into one or several metabolically hyperactive CCs, the other one exhibits selective degenerative autolysis (Esau, 1969; Lucas *et al.*, 2013; van Bel, 2003). In fact, as the SE matures, the nucleus and vacuoles are degraded, while ribosomes, Golgi apparatus and mitochondria are greatly reduced in number. The mature SEs present only the endoplasmic reticulum and some mitochondria closely related to the plasma membrane and a thin marginal cytoplasm area, the cytoskeleton and phloem-specific proteins and plastids (van Bel, 2003; Hafke *et al.*, 2013). Moreover, SEs develop perforated walls at the cell junctions within the sieve tube, forming sieve plates and establishing a symplastic continuity throughout the sieve tube (van Bel, 2003; van Bel and Thompson, 2013). The reorganization of the cellular contents creates an effective transport route (Lucas *et al.*, 2013; van Bel and Thompson, 2013) and, at the same time, maintains SEs still alive, thanks to plasmodesma pore units (PPUs), which symplastically interconnect the SEs to their neighbouring CCs (Kempers and van Bel, 1997; Knoblauch and van Bel, 1998; Hafke *et al.*, 2013). In fact, CCs are responsible for SE survival,

providing metabolites, energy-carrying substances, messages and probably genetic information (van Bel, 2003). Moreover, CCs allow the translocation of photoassimilates between parenchyma cells and SEs (Taiz and Zeiger, 1998).

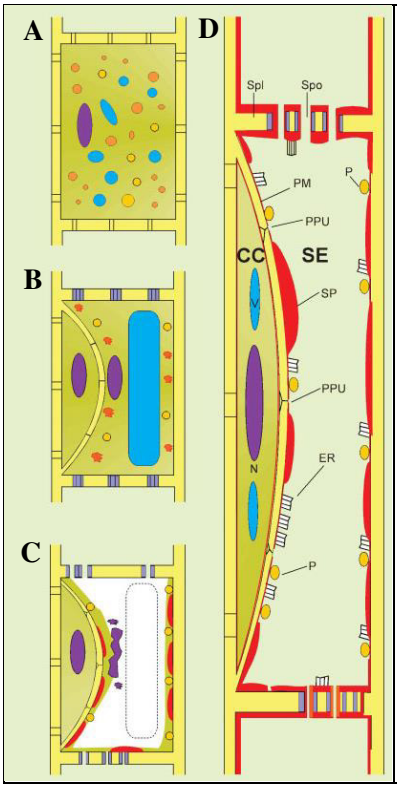

Figure 3. Development and organization of the SE-CC complex. SE and CC are derived from the same meristematic cell (A). Mother cell divides differently. While the immature CC keeps a dense cytoplasm, the immature SE vacuolizes strongly (blue) and forms conspicuous protein bodies (red) and plastids (yellow) (B). In immature SE, nucleus (violet), ribosomes, cytoskeleton, Golgi apparatus and vacuole membrane disappear. On the other hand, the CC retains its equipment. (C). After completion of the growth of the length of the cells, the SE has only one plasma membrane (PM), parietal ER network (ER), sieve element plastids (P), some mitochondria and phloem-specific, structural proteins (SP) (D). Furthermore, the simple plasmodesmata connecting SE and CC are modified in branched connections called plasmodesma pore units (PPUs). In this process, the wall connecting two SEs perforates forming sieve plates and establishing a symplastic continuity throughout the sieve tube. Image from van Bel and Hess (2003).

Phloem transports a complex mixture of organic and inorganic substances (Heo *et al.*, 2014; Komor *et al.*, 1996). Analyses of the phloem exudates from various plants have shown that the major phloem sap components are carbohydrates and amino acids. Sucrose is the main sugar in phloem sap (Fukumorita and Chino, 1982; Liu *et al.*, 2012; Patrick *et al.*, 2001), while amino acids are the main form of reduced nitrogen in phloem sap (Dinant *et al.*, 2010; Douglas, 2006). Absolute and relative concentrations of these compounds vary among species (Dinant *et al.*, 2010; Douglas, 2006). Furthermore, sieve tubes are not only efficient pipes for the photosynthate transport: they also mediate long-distance signalling by transporting hormones, peptides, proteins, and RNAs (Bishop *et al.*, 2011; Dinant *et al.*, 2010; Heo *et al.*, 2014; van Bel, 2003). Signalling substances are responsible for the integration of functioning, growth and development of the plant and play an important role in defence against pests and predators (Dannenhoffer *et al.*, 2001; Dinant *et al.*, 2010; Furch *et al.*, 2014; Hijaz and Killiny, 2014). On the other hand, precisely for its high transport efficiency along the plant, phloem provides an excellent vehicle for distribution of micro-organisms (Nelson and van Bel, 1998; Oparka and Santa Cruz, 2000; Bové and Garnier, 2003; Hijaz and Killiny, 2014).

1.3. Plant-pathogen interaction step 1: pathogen recognition.

Plants have developed multiple layers of a sophisticated apparatus for pathogen recognition and response. Even if recent literature suggests that plant response is an integrative and essentially stochastic process combining different surveillance and response mechanisms (Pritchard and Birch, 2014; Thomma *et al.*, 2011), plant response to pathogen attack is considered to consist of at least two phases, described by the so called "zig-zag model" (Fig. 4) (Jones and Dangl, 2006).

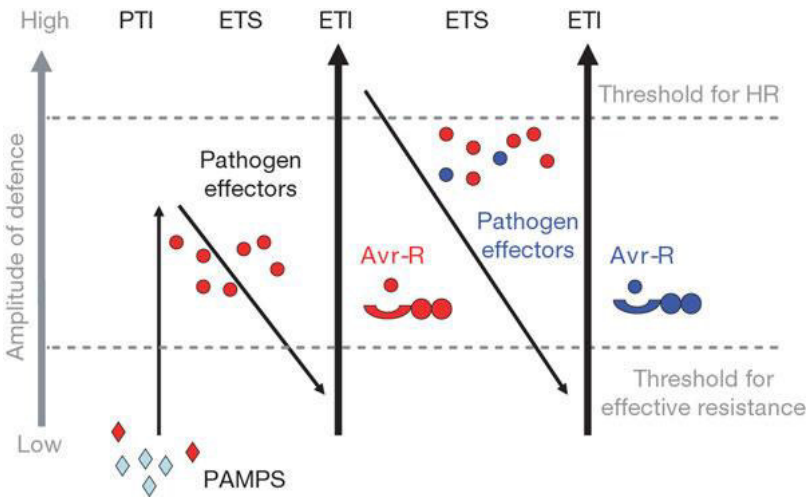

Figure 4. The zig-zag model. Plant surface receptors, called pattern recognition receptors (PRRs), recognize pathogen-associated molecular patterns (PAMPs) and activate an innate immune response, called PAMP-triggered immunity (PTI). Successful pathogens are able to overcome PTI, secreting effectors that suppress PTI responses and causing in the plant the so-called effector-triggered susceptibility (ETS). Nevertheless, plants respond to these effectors through the development of cytoplasmic R proteins that recognize single effectors and activate the so-called effector-triggered immunity (ETI). Finally, as a result of the selection pressure on both actors, there will be the loss or the gain of effectors over evolutionary time. Image from Jones and Dangl, 2006

Pathogen extracellular presence is first detected by the plant pattern recognition receptors (PRRs), which recognize pathogen associated molecular patterns (PAMPs) and activate the PAMP-triggered immunity (PTI). Successful pathogens employ virulence proteins (called effectors) that provide a beneficial environment for bacterial multiplication inside the host, suppressing PTI and causing the effector-triggered susceptibility (ETS). The second phase, consists in the recognition of the pathogen effectors by the plant resistance (R) proteins, resulting in the effector-triggered immunity (ETI). ETI is a more efficient form of resistance and it is frequently associated with the hypersensitive response (HR), characterized by deliberate plant cell suicide at the site of infection, and systemic acquired resistance (SAR), a long-lasting, broad-spectrum immune response that is induced throughout the entire plant following attempted local infection (Jones and Dangl, 2006; Katagiri and Tsuda, 2010; Schwessinger and Zipfel, 2008). Pathogen recognition results in several plant defence response, like

activation of enzymes and generation of reactive oxygen species (ROS) (Baxter *et al.*, 2014; Thakur and Sohal, 2013), accumulation of salicylic acid (SA), jasmonic acid (JA), ethylene and lipid-derived molecules implicated in systemic signalling and the production of antimicrobial compounds, such as pathogenesis-related (PR) proteins (Durrant and Dong, 2004; Fu and Dong, 2013; Thakur and Sohal, 2013; van Loon and van Strien, 2009; Wani *et al.*, 2016). As a result of selection pressure on both plants and microbes, a coevolutionary arm race will continue with the loss or the gain of effectors and pathogen-recognition molecules over time (Deslandes and Rivas, 2012).

As regards phytoplasmas, the knowledge about the molecular mechanisms involved in the pathogenicity and in the host plant response has been limited primarily by the inability to culture phytoplasmas *in vitro* (Contaldo *et al.*, 2012). Moreover, in contrast with other bacteria, phytoplasmas are directly introduced and confined inside living sieve cells (Bertaccini *et al.*, 2014). Because of the fact that PRR-mediate immune responses occur in the extracellular space (Bent and Mackey, 2007; Deslandes and Rivas, 2012; Schwessinger and Zipfel, 2008), phytoplasmas have the ability to hide from host recognition and immune defence reaction inside the phloem cells (Hogenout *et al.*, 2008). On the other hand, effector proteins into the cytoplasm can be recognized intracellularly and R-mediated ETI can be triggered (Bent and Mackey, 2007). Like other pathogens, also phytoplasmas produce effectors, which can interact directly with vector and host to influence developmental processes (Hogenhout and Loria, 2008; Hogenhout and Segura, 2010; Sugio *et al.*, 2011). Effectors could enhance phytoplasma fitness, modifying the plant development in accordance with pathogen needs, for example generating more vegetative tissues to attract the insect vectors, prolonging the vegetative growth phase of the plant to postpone plant death and suppressing inducible plant defence pathways (Lu *et al.*, 2014; MacLean *et al.*, 2014; Sugio *et al.*, 2011). In response to effector release, host plant may activate resistance genes, to detect pathogen virulence factors and to initiate an immune response (Jones and Dangl, 2006). It is unclear whether ETI can be induced by sieve cells, since they lack the organelles reputed indispensable for most plant immune responses (like the nucleus, chloroplasts or the Golgi-apparatus) (Knoblauch and van Bel, 1998; Sugio *et al.*, 2011). Since effector proteins are produced in the phloem, but accumulate in nuclei of cells beyond the phloem (Bai *et al.*, 2009), the neighbouring cells could have a role in their recognition (Hoshi *et al.*, 2009). Effector protein transport is assumed to be achieved through plasmodesmata passage (Hogenhout and Loria, 2008).

1.4. Plant-pathogen interaction step 2: biochemical changes.

1.4.1. Signalling molecules.

Pathogen presence and activity, as well as its recognition by the host plant, drive to many biochemical changes indicating the activation of plant defence response. Phytoplasma infection induces Ca^{2+} influx into the SEs, leading to sieve-tube blockage (Musetti *et al.*, 2013; Musetti and Favali, 2003). In addition, Ca^{2+} signals are decoded and relayed by signalling molecules, generating various intracellular cascades leading to changes in metabolism and gene expression (Kudla *et al.*, 2010; McAinsh and Pittman, 2009; van Bel *et al.*, 2014).

Phytoplasma infection can lead to the involvement of other important signal and defence molecules such as hydrogen peroxide (H_2O_2) (Musetti *et al.*, 2004; 2005; Sanchez-Rojo *et al.*, 2011) and different phytohormones (Minato *et al.*, 2014; Punelli *et al.*, 2016; Zimmermann *et al.*, 2015). H_2O_2 and other reactive oxygen species (ROS) can directly have a toxic effect on the pathogenic bacteria but can also function as signalling molecules (Apel and Hirt, 2004; Scheler *et al.*, 2013), activating a variety of defence responses including enhancement of cell wall strength, synthesis of phytoalexins, synthesis of pathogenesis-related proteins, and suppression of pathogen growth by programmed cell death (Lamb and Dixon, 1997). Nevertheless, it seems that H_2O_2 accumulation depends on the phytopathological condition of the plants, being relegated to recovery, a spontaneous remission of symptoms in phytoplasma-infected plants (Musetti *et al.*, 2004; 2005; 2007). On the other hand, phytohormones play a regulatory role before or within symptom appearance (Kazan and Lyons, 2014; Punelli *et al.*, 2016). Phytohormones are small molecules that occur at low concentration and regulate numerous aspects of plant growth, development, and response to stress, functioning in complex signalling networks, with interactive effects, referred to as crosstalk (Kazan and Lyons, 2014; Pieterse *et al.*, 2009; Robert-Seilaniantz *et al.*, 2011). Primary defence hormones are jasmonates (JAs), salicylates (SAs), and ethylene (ET). Other phytohormones, such as abscisic acid (ABA), auxins (indole-3-acetic acid [IAA]), cytokinins (CKs), brassinosteroids (BRs), gibberellins (GA), and strigolactones, are better known for their roles plant growth and development, but they also regulate plant defence (Pieterse *et al.*, 2009; Robert-Seilaniantz *et al.*, 2011).

Traditionally, SA signalling activates resistance against biotrophic and hemibiotrophic pathogens, while a combination of JA and ET signalling induces resistance against necrotrophic pathogens (Kazan and Lyons, 2014; Pieterse *et al.*, 2009; Robert-Seilaniantz *et al.*, 2011). Phytoplasmas are biotrophic pathogens, thus the increase in SA level and the consequent decrease of JA level was supposed and demonstrated (Minato *et al.*, 2014; Musetti *et al.*, 2013; Patui *et al.*, 2013; Sugio *et al.*,

2011; Zimmermann *et al.*, 2015). Nevertheless, the concentration of these two hormones seems to be dependent on many factors, such us the tissue age (Sugio *et al.*, 2011), the moment of vegetative cycle (Janik *et al.*, 2016), the phytoplasma strain (Ahmad *et al.*, 2013), probably due to distinct sets of virulence factors (Zimmermann *et al.*, 2015) and the phytosanitary state of the plant (Musetti *et al.*, 2013). Another phytohormone significantly compromised in different phytoplasma infections, is IAA, whose level and biosynthesis pathway activity drop dramatically (Chang, 1998; Gai *et al.*, 2014; Hoshi *et al.*, 2008; Zafari *et al.*, 2012). Many phytoplasma-associated disorders are grouped as auxonic plant diseases (Musetti, 2010). In fact, considering that IAA controls cell division and cell elongation in plants during developmental processes, including stem elongation and apical dominance, stunting and witches' broom symptoms could be explained by an imbalance of these growth regulators (Gai *et al.*, 2014; Hoshi *et al.*, 2008).

It is important to underline that phytoplasma-triggered hormonal imbalance is not only related to plant defence response, but could be directly caused by pathogen activity. Up to date, it is not known whether phytoplasmas synthesize plant growth regulators, like some walled plant-pathogenic bacteria (Kazan and Lyons, 2014; Robert-Seilaniantz *et al.*, 2011), or if phytoplasmas change the natural level of one or more of the endogenous plant hormones. Nevertheless, two phytoplasma effectors have been discovered to regulate JA biosynthesis in a negative manner rendering the plants highly susceptible to phytoplasma vectors (Sugio *et al.*, 2011): secreted AY-WB protein 11 (SAP11) and tengu-su inducer (TENGU) (Hoshi *et al.*, 2008; Minato *et al.*, 2014; Sugio *et al.*, 2011).

1.4.2. Photosynthetic activity and carbohydrate metabolism.

Different authors reported a downregulation of photosynthetic proteins in phytoplasma-infected plants (Ji *et al.*, 2009; Hren *et al.*, 2009; Taheri *et al.*, 2011), accompanied by a reduction of total chlorophyll content (Bertamini *et al.*, 2002a; 2002b; Junqueira *et al.*, 2004; Zafari *et al.*, 2011). The limited expression of the photosynthetic proteins induces alteration in the photosynthetic whole chain (mainly affecting photosystem II activity), compromising the whole photosynthetic process (Musetti, 2010). This inhibition seems to have an impact on the carbohydrate metabolism, particularly on the accumulation of soluble carbohydrates and starch, as observed in source leaves of plants infected by phytoplasmas (Ji *et al.*, 2009; Junqueira *et al.*, 2004; Lepka *et al.*, 1999; Maust *et al.*, 2003; Pagliari *et al.*, 2016). It has been proposed that, following infection, photosynthesis must be switched off to initiate respiration and other processes for plant defence against pathogens (Scharte *et al.*, 2005). On the other hand, an increase in soluble carbohydrate concentration and elevated invertase activity could also suggest the establishment of a pathogen-induced carbohydrate sink (Santi *et al.*, 2013). Thus,

altered expression of genes coding for enzymes involved in carbohydrate metabolism may be caused by phytoplasma necessity to satisfy their requirements for energy, growth and spread using the host plant's phloem system (Giorno *et al.*, 2013). On the other hand, sugar can also act as a signalling molecule in plant immunity, preparing the plant to a fast and strong defence response, without however triggering any response before the actual manifestation of the stress condition (Moghaddam and van den Ende, 2012).

1.4.3. Protein content.

It has been hypothesized that photosynthesis impairment and the following decrease in synthesis of ribulose-1, 5-biphosphate carboxylase, the major soluble protein of the leaf (Bertamini *et al.*, 2003), could be related with the reduction in total soluble proteins observed in many phytoplasma-infected plants (Favali *et al.*, 2001, Bertamini *et al.*, 2002a; 2002b, Musetti *et al.*, 2007). Despite the decrease of the total protein content, following pathogen infection, a lot of proteins are produced by the host plant. Most of them are related to the defence mechanisms and are called pathogenesis-related-proteins (PR-proteins) (Junqueira *et al.*, 2004; Margaria and Palmano, 2011; Musetti *et al.*, 2013; Santi *et al.*, 2013; Zhong and Shen, 2004). PR proteins accumulate locally in the infected leaves and are also induced systemically, dealing to the development of systemic acquired resistance (SAR) (van Loon, 1999). To date, 17 families of PR proteins have been identified in numerous plant species (Ebrahim *et al.*, 2011). This great variability reflects the wide range of roles they are supposed to cover, that include peroxidases, chitinases and β-1, 3-glucanases (Ebrahim *et al.*, 2011; Sels *et al.*, 2008; van Loon, 1999). However, a direct functional role in defence could not be demonstrated for all of them (Sels *et al.*, 2008).

1.4.4. Phenolics.

Despite the lack of information on the topic, polyphenols seem to play an important chemical and biological role in plant resistance against phytoplasmas. In fact, in many pathosystems a significant increase in phenolic compounds was observed in relation to the inhibition of the pathogen inside the phloem cells (Choi *et al.*, 2004; Junqueira *et al.*, 2004; Musetti *et al.*, 2000; 2007). Moreover, Hren and co-authors (2009) demonstrated a significant reprogramming of the transcriptome following phytoplasma infection, because 19 out 22 genes from secondary metabolism, mainly flavonoids and chalcones, were involved in up-regulated processes. Nevertheless, studying two different cultivars,

Margaria and co-authors (2014) hypothesized that flavonoid accumulation is a physiological consequence of phytoplasma infection but does not affect phytoplasma multiplication.

1.5. Plant-pathogen interaction step 2: morphological and ultrastructural plant modifications following phytoplasma infection.

Following phytoplasma infection, a deep architectural modification of the host cell structure occurs, due to the alteration of metabolism, hormone and development balances, which pathogen presence implies (Albertazzi *et al.*, 2009; Buxa *et al.*, 2015; Ehya *et al.*, 2013; Musetti *et al.*, 2005, 2010; Pagliari *et al.*, 2016; Zimmermann *et al.*, 2015). A stable association between the necrosis of the phloem elements and the formation of new ones, due to the cambium hyperactivity (hyperplasia), was reported in many phytoplasma-plant interactions (Braun and Sinclair; 1979; Garcion *et al.*, 2014; Iriti *et al.*, 2008; Oshima *et al.*, 2001; Pagliari *et al.*, 2016; Sinclair *et al.*, 1976) and it could be explained as a plant response to limit phloem functionality that occurred in infected tissue (Oshima *et al.*, 2001) or as a result of pathogen effector action (Bai *et al.*, 2009; Sugio *et al.*, 2011). Transmission electron microscopy (TEM) images revealed cell wall thickening and distortion in the phloem of different plant hosts infected by phytoplasma (De Marco *et al.*, 2016; Musetti *et al.*, 2000, 2013; Pagliari *et al.*, 2016; Santi *et al.*, 2013), probably due to defensive depositions of phenolic (Messiaen *et al.*, 1993) and/or homogalacturonans (Cosgrove, 2005). The SE plasma membrane also deforms due to phytoplasma infection, invaginating or undulating, and incoming in close contact with the phytoplasma membrane (Buxa *et al.*, 2015), to form a structure that anchors the phytoplasma body to the SE plasma membrane (Musetti *et al.*, 2016).

Phytoplasmas also interact with the plant and insect cytoskeleton by the immunodominant membrane proteins (IMP) (Boonrod *et al.*, 2012; Galetto *et al.*, 2011), imposing SE actin reorganization (Buxa *et al.*, 2015). It is known that actin is stimulated by intracellular bacteria for promoting their motility (Borisy and Svitkina, 2000; Haglund and Welch, 2011; Opalski *et al.*, 2005). Considering that phytoplasmas lack genes coding for movement, actin binding could be involved in phytoplasma movement within SEs and through the sieve plates.

Starch accumulation and general disorganization of thylakoids (Braun and Sinclair, 1978; Junqueira *et al.*, 2004; Maust *et al.*, 2003; Musetti *et al.*, 2010), together with impaired photosynthesis (Bertamini *et al.*, 2001; Lepka *et al.*, 1999; Maust *et al.*, 2003) and stoma closure (Matteoni and Sinclair, 1983; Vitali *et al.*, 2013) are often described in phytoplasma infection and seem to be related to the inhibition of phloem transport (Bertaccini and Duduk, 2009). Limited phloem translocation may be not exclusively linked with high phytoplasma level clogging SE lumen. In fact, a lower

translocation has also been seen in plants with a low phytoplasma titre (Christensen *et al.*, 2005). Two characteristic plant responses, such as structural phloem protein in sieve elements (SE-protein) filament formation and agglutination and callose deposition at sieve plate level, have been hypothesised to limit phloem mass flow and, consequently, to prevent pathogen spread by SE occlusion (Braun and Sinclair, 1978, Gamalero *et al.*, 2010; Lherminier *et al.*, 2003; Musetti *et al.*, 2010; 2013; Sinclair *et al.*, 1976).

Callose is a structural component of the SE (Ehlers *et al.*, 2000; van Bel *et al.*, 2002), but its activity in case of biotic and abiotic stress is extensively reported (Barratt *et al.*, 2011; Furch *et al.*, 2007; Knoblauch and van Bel, 1998; Xie *et al.*, 2011). This site-specific plant response (De Marco *et al.*, 2016; Pagliari *et al.*, 2016) occurs mainly around sieve pores after the increase in Ca^{2+} concentration inside the SEs and takes several minutes to occlude the sieve pores (Furch *et al.*, 2007; 2008; 2010; van Bel *et al.*, 2014), probably for the necessity of a *de novo* synthesis (Chen and Kim, 2009; Xie *et al.*, 2011) or the relatively high Ca^{2+} threshold level necessary to evoke this response (van Bel *et al.*, 2014). Thanks to a sort of "safety design" (van Bel *et al.*, 2014), the time necessary for callose deposition is covered by SE-protein occlusion mechanism.

1.5.1. SE-proteins in Fabaceae plants: forisomes.

Differently from callose, SE-proteins are structural components of the SEs, which do not require a *de novo* synthesis (van Bel, 2003). Moreover, as callose deposition, SE-protein agglutination is a Ca^{2+}-mediated response, but its threshold level seems to be considerably lower (van Bel *et al.*, 2014). For these reasons, the agglutination of SE-protein filaments is an immediate and reversible process that acts in the time frame of seconds (Furch *et al.*, 2007; Srivastava *et al.*, 2015; van Bel, 2003).

SE-proteins are encoded by members of the widespread sieve element occlusion (*SEO*) gene family, first described in Fabaceae and then individuated in many other angiosperms (Ernst *et al.*, 2011; 2012; Froelich *et al.*, 2011; Pelissier *et al.*, 2008; Rüping *et al.*, 2010). In Fabaceae, SEO proteins encode forisome components (Pélissier *et al.*, 2008). Forisomes are synthesized in the cytoplasm of immature SE, forming giant, electron-dense SE-proteins bodies (Cronshaw and Esau, 1967; Fisher, 1975; Steer and Newcomb, 1969; Wergin and Newcomb, 1970). During the maturation and the selective autolysis of the SE, forisomes maintain their spindle-shaped morphology. In case of biotic or abiotic stress, forisomes can undergo to a reversible calcium-induced change in its conformation, from spindle to dispersed state, reaching up to six times their contracted volume and temporary occluding sieve pores (Fig. 5) (Furch *et al.*, 2007; Knoblauch and Oparka, 2012;

Knoblauch *et al.*, 2001, 2003; Peters *et al.*, 2006). It has been speculated that this mechanism reduces photoassimilate leakage in case of injury (Srivastava *et al.*, 2015; van Bel *et al.*, 2014). Moreover, results obtained in *in vivo* studies with phytoplasma-infected *Vicia faba* plants demonstrated that structural modification of forisomes could also be triggered by phytoplasmas, suggesting a putative role in pathogen restriction (Musetti *et al.*, 2013).

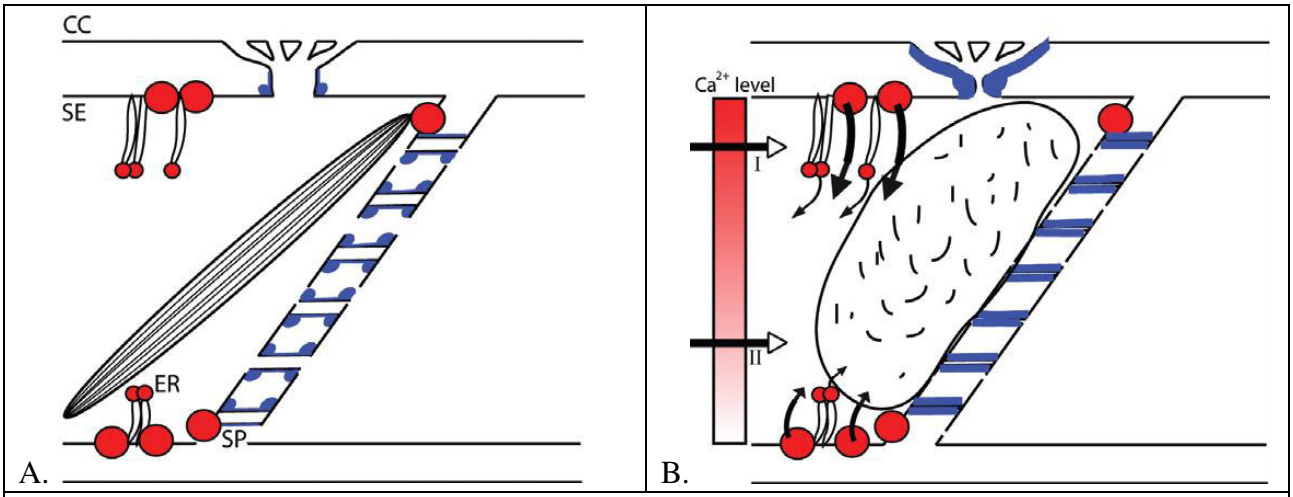

Figure 5. Structural modification occurring in forisomes. The intact SE presents condensed forisomes, showing typical spindle shape, and low degree of callose deposition (blue areas) (A). Following an increase in the Ca2+ concentration in SEs, due to the activation of Ca2+-permeable channels (red circles), forisome dispersion and callose synthesis occur.
CC: companion cell; ER: endoplasmic reticulum; SE: sieve element; SP: sieve plate

Picture from Furch *et al.*, 2007

1.5.2. SE-proteins in non-Fabaceae plants.

In non-Fabaceae plants, conventional SE-proteins are supposed to share many structural and functional features with forisomes (Ernst *et al.*, 2012; Rüping *et al.*, 2010; Srivastava *et al.*, 2015), but instead of protein giant bodies, they consist of electron dense, variously branched, protein strands (Batailler *et al.*, 2012; Ernst *et al.*, 2012; Jekat *et al.*, 2013; Sjolund, 1997). Moreover, even if, like forisomes, they are synthesized in the cytoplasm of immature SEs as large electron-dense proteins bodies, conventional SE-proteins disperse during SE maturation forming a parietal layer at the sieve element wall (Ehlers *et al.*, 2000; Ernst *et al.*, 2012; Evert *et al.*, 1972; Froelich *et al.*, 2011).

SEO genes have been found conserved through Dicots (Ernst *et al.*, 2011, 2012; Pélissier *et al.*, 2008; Rüping *et al.*, 2010). In Arabidospis, SE-protein filament formation requires two *SEO* genes, *AtSEOR1* (At3g01680) and *AtSEOR2* (At3g01670) (Anstead *et al.*, 2012). These two contiguous genes, together with one pseudogene (At1g67790), are located on chromosome 3 and are the sole *SEO* genes individuated in *A. thaliana* (Anstead *et al.*, 2012; Rüping *et al.*, 2010). No functional

redundancy between the corresponding proteins has been detected (Anstead *et al.*, 2012). The heterodimer formation mechanism is still uncertain and AtSEOR1 and AtSEOR2 interaction seems to require one or more additional unknown proteins (Anstead *et al.*, 2012; Jekat *et al.*, 2013). Even if AtSEOR1 and AtSEOR2 remain the sole proteins reputed necessary for SE-protein filament formation, Batailler and coauthors (2012) reported that the protein AtPP2-A1, encoded by the gene At4g19840, is also associated with SE-protein filaments in Arabidopsis. In *Cucurbita* spp., phloem protein 2 (PP2) and phloem protein 1 (PP1) have been associated with the structural SE-protein filaments (Allen, 1979; Cronshaw and Sabnis, 1990; Read and Northcote, 1983; Sabnis and Hart, 1978). While *PP1* gene belongs to a family found only in Cucurbitaceae (Clark *et al.*, 1997; Lin *et al.*, 2009), *PP2*-like genes have been found widely among angiosperms and gymnosperms (Dinant *et al.*, 2003). Moreover, phloem lectin PP2 is known to play a role in different phloem-specific defence mechanism, induced by both biotic and abiotic stresses (Bencharki *et al.*, 2010; Beneteau *et al.*, 2010; Lee *et al.*, 2014; Zhang *et al.*, 2011).

Despite the solid knowledge acquired on forisome functions (Knoblauch and Peters, 2004; Srivastava *et al.*, 2015; Musetti *et al.*, 2013), up to now, the role of SE-protein filaments in non-Fabaceae, in physiological and stress conditions is not well understood and, for this reason, it is still matter of debate.

In *Cucurbita* spp., PP2 and PP1 proteins are the candidates for sieve tube occlusion in case of abiotic stress. In fact, after wounding, PP2 covalently interacts with PP1 and sieve tubes and cut surfaces are rapidly occluded by exudate gelling (Alosi *et al.*, 1988; Clark *et al.*, 1997; Dinant *et al.*, 2003; Furch *et al.*, 2010; Lough and Lucas, 2006; Read and Northcote, 1983). On the other hand, in *Cucurbita maxima* a SEO-like protein (CmSEO1) has been also found and it has been supposed to have a role in wound sealing (Ernst *et al.*, 2012; Zhang *et al.*, 2010). This phenomenon could be explained by the significant differences between the fascicular and the extrafascicular phloem system characteristic of *C. maxima* (Zhang *et al.*, 2010).

Having a general view on non-Fabaceae plants, following biotic or abiotic stresses, such as injury or pathogen infection, SE-protein filaments are displaced from their parietal position and organized in SE lumen as strands or meshwork to plug the sieve plate (Batailler *et al.*, 2012, Ernst *et al.*, 2012; Jekat *et al.*, 2013; Sjolund, 1997). Dealing with the further step of this mechanism, different experiments drove to opposite conclusions (Froelich *et al.*, 2011; Ernst *et al.*, 2012; Jekat *et al.*, 2013), generating a lively debate about the real impact of SE-protein plugs on phloem mass flow and photoassimilate translocation (Knoblauch *et al.*, 2014). Moreover, it is not even clear if the supposed plug could really affect pathogen spread. In fact, this assumption is only based on indirect evidences

(Gamalero *et al.*, 2010; Lherminier *et al.*, 2003; Musetti *et al.*, 2013).

2. Aims.

As previously described, phytoplasmas represent worldwide a severe problem to agriculture, causing huge damages in plant productivity. The lack of effective traditional curative strategies has pressed for the development of genetic-based approaches and thus the detailed knowledge on plant response mechanisms to phytoplasma infection is mandatory.

Following infection, many morphological and biochemical changes occur. Even if the macroscopic consequences of phytoplasma activity in the host plants have been amply described, phytoplasma relationships and effects on the sieve-element physiology and ultrastructure have been poorly investigated. SE-protein agglutination and callose deposition at sieve pore level have been proposed as plant response to limit pathogen spread, but unequivocal evidences about the identity of actors in phytoplasma-mediated sieve-tube occlusion and their possible consequences on pathogen fitness are lacking thus far. In this work, the interactions between SE-protein and phytoplasmas have been investigated, using wild-type and *AtSEOR* and *AtPP2-A1* mutant Arabidopsis lines. For the first time, SE-protein morphology and functionality were studied both in healthy and pathogen-stimulated SEs. Two main goals have been attempted to achieve: elucidating the role of SE-proteins on phloem mass flow and their affection on phytoplasma infection.

Various microscopic techniques were used, in order to observe both fresh and embedded tissue, gaining information both on ultrastructural and physiological modifications in SEs following phytoplasma infection. Trying to have a view as wide as possible, a multidisciplinary approach was followed, interpenetrating microscopy investigations with molecular and biochemical analyses.

3. Setting of the experimental system.

3.1. Pathosystem.

3.1.1. The pathogen: '*Candidatus* Phytoplasma asteris'.

'*Candidatus* Phytoplasma asteris' is a member of the Aster Yellows (AY) phytoplasma group or 16SrI group (IRPCM, 2004; Lee *et al.*, 2004a). On the basis of 16S rRNA gene sequence analysis, the AY phytoplasma group is relatively homogeneous (Lee *et al.*, 2004a), but, despite this, the AY phytoplasma group could be subdivided into several distinct restriction fragment length polymorphism (RFLP) subgroups (16SrI subgroups), basing on extensive RFLP analysis of 16S rRNA gene sequences (Lee *et al.*, 2004a; 2007; Jomantiene *et al.*, 2011; Wei *et al.*, 2011).

16SrI is the most widespread phytoplasma group (Marcone *et al.*, 2000; Lee *et al.*, 2004a; Jomantiene *et al.*, 2011). It appears to have a wide host range, mostly infecting herbaceous dicotyledonous plant hosts and spreads naturally by several leafhoppers as insect vectors (Lee *et al.*, 1998; 2004a; Weintraub and Beanland, 2006).

3.1.2. The plant host: *Arabidopsis thaliana*.

A. thaliana, a member of the Brassicaceae family, is a herbaceous winter annual plant with a relatively short life cycle. Native to Europe, Asia, and north-western Africa, nowadays Arabidopsis presents a cosmopolitan diffusion (Hoffmann, 2002). While *A. thaliana* impact is not directly significant in agricultural or economic fields, in the last decades it has imposed in the biologic research scenario as the model plant per excellence, becoming probably the most widely studied plant species (Huala *et al.*, 2001; Koornneef and Meinke, 2010; Meinke *et al.*, 1998). In fact, *A. thaliana* has many advantages, including a relative small genome size, fully sequenced in 2000 (Kaul *et al.*, 2000), a fast growth cycle, small size, autogamous breeding system and the ability to grow on various media (Koornneef and Meinke, 2010). Moreover, mutants can be obtained easily, by transformation process or, when available, by request to stock centres, open to the scientific community (Koornneef and Meinke, 2010).

3.2. Classification of the putative phytoplasma strain.

In *A. thaliana* infection process, infected *Chrysanthemum* plants were used as sources of phytoplasma acquisition for the insect vectors. The effective presence of '*Ca.* P. asteris' in daisy plants was previously checked by PCR and restriction fragment length polymorphism (RFLP) technique.

For each plant, 1 g of randomly-selected leaf tissue was collected. Total Genomic DNA was extracted using the CTAB extraction method (Doyle and Doyle, 1990) modified according to Martini and co-authors (2009). Briefly, leaf tissue was placed in a sterile mortar with 4 ml of CTAB extraction buffer and homogenized with a sterile pestle. 1 ml of the total homogenate was collected in a 2-ml microfuge tube, vortexed, and thawed at 70°C for 25 minutes. After centrifugation at 10000 rpm for 10 min, the supernatant was transferred to another sterile microfuge and an equal volume of chloroform:isoamyl alcohol (24:1) was added. Tubes were vortexed and centrifugated at 8000 rpm for 10 min. Then the supernatant was transferred to another sterile microfuge tube and 2/3 volume of cold isopropanol was added. After having gently mixed by inverting several times, the tubes were then centrifuged at 12000 rpm for 15 min at 4°C. The pelleted DNA was separated from the supernatant and washed with 0.5 ml of cold 70 % ethanol. Following a 5-minute centrifugation at 12000 rpm at 4°C, the supernatant was discarded and the DNA pellets were then dried by a HetoVac vacuum and diluted in 200 µl of TE buffer. DNA concentration and purity were determined using a NanoDrop 1000 Spectrophotometer (Thermo Fisher Scientific, Wilmington, DE, USA).

For polymerase chain reaction (PCR) analysis, the 16S rRNA gene, commonly used for phytoplasma diagnosis (Lee *et al.*, 2000), was chosen as a target for amplification using the universal primer pair, R16F2n/R16R2 (Gundersen and Lee, 1996; Marcone *et al.*, 2000). PCR was performed in a reaction volume of 25 µl containing 200 mM of each dNTP, 0.4 mM of each primer, 1.5 mM $MgCl_2$, 5ml of 5×PCR buffer, 0.625 U of GoTaq Flexi polymerase (Promega, USA) and 20 ng of total DNA. A negative control lacking DNA templates in the reaction mix was included. Cycling conditions were as follows: 94 °C for 2 min, 40 cycles of 94 °C for 1 min, 55 °C for 1 min, 72 °C for 2 min, followed by a final extension at 72 °C for 8 min. Amplification products were analysed by 1% agarose gel electrophoresis, stained with GelRedTM (10000× Biotium, USA) and visualized under UV light. The PCR products (6–8 ml) were digested singly with each of the restriction enzymes (MseI, HpaII, AluI, HhaI, HinfI, HaeIII), which were selected to differentiate among phytoplasma groups and subgroups inside the AY group (16SrI) (Marcone *et al.*, 2000). The restriction products were then separated by electrophoresis through a 2.5% agarose gel for 30 min at 120V and 60 min at 100 V, stained with GelRedTM (10000×Biotium, USA), and visualized with a UV transilluminator.

As showed in figure 6, RFLP profiles of infected chrysanthemum sample were identical to the profiles of the strains belonging to group 16Sr-IB (Marcone *et al.*, 2000).

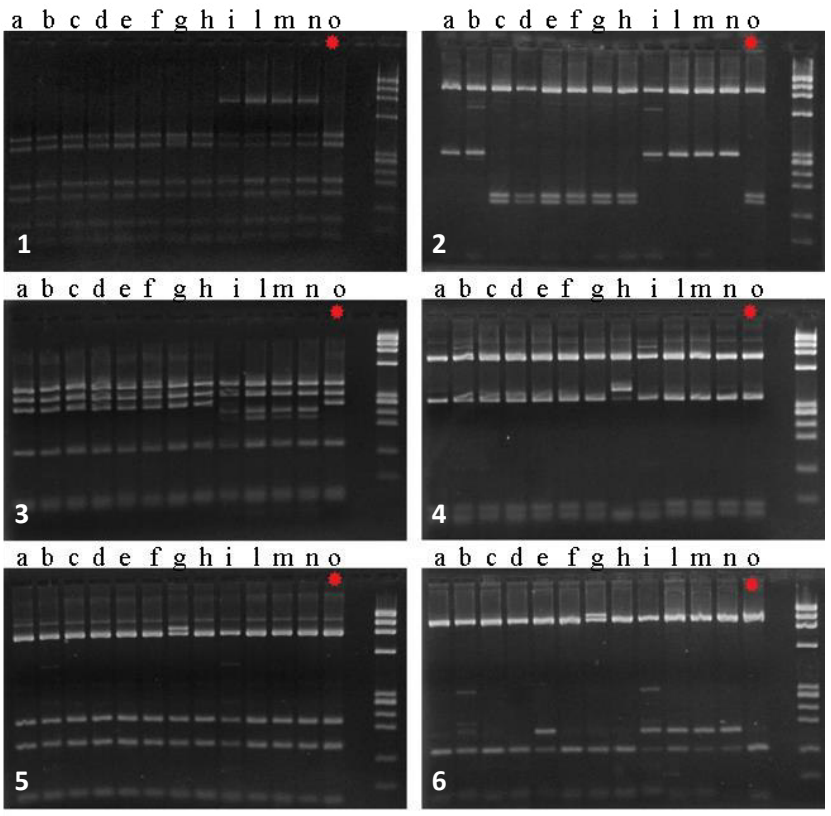

Strains and 16Sr-I subgroups

a.	Aster yellows witches' broom (NJAY)	A
b.	Grey dogwood stunt (GD1)	A
c.	Onion yellows mild strain (NA)	B
d.	Silene vulgaris yellows (SIL)	B
e.	Acetosella witches' broom (SA)	M
f.	Periwinkle yellows (OS)	B
g.	Tagetes witches' broom (TWB)	B
h.	Maryland aster yellows (AY1)	L
i.	Clover phyllody (Cph)	C
l.	Carrot yellows (CA)	C
m.	Leontodon yellows (LEO)	C
n.	Canada Clover phyllody (CCph)	C
o.	Putative strain	B

Figure 6. RFLP classification of the putative phytoplasma strain. The PCR products of infected chrysanthemum plants were digested singly with each of the restriction enzymes: AluI (1), HhaI (2), MseI (3), HinfI (4), HpaII (5) and HaeIII (6). RFLP profiles from infected chrysanthemum sample (indicated with letter o) were identical to the profiles of the strains belonging to group 16Sr-IB (letter c,d,f,g).

3.3. Infection protocol.

A. thaliana plants, ecotype Col-0, were infected with Chrysanthemum yellows (CY) phytoplasma, a '*Ca.* P. asteris'-related strain (16SrI-B subgroup) (Lee *et al.*, 2004a), using infected daisy plants (*Chrysanthemum carinatum* Schousboe) as the source of inoculum.

Both the insect vector *Euscelidius variegatus* and *A. thaliana* plants were grown at 20/22 °C under short-day conditions (9hL/15hD period). Fourth and fifth instar *E. variegatus* nymphs were taken from healthy colonies grown on *Avena sativa* and transferred to CY-infected daisy plants for a 7-day acquisition-feeding period. The choice of juvenile stages depended on the necessity to ensure the survival of the insects at the end of the latency period and consequently the possibility to infect the host plant. The minimum number of days required for the acquisition `was estimated to be 3 days, however, the insects remained on chrysanthemum for 7 days, to increase the vector phytoplasma titre

and consequently the probability for a successful infection (Palermo *et al.*, 2001). Thirty days after nymph transfer, 45-day-old *A. thaliana* plants [corresponding to the 3.50 growth stage, according to Boyes *et al.*, (2001)] were individually exposed to 3 infective insects. Healthy control plants were exposed to healthy insects. At the end of the 7-day inoculation-feeding period, insects were manually removed.

3.4. Arabidopsis as a model plant for studying plant-phytoplasma interaction.

Phytoplasmas are strictly dependent on metabolic compounds from their hosts (Bai *et al.*, 2006; Oshima *et al.*, 2004) and for this reason many attempts to culture them *in vitro* failed (Contaldo *et al.*, 2012). The necessity to study the fine mechanisms regulating plant-phytoplasma interaction and thus to control experimental and environmental condition, makes investigation in natural plant hosts particularly limiting. Therefore, in the last decade some authors have started to use *A. thaliana* as model plant for studying phytoplasma-plant interactions (Bressan and Purcell, 2005; Cettul and Firrao, 2011; Hogenhout and Music, 2010; Hoshi *et al.*, 2009; MacLean *et al.*, 2011). Nevertheless, ultrastructural modifications occurring in *A. thaliana* tissues following phytoplasma infection have never been described in detail.

Paper published by Micron Journal (2016).

Micron 89 (2016) 1–11

Contents lists available at ScienceDirect

Micron

journal homepage: www.elsevier.com/locate/micron

Looking inside phytoplasma-infected sieve elements: A combined microscopy approach using *Arabidopsis thaliana* as a model plant

Laura Pagliari, Marta Martini, Alberto Loschi, Rita Musetti*

Department of Agricultural, Food, Environmental and Animal Sciences, University of Udine, Via delle Scienze, 206, I-33100 Udine, Italy

ARTICLE INFO

Article history:
Received 3 May 2016
Received in revised form 11 June 2016
Accepted 18 July 2016
Available online 21 July 2016

Keywords:
Phytoplasma
Arabidopsis thaliana
Phloem
Combined microscopy

ABSTRACT

Phytoplasmas are phloem-inhabiting plant pathogens that affect over one thousand plant species, representing a severe threat to agriculture. The absence of an effective curative strategy and the economic importance of many affected crops make a priority of studying how plants respond to phytoplasma infection. Nevertheless, the study of phytoplasmas has been hindered by the extreme difficulty of culturing them *in vitro* and by impediments to natural host plant surveys such as low phytoplasma titre, long plant life cycle and poor knowledge of natural host-plant biology. Stating correspondence between macroscopic symptoms of phytoplasma infected *Arabidopsis thaliana* and those observed in natural host plants, over the last decade some authors have started to use this plant as a model for studying phytoplasma-plant interactions. Nevertheless, the morphological and ultrastructural modifications occurring in *A. thaliana* tissues following phytoplasma infection have never been described in detail. In this work, we adopted a combined-microscopy approach to verify if *A. thaliana* can be considered a reliable model for the study of phytoplasma-plant interactions at the microscopical level.

The consistent presence of phytoplasma in infected phloem allowed detailed study of the infection process and the relationship established by phytoplasmas with different components of the sieve elements. In infected *A. thaliana*, phytoplasmas induced strong disturbances of host plant development that were mainly due to phloem disorganization and impairment. Light microscopy showed collapse, necrosis and hyperplasia of phloem cells. TEM observations of sieve elements identified two common plant-responses to phytoplasma infection: phloem protein agglutination and callose deposition.

1. Introduction

Phytoplasmas, which are plant pathogenic prokaryotes belonging to the *Mollicutes* (Lee et al., 2004), are associated with several hundred diseases affecting over one thousand plant species, including many economically important crops (Marcone et al., 2014), and they cause severe yield losses worldwide. Their impact in agriculture is expected to grow by the continuing association of phytoplasma with newly emerging diseases (Bertaccini and Duduk, 2010) and by global warming, advantageous to cold-sensitive insect vectors (Hogenhout et al., 2008). There is no effective curative strategy available so far, and the most common ways to limit the outbreaks of phytoplasma epidemics are the use of insecticides and the removal of symptomatic plants (Bertaccini et al., 2014).

Phytoplasmas are obligate pathogens of plants and phloem-feeding insects. With a unique life cycle, they are able to replicate intracellularly in both (Hogenhout et al., 2008). While in plants phytoplasmas are confined to phloem tissue, in insects they move from the intestinal tract to the salivary glands and are then released in new host plants by feeding activity (Hogenhout et al., 2008).

Although not all phytoplasma infections are necessarily deleterious, symptoms in diseased plants suggest strong disturbances to phloem functions and imbalances in plant growth regulators (Lee et al., 2000). Phloem impairment results in foliar yellowing and reddening, small leaves, leaf roll and curl, vein clearing and enlargement, vein necrosis, growth stunting and general plant decline. Phloem impairment is caused by occlusion of the sieve elements (SEs) due to phloem-protein (PP) agglutination and callose deposition (Musetti et al., 2013), followed by necrosis and collapse of SEs (Lee et al., 2000; Musetti et al., 2013). Reduced phloem translocation is histologically demonstrated by starch accumulation in the chloroplasts of source leaf tissues, which leads to thylakoid disorganization (Musetti, 2010) and to a consequent alteration in photosynthesis activity (Bertamini et al., 2002; Lepka et al., 1999).

Since their discovery by Doi et al. (1967), the study of phytoplasmas has been hindered by the extreme difficulty of culturing them

* Corresponding author.
E-mail address: Rita.Musetti@uniud.it (R. Musetti).

http://dx.doi.org/10.1016/j.micron.2016.07.007
0968-4328/

in vitro (Contaldo et al., 2012). This is due to the high dependence of phytoplasmas on metabolic compounds from their hosts, due to their loss of many endogenous metabolic genes (Bai et al., 2006; Oshima et al., 2004). Moreover, investigations in natural plant hosts are often limited by environmental conditions, long plant-host life cycles and poor knowledge of host-plant biology. Therefore, in the last decade some authors have started to use *Arabidopsis thaliana* as model plant for studying phytoplasma-plant interactions. This choice was supported by the correspondence between macroscopic symptoms present in infected *A. thaliana* and those observed in natural host plants (Bressan and Purcell, 2005; Cettul and Firrao, 2011; Hogenhout and Music, 2010; Hoshi et al., 2009; MacLean et al., 2011). Nevertheless, ultrastructural modifications occurring in *A. thaliana* tissues following phytoplasma infection have never been described in detail.

In this work we combined different microscopy approaches, focusing on phloem tissue of *A. thaliana* infected with a strain of '*Candidatus* Phytoplasma asteris' ('*Ca.* P. asteris', Lee et al., 2004), to detect ultrastructural modification occurring in Arabidopsis following phytoplasma challenge, with the aim of evaluating whether this plant species is a reliable tool for studying phytoplasma-host plant interactions at the cytological level.

2. Materials and methods

2.1. Plant materials and insect vectors

A. thaliana plants, ecotype Col-0, were infected with Chrysanthemum yellows (CY) phytoplasma, a '*Ca.* P. asteris'-related strain (16SrI-B subgroup) (Lee et al., 2004), using infected daisy plants (*Chrysanthemum carinatum* Schousboe) as the source of inoculum and *Euscelidius variegatus* as the insect vector (Bosco et al., 1997). Both the insect vector and *A. thaliana* plants were grown at 20/22 °C under short-day conditions (9hL/15hD period). Fourth and fifth instar *E. variegatus* nymphs were taken from healthy colonies grown on *Avena sativa* L. and transferred to CY-infected daisy plants for a 7-day acquisition-feeding period. Thirty days after nymph transfer, 45-day-old *A. thaliana* plants [corresponding to the 3.50 growth stage, according to Boyes et al. (2001)] were individually exposed to 3 infective insects. Healthy control plants were exposed to healthy insects. At the end of the 7-day inoculation feeding period, insects were manually removed.

For the molecular detection and microscopy analyses diseased-symptomatic and healthy control *A. thaliana* plants were analysed 20 days after inoculation, corresponding to the 3.90 growth stage (Boyes et al., 2001). For macroscopic full-symptom evaluation, symptomatic and healthy control *A. thaliana* plants were analysed 40 days after inoculation, corresponding to the 6.50 growth stage (Boyes et al., 2001).

2.2. Phytoplasma molecular detection

The polymerase chain reaction (PCR) was performed to detect phytoplasmas in ten diseased-symptomatic and ten healthy control *A. thaliana* plants. For each plant, 500 mg of randomly-selected fully-expanded leaf tissue were collected from the rosette. Total genomic DNA was extracted using a CTAB extraction method (Doyle and Doyle, 1990) modified according to Martini et al. (2009). DNA concentration and purity were checked using a NanoDrop 1000 Spectrophotometer (Thermo Fisher Scientific, Wilmington, DE, USA). The 16S rRNA gene, commonly used for phytoplasma diagnosis (Lee et al., 2000), was chosen as a target for amplification using the universal primer pair, R16F2n/R16R2 (Gundersen and Lee, 1996; Marcone et al., 2000).

PCR was performed in a reaction volume of 25 μl containing 200 μM of each dNTP, 0.4 μM of each primer, 1.5 mM MgCl2, 5 μl of 5 × PCR buffer, 0.625 U of GoTaq Flexi polymerase (Promega, USA) and 20 ng of total DNA. A negative control lacking DNA templates in the reaction mix was included. Cycling conditions were as follows: 94 °C for 2 min, 40 cycles of 94 °C for 1 min, 55 °C for 1 min, 72 °C for 2 min, followed by a final extension at 72 °C for 8 min. Amplification products were analysed by 1% agarose gel electrophoresis, stained with GelRed™ (10000× Biotium, USA) and visualized under UV light.

Restriction fragment length polymorphism (RFLP) analysis of PCR products was used for the identification of the putative phytoplasmas. The PCR products (6–8 μl) were digested singly with each of the restriction enzymes (*Mse*I, *Hpa*II, *Alu*I, *Hha*I, *Hinf*I, *Hae*III), which were selected to differentiate among phytoplasma groups and subgroups inside the AY group (16SrI) (Marcone et al., 2000). The restriction products were then separated by electrophoresis through a 2.5% agarose gel for 30 min at 120 V and 60 min at 100 V, stained with GelRed™ (10000× Biotium, USA), and visualized with a UV transilluminator.

2.3. Transmission electron microscopy

For transmission electron microscopy (TEM) analysis, ten fully symptomatic and ten healthy control *A. thaliana* plants were used. To preserve phloem tissue structure, a gentle preparation method was adopted, modifying the protocol by Ehlers et al. (2000), to adapt it to Arabidopsis leaves as recently reported for tomato (De Marco et al., 2016). From each plant, a midrib portion, 30 mm-long, was excised from three randomly selected, full-expanded leaves of the rosette. The midrib segments were immediately submerged in a buffer (10 mM NaOH-2-(*N*-morpholino) ethanesulfonic acid, 2 mM $CaCl_2$, 1 mM $MgCl_2$, 0.5 mM KCl and 200 mM mannitol, pH 5.7) for two hours at room temperature. A fixation solution of 3% paraformaldehyde and 4% glutaraldehyde in 50 mM sodium cacodylate buffer plus 2 mM $CaCl_2$, pH 7.2, was used and substituted every 30 min for 6 h. Samples were rinsed for 1 h at 4 °C in 50 mM sodium cacodylate buffer (2 mM $CaCl_2$, pH 7.2) and post-fixed overnight with 2% (w/v) OsO_4 in the previous buffer at 4° C. Samples were dehydrated in a graded ethanol series and then transferred into propylene oxide. From the central part of each midrib, a 6–7 mm long piece was finally excised and embedded in Epon/Araldite epoxy resin (Electron Microscopy Sciences, Fort Washington, PA, USA). Ultrathin sections (60–70 nm in thickness) were cut using an ultramicrotome (Reichert Leica Ultracut E ultramicrotome, Leica Microsystems, Wetzlar, Germany), collected on uncoated copper grids, stained with uranyl acetate and lead citrate (Reynolds, 1963), and then observed under a PHILIPS CM 10 (Eindhoven, The Netherlands) TEM, operating at 80 kV. Five non-serial cross sections from each sample were analysed.

2.4. Light microscopy

For phloem visualization at the histological level, semithin sections (1 μm in thickness) of resin-embedded tissue, prepared as described above, were cut using an ultramicrotome (Reichert Leica Ultracut E ultramicrotome), stained with 1% toluidine blue and examined using a Zeiss Axio Observer Z1 microscope (Carl Zeiss GmbH, Munich, Germany). Five non-serial cross sections from each sample were analysed.

2.5. Callose aniline blue staining and epifluorescence microscopy

Three entire Arabidopsis leaves, selected as described above from five healthy and five infected plants, were cut and submersed immediately in 4% paraformaldehyde and 0.1% glutaraldehyde in

0.2 M Sorensen's phosphate buffer, pH 7.2, overnight in the dark at 4 °C. A segment, 4 mm in length, was excised from the midrib of each sampled leaf. It was immediately washed and submerged overnight in a graded sucrose series in 0.1 M Sorensen's phosphate buffer (Lee et al., 2011) as follows: 0.7 M sucrose for 4 h, 1.5 M sucrose for 4 h and 2.3 M overnight. Samples were finally embedded in Jung Tissue Freezing Medium embedding matrix (Leica Instruments GmbH, Nussloch, Germany), overnight at 4 °C. Forty μm-thick transversal sections of frozen samples were cut using a cryostat (Jung CM 1500, Leica Instruments, GmbH, Nussloch, Germany) operating at −20 °C. Sections were stained for 5 min at room temperature using a solution containing 0.05% (w/v) aniline blue (Carlo Erba Reagents, Milano, Italy) in phosphate buffer. They were then rinsed in buffer solution and examined using a Zeiss Axio Observer Z1 epifluorescence microscope (EFM), using a 405 nm excitation filter and a 435–490 nm emission filter.

As controls, unstained sections were observed at the same excitation wavelength used for the fluorochrome (405 nm) (Fig. 3A and B).

At least 10 thin sections were analysed for both healthy and infected Arabidopsis leaves.

2.6. Statistical analysis

To compare phloem development in healthy and phytoplasma-infected leaf tissues, phloem cell layers observed under the LM were counted and phloem size was measured. Three different measuring points, as indicated by the lines drawn in Fig. 2, were chosen in three different non-serial cross sections from five healthy and five infected samples. Comparable vascular bundles from leaves at the same developmental age were detected.

The level of aniline fluorescence in the phloem tissue was measured and compared in healthy and diseased samples by computerized image analysis in 3 non-serial sections per plant, using ImageJ 1.49 m software (National Institutes of Health, Bethesda, MD, USA) (Bacci et al., 2008). The grey level (in arbitrary units; 0 = black, *i.e.* absence of signal; 255 = white) was measured on the tissue in an area devoid of signal at visual inspection and assumed as background; the threshold was then set at 2 times the background and the surface area and mean grey intensity were measured for all phloem areas above threshold. The background was subtracted from the mean grey intensity and the result was multiplied for the surface area above threshold, to get the signal intensity for every field (in arbitrary units) (Bacci et al., 2008).

To compare the distribution of sieve-element reticulum (SER) in healthy and phytoplasma-infected SEs, SER stacks observed by TEM were counted and recorded in five healthy or five phytoplasma-infected SEs (SE) from five different non-serial sections (Bamunusinghe et al., 2009).

Unpaired *t*-tests were performed using the InStat GraphPad software package (La Jolla, CA, USA) to determine statistically significant differences between healthy and infected samples. A level of $P < 0.005$ was considered statistically significant.

3. Results

3.1. Development of symptoms and molecular phytoplasma detection

All plants exposed to infective insects exhibited symptoms within 20 days of inoculation. In comparison to controls (Fig. 1A), infected plants showed yellowing, reduced growth and general stunting, although this did not result in rapid plant decline or death (Fig. 1H).

Table 1
Phloem hyperplasia: phloem development in healthy and infected plants.

Phloem cell layers (±SD)			Phloem thickness (μm) (±SD)		
Fields	Healthy plants	Infected plants	Fields	Healthy plants	Infected plants
15	3.47 ± 0.2	6.47 ± 0.43	15	10.86 ± 0.94	21.66 ± 1.04

Fields are defined as the three non-serial cross sections of five healthy and five infected plants. Unpaired *t*-test, P-values < 0.0002. SD: standard error.

Table 2
Measurements of the aniline blue fluorescence intensity in healthy and infected midribs.

Condition	Fields	Dot number (±SD)	Total Area (±SD)	Signal Intensity (± SD)
Healthy	15	7.67 ± 2.51	84.67 ± 18.61	10027.25 ± 1445.47
Infected	15	20.61 ± 5.15	391.51 ± 100.20	43428.31 ± 6214.20

Fields are defined as the three non-serial cross sections of five healthy and five infected plants. Unpaired *t*-test, P-values < 0.0002. SD: standard error.

Leaves that emerged after phytoplasma inoculation were shorter, with a thick main vein and closely spaced, causing bushy appearance in the plants (Fig. 1H). Many leaves showed progressive yellowing, while reddening was detected in rare cases at the end of observation period (Fig. 1B and C, right side). Flower virescence and phyllody were generally observed (Fig. 1E). Flower abnormalities caused fruit anomalies or sterility. Siliquae appeared shorter and enlarged, with a profile characterized by a swollen top (Fig. 1G).

Direct PCR analysis allowed the amplification of a 1250-bp-fragment, confirming the presence of phytoplasmas only in the symptomatic plants. RFLP analysis confirmed the inclusion of PCR products into the 16SrI-B subgroup (not shown).

3.2. Plant responses at the histological level

Semithin sections and light microscopy (LM) observation of midribs from healthy *A. thaliana* plants allowed the visualization of vascular bundles with a regular collateral pattern and no cell alteration (Fig. 2A). Phytoplasma-infected leaf tissues were characterized by a general disorganization of the vascular bundles, with slight aberration in bundle disposition (Fig. 2B). Many phloem components possessed dense withdrawn protoplasts, probably due to the presence of phytoplasma or necrotic processes (Fig. 2B). Moreover, cambial tissue appeared in a hyperactivity state, showing many layers and a massive production of new phloem components, leading to phloem hyperplasia. New phloem cells appeared to have small lumens and an irregular shape associated with thick and distorted walls (Fig. 2B).

The phloem tissue in infected plants was approximately two times thicker than in the controls; at the same time cell layers of infected phloem were almost two times more numerous than in control tissue (Table 1). In spite of a small variation in xylem arrangement and vessel wall thickness, no new xylem formation or other significant changes in vessel morphology were detected (Fig. 2B).

Callose was detected in healthy and phytoplasma-diseased *A. thaliana* midribs by aniline blue staining under the EFM (Fig. 3). Healthy tissues were characterized by a modest callose presence, indicated by a number of fluorescent dots in correspondence to phloem tissue (Fig. 3C). In infected samples, intense aniline blue signals revealed a considerable increase in callose deposits (Fig. 3D). The level of fluorescence was measured and compared in healthy and infected samples, resulting in a significant increase in the latter compared to the former (Table 2).

No fluorescence signal was identified in chlorenchyma.

Fig. 1. Phytoplasma infection alters the phenotype of Arabidopsis, producing classic phytoplasmosis symptoms. (A) Healthy plants show regular growth. (B) Infected plants are characterized by stunted growth and bushy phenotype. (C and D) Leaves are shorter, with a thick main vein. Yellowing is manifested on the leaf lamina, while reddening occurs only in leaf veins (arrow) (left: a leaf from healthy plant, right: a leaf from infected plant). (E) Flowers in healthy plants have regular morphology. (F) Flowers in infected plants show virescence (green petals and stamens) and phyllody (leaf-like sepals and petals). (G) Siliquae in healthy plants are linear and elongated. (H) In infected plants siliquae have enlarged and distorted carpels. Bars correspond to 10 mm (For interpretation of the references to color in this figure legend, the reader is referred to the web version of this article.)

3.3. *Phytoplasma morphology and localization*

TEM observations confirmed the presence of phytoplasma exclusively in the SEs of every symptomatic *A. thaliana* plant. The phytoplasma colonization pattern often seemed uneven, with some SEs filled by phytoplasma cells and others less populated (Fig. 4A). Phytoplasmas appeared well preserved, with their typical pleomorphic shape (Fig. 4B). An electron-dense membrane, holding ribosome granules and dispersed DNA strands, delimited phytoplasma cells (Fig. 4B, inset i). In the SE lumen free-floating, dividing phytoplasmas were detected (4 B) with others partly located within the sieve pores (Fig. 4B and C). Other phytoplasmas adhered to SE plasma membrane by an “adhesion structure”. Contact structures connecting phytoplasmas with SER stacks were also visible

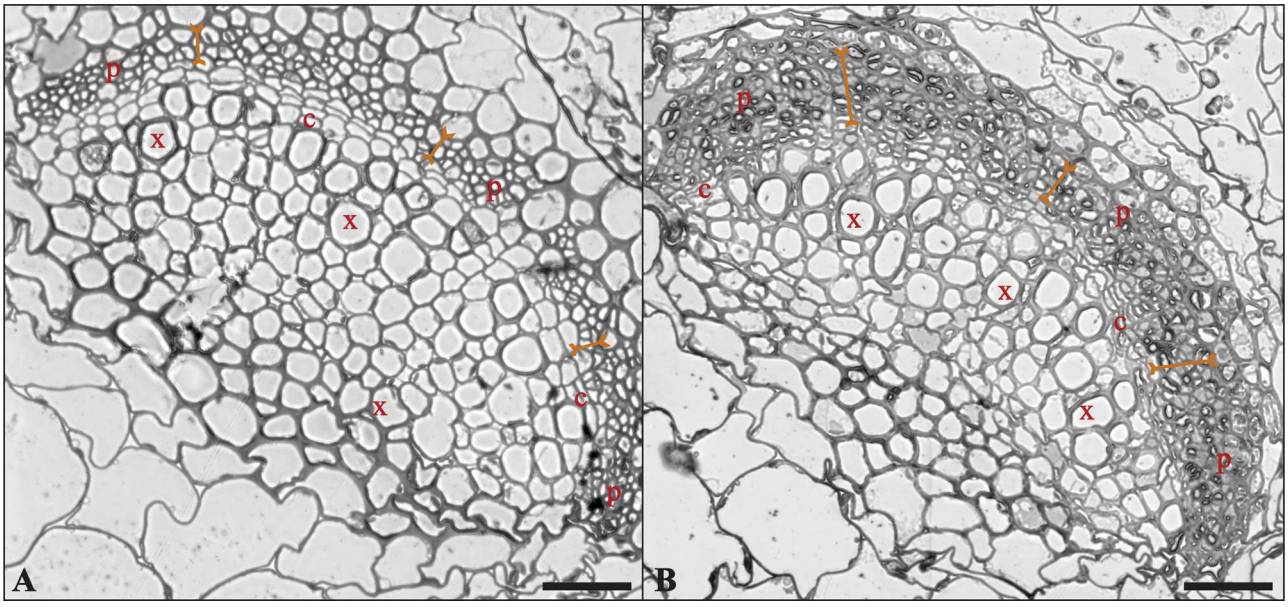

Fig. 2. Semithin sections of midribs from healthy and infected *A. thaliana* plants. (A) In healthy plants vascular bundles have a regular collateral pattern and no cell alteration. (B) In infected leaf tissues many phloem components show plasmolysis, collapse or necrosis. Moreover, massive production of new phloem components causes phloem hyperplasia. Amber segments indicate phloem thickness measuring lines. Bars correspond to 25 μm. c: cambium; p: phloem; x: xylem.

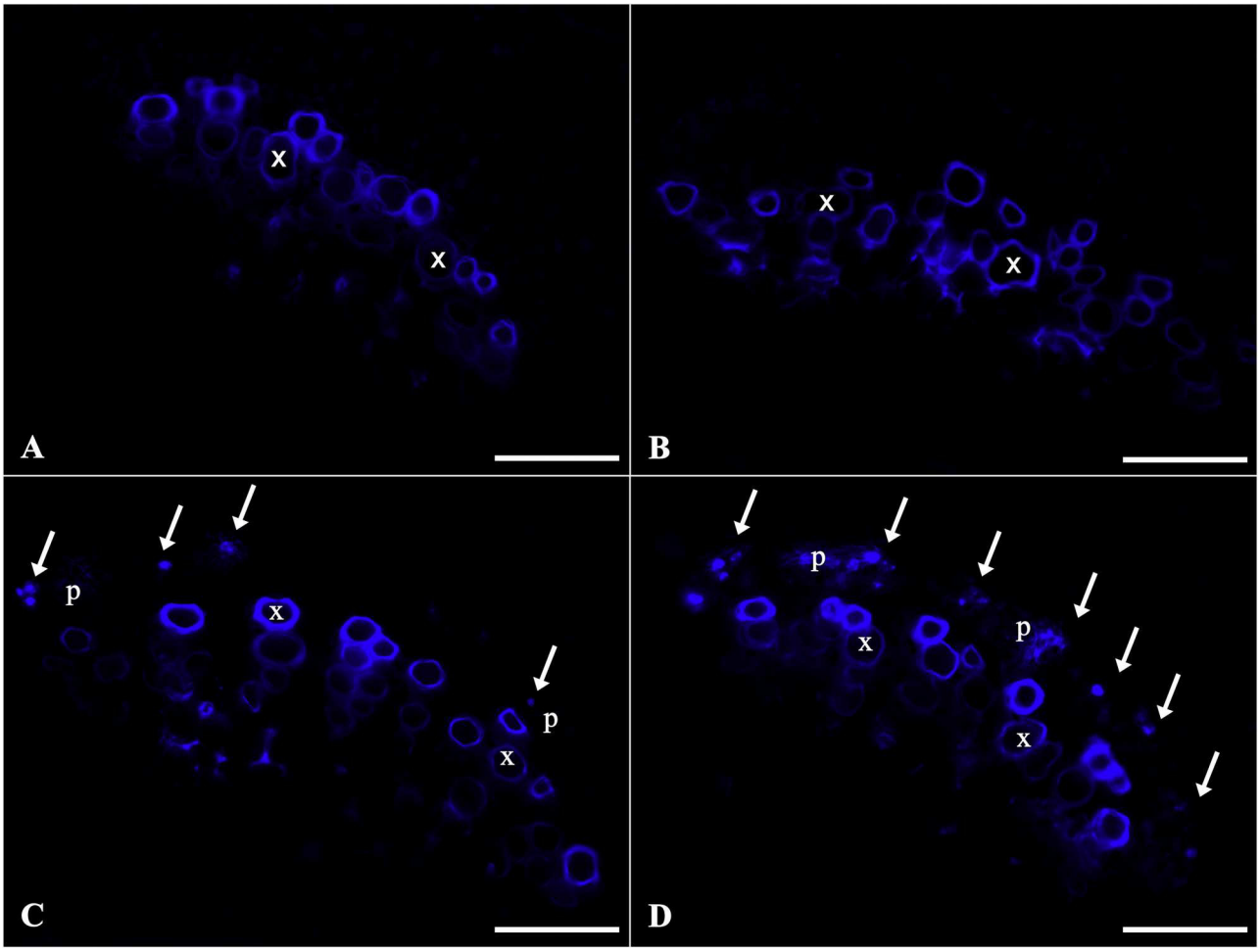

Fig. 3. Epifluorescence images of *A. thaliana* midrib cross-sections. (A) Healthy and (B) infected unstained samples do not emit fluorescence when observed at the same excitation wavelength used for the fluorochrome (405 nm). (C) After aniline blue staining of healthy tissue, fluorescent dots corresponding to the phloem indicate callose deposition (arrows). (D) In infected tissue, intense aniline blue signals reveal consistent callose deposition. Bars correspond to 50 μm. p: phloem; x: xylem. (For interpretation of the references to color in this figure legend, the reader is referred to the web version of this article.)

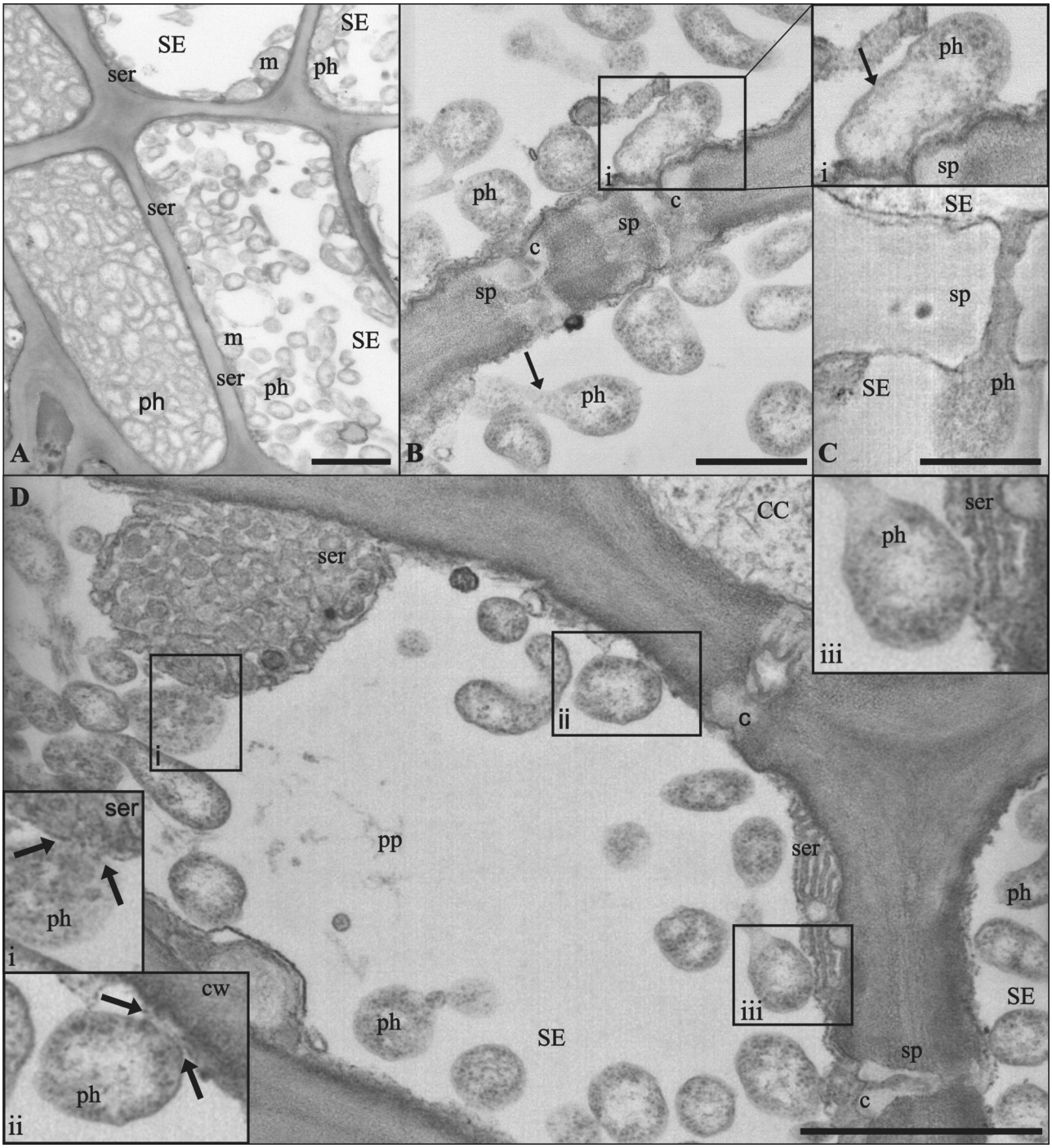

Fig. 4. TEM micrographs showing phytoplasmas in infected SEs. (A) The presence of phytoplasma is consistent, even though the colonization pattern is often uneven. (B). Phytoplasmas show a typical pleomorphic shape, delimited by an electron-dense membrane (inset i, arrow). Many free-floating phytoplasmas divide in SE lumen (arrow) and may spread by passing through sieve pores. (C) Passage through the sieve-pore may involve the narrowing and elongation of the phytoplasmas as observed within the sieve plate. (D) Phytoplasmas adhere to the SE plasma membrane (inset ii) or to SER cisternae (insets i and iii). Contact structures, connecting phytoplasmas with the stacks of SER, are visible (arrows). In (A) and (D) the bars correspond to 1000 nm; in (B) and (C) the bars correspond to 500 nm. c: callose; CC: companion cell; cw: cell wall; ph: phytoplasma; pp: P-protein; sp: sieve pore; SE: sieve element; ser: sieve-element reticulum.

(Fig. 4D, insets i and iii). The SER seemed to have proliferated with an increased number of stacks (Table 3) as well as expansion and deformation of the cisternae (Fig. 4D).

3.4. Plant response at the ultrastructural level

TEM observations confirmed and refined the description of phloem cell morphology obtained by LM observations. In healthy *A. thaliana* plants, SEs and companion cells (CCs) looked well differentiated, with a regular shape and no signs of necrosis or subcellular aberrations (Fig. 5A and B). In mature SEs, small smooth SER and mitochondria were easily visible (Fig. 5F). Dispersed phloem protein (P-protein) filaments were located in the lumen and along the SE plasma membrane (Fig. 5A). Filaments consisted of electron dense strands that could be straight, branched or even organized into thin networks (Fig. 5C). P-proteins had an irregular frequency

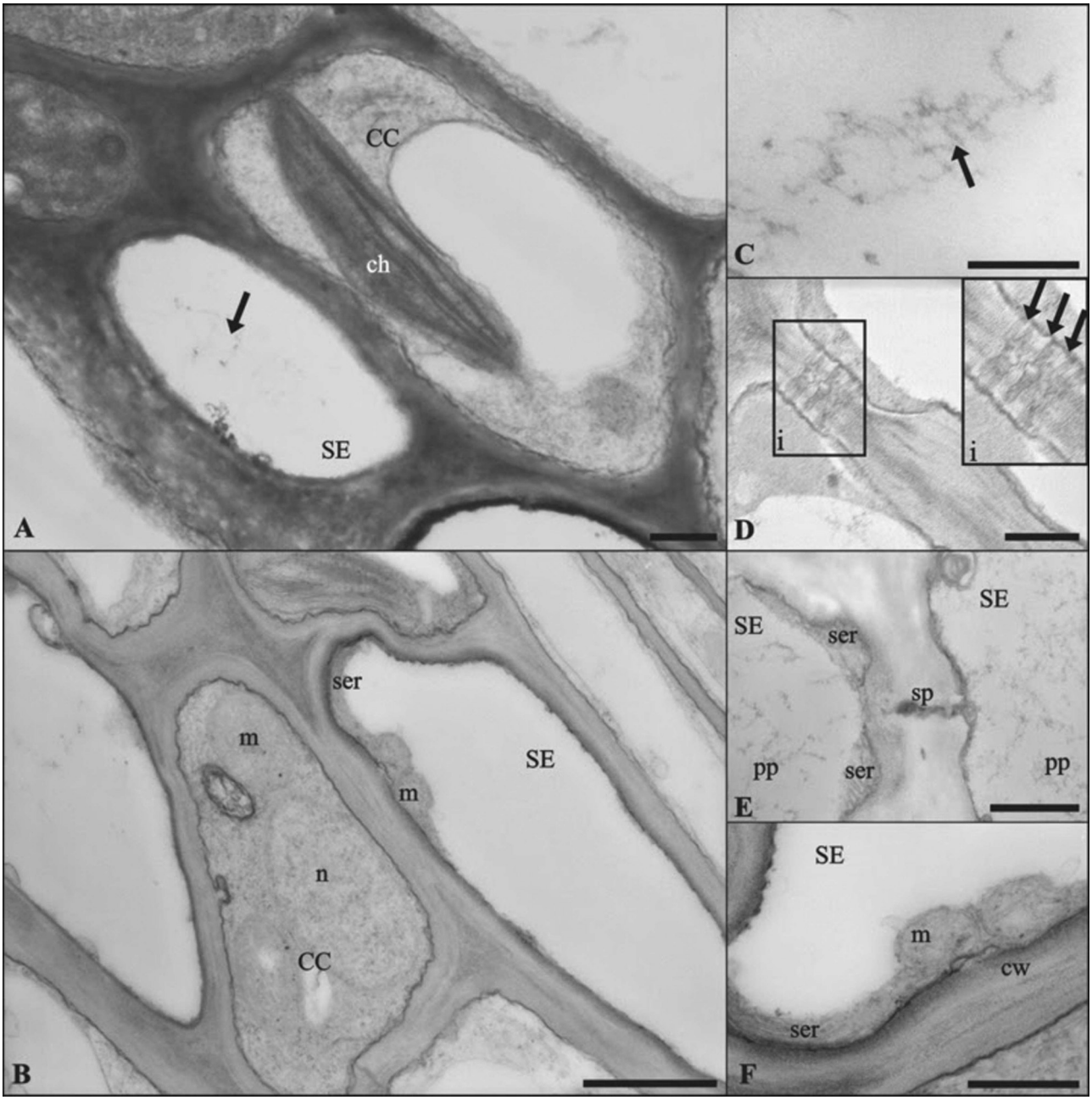

Fig. 5. TEM micrographs of midrib tissue from healthy plants. (A) and (B) Phloem components appear well preserved. Some P-protein filaments (arrow) are visible. (C) P-protein filaments consist of electron dense strands, organized in thin networks (arrow). (D) The plasmodesmata are open and well structured (inset i, arrows). (E) No callose deposits or P-protein plugs surround the sieve pores. (F) Compact cisternae of the SER observed in parietal position. In (A) and (B) the bars correspond to 1000 nm; in (C) the bar corresponds to 300 nm, in (D), (E) and (F) the bars correspond to 500 nm. CC: companion cell; ch: chloroplast; cw: cell wall; m: mitochondrion; n: nucleus; ph: phytoplasma; pp: P-protein; sp: sieve pore; SE: sieve element; ser: sieve-element reticulum.

Table 3
Number of SER stacks per SE in healthy and infected samples.

Fields	SER stacks in healthy samples (±SD)	Fields	SER stacks in infected samples (±SD)
25	1 ± 0.14	25	3 ± 0.10

Fields are defined as the cross sections of five SEs observed in five non-serial sections. Unpaired *t*-test, P-values < 0.0002. SD: standard error.

and density within the SE cells (Fig. 5A–C). Sieve pores and plasmodesmata appeared open and free from callose deposition (Fig. 5D and E).

In infected plants, the presence of new phloem cells and severe ultrastructural disorders of mature cells were observed. Several phloem cells belonging to different phloem components showed electron-dense content or were altered in shape and morphology (Fig. 6A). The plasma membrane of these cells was irregular and often detached from the cell wall, which appeared thick and distorted (Fig. 6A). In many SEs, the SER was expanded along the plasma membrane or into the lumen (Figs. 4D and 6B). An increase in the number of SER stacks per SE was also observed (Fig. 6B; Table 3). The lumen of infected SEs was characterized by a consistent P-protein filament presence, also enveloping phytoplasma cells (Fig. 6C). In contrast to control SEs, P-protein occasionally plugged sieve pores (Fig. 6D). SEs also had considerable callose accumulation mainly at the sieve pores (Figs. 4B and D; 6D and E). Callose was occasionally detected at the PPUs (Figs. 4D and

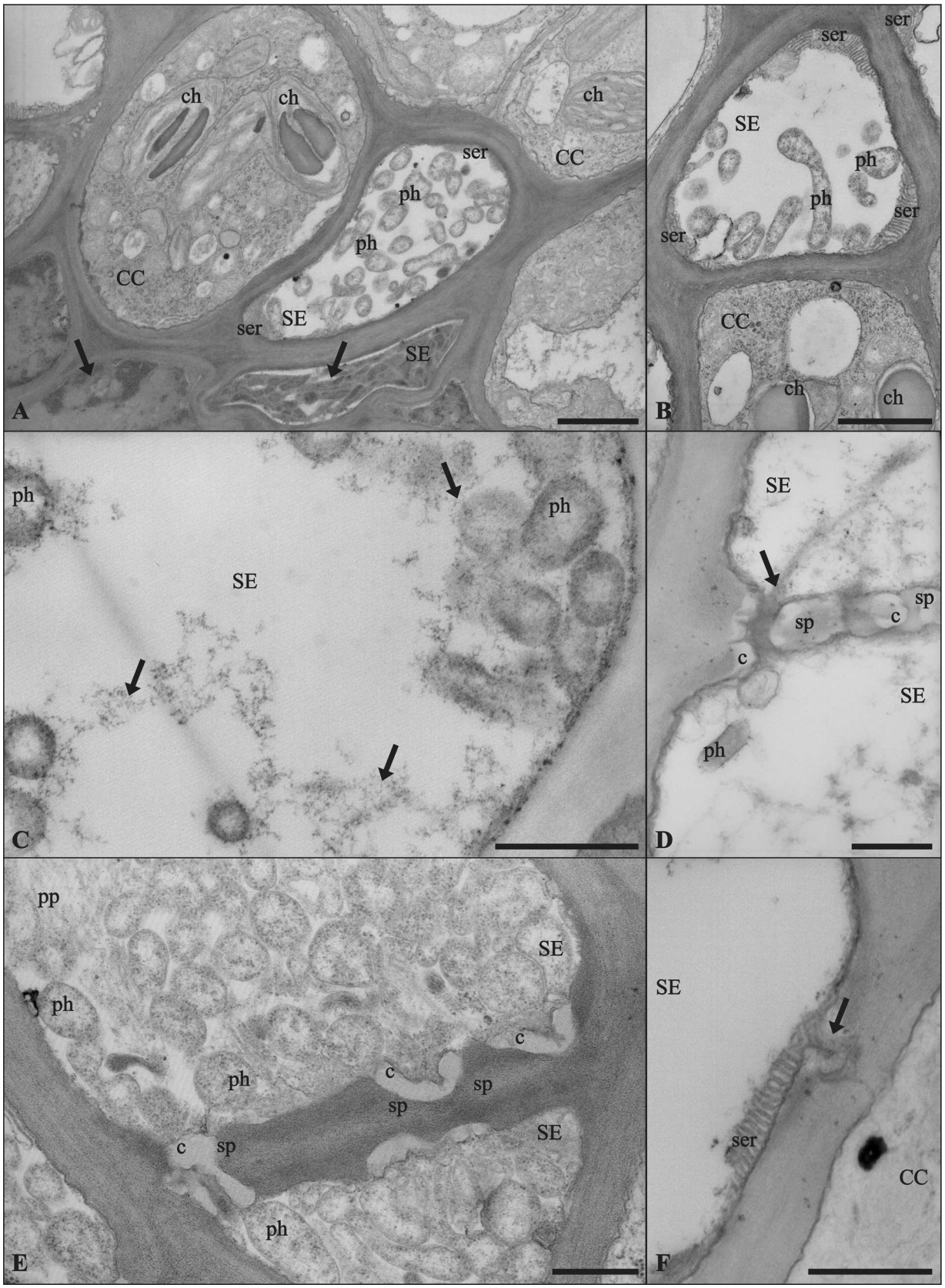

Fig. 6. TEM micrographs of midrib tissue from infected plants. (A) Several phloem components present alterations in shape and morphology (arrows). Chloroplasts in companion cells show various degrees of swelling and large starch grains provoke a distortion of the thylakoid membrane system. (B) The presence of phytoplasma is associated with SER stack proliferation and (C) P-protein filament agglutination (arrows). (D) Sieve pores are narrowed or obstructed by P-protein agglutination (arrow) and (E) callose deposits. (F) PPUs are generally not affected by callose deposition (arrow). In (A) and (F) the bars correspond to 1000 nm; in (B), (C), (D) and (F) the bars correspond to 500 nm. c: callose; CC: companion cell; ch: chloroplast; ph: phytoplasma; pp: P-protein; sp: sieve pore; SE: sieve element; ser: sieve-element reticulum.

6F), apparently without occluding them. No callose deposits were detected in other phloem components or in other leaf tissues.

CC ultrastructure seemed generally well preserved. In contrast with chloroplasts in control plants (Fig. 5A), those in infected tissues had lost their typical elongated shape, presenting various degrees of swelling (Fig. 6A and B). Large starch grains occupied a significant amount of the chloroplast profile and were accompanied by a distortion of the thylakoid membrane system. This modification was also associated with the disorganization of the parallel pattern of the lamellae and a reduction in the grana (Fig. 6A).

4. Discussion

As previously described by different authors (Bressan and Purcell, 2005; Cettul and Firrao, 2011; Hogenhout and Music, 2010; Hoshi et al., 2009; MacLean et al., 2011), at the macroscopic level, infected *A. thaliana* manifested classic phytoplasma-disease symptoms without suffering a rapid decline. Stunted and yellowed plants were indicative of strong disturbance of phloem functions (Maust et al., 2003), while auxilary shoot proliferation and flower abnormalities, such as virescence and phyllody, suggested disturbances in the normal balance of plant hormones (Bertaccini et al., 2014).

The presence of typical phytoplasma-disease symptoms matched with an easily detectable phytoplasma presence, using both molecular and microscopy diagnostic tools. In fact, in contrast to natural woody host plants, it was not necessary to set up any particular DNA extraction protocol for phytoplasma enrichment, PCR assay did not require nested steps and TEM observations immediately led to phytoplasma visualization. The ease of detection is also characteristic of other herbaceous plants used to study phytoplasma-plant interactions, such as *Catharanthus roseus* (Musetti et al., 2011) or *Solanum lycopersicum* (Buxa et al., 2015). Nevertheless, *A. thaliana* has emerged in the last thirty years as model system for research in plant biology. The Arabidopsis genome was the first plant genome to be completely sequenced, the functions of many genes have been identified and mutants can be obtained easily, by transformation process or, when available, by request to stock centres, open to the scientific community (Koornneef and Meinke, 2010). For these reasons, the choice of Arabidopsis as a model for experiments in plant pathology could benefit from the large body of existing physiological data on this species and provide a novel contribution to the Arabidopsis research community.

The extensive TEM observations and the phytoplasma abundance in infected SEs reinforced the hypothesis about diverse sites of interaction in phytoplasma-infected SEs, as recently described in tomato (Musetti et al., 2016). In fact, as in tomato, an “adhesion structure” that joined the phytoplasmas and SE plasma membrane was highly visible in Arabidopsis. Concerning the SER, in addition to the stack deformation and proliferation described previously (Buxa et al., 2015; Musetti et al., 2016), a contact structure connecting the phytoplasma membrane and SER cisternae has been described here for the first time. Connection structures, joining the bacterial surface with the endoplasmic reticulum have been reported in pathogenic endocellular bacteria, with the function of acquiring proteins from the host (Kagan et al., 2004; Tilney et al., 2001). The finding of SER-phytoplasma contact structures supports the hypothesis of a role of SER in phytoplasma nutrition (Musetti et al., 2016). The increase in the number of SER stacks reported in infected SEs could be a consequence of this nutritional interaction (Musetti et al., 2016).

Phytoplasma multiplication and spread was documented by the presence of dividing phytoplasma cells and their presence inside sieve pores, suggesting passage from one cell to another, which was easily observed in Arabidopsis leaf tissue.

Regarding the plant response to CY phytoplasma, necrosis and altered cell morphology were visualized in infected plants by LM and TEM; these observations matched evidence known from other phytoplasma-infected plants (Buxa et al., 2015; Kartte and Seemüller, 1991; Musetti, 2010; Rudzinska-Langwald and Kaminska, 2001). In fact, modifications in cell wall structure and morphology were observed in other phytoplasma hosts (Kaminska et al., 2001; Musetti et al., 2013; Santi et al., 2013) and are supposedly formed by calcium-dependent phenolic depositions (Messiaen et al., 1993). Necrotized cells were sometimes detected in Arabidopsis phloem tissue and the presence of dead cells was balanced by excessive procambial or cambial activity, leading to phloem hyperplasia, as reported in many phytoplasma-plant interactions (Braun and Sinclair, 1976, 1979; Garcion et al., 2014; Iriti et al., 2008; Oshima et al., 2001; Schneider, 1977; Uehara et al., 1999). New phloem cells did not look smaller, but the cell lumens appeared restricted by cell wall thickening. In fact, following infection, phloem cell layers roughly doubled and the tissue thickness showed the same trend. Hyperplasia may be explained as a plant response to limited phloem functionality (Oshima et al., 2001) or as a result of pathogen effector action (Bai et al., 2009; Sugio et al., 2011).

P-protein agglutination and callose deposition, observed in infected SEs of *A. thaliana* have been previously described in different plant/phytoplasma interactions (Gamalero et al., 2010; Lherminier et al., 2003; Luna et al., 2011; Musetti et al., 2010, 2013). P-proteins filaments, constituted by heterogeneous subunits dispersed in SE lumina of most angiosperms (Ernst et al., 2012; Knoblauch et al., 1998), clump during abiotic and biotic stresses (Batailler et al., 2012; Knoblauch et al., 2001; Musetti et al., 2013; van Bel et al., 2014). In infected *A. thaliana* plants, P-protein agglutination led to SE lumen filling and sieve-pore plugging. This phenomenon is interpreted as a fast and straightforward plant response to physically limit pathogen spread (Lherminier et al., 2003; Musetti et al., 2010, 2013), and might be associated with the activation of systemic-defence processes connected to P-protein-mediated long-distance signalling (Read and Northcote, 1983; van Bel, 2003).

While P-protein clumping is an immediate and reversible process, callose deposition is a long-term plant response to phytoplasma infection (Braun and Sinclair, 1976; Gamalero et al., 2010; Leljak-Levanić et al., 2010; Musetti et al., 2010). Even though callose synthesis occurs during basic developmental processes in plant tissues (Barratt et al., 2011; Xie et al., 2011), the local deposition of callose is induced only by stress (Jacobs et al., 2003; Nishimura et al., 2003). Fluorescence microscopy observations showed an evident increase in aniline blue signal in infected compared to healthy phloem. In infected *A. thaliana* plants, callose deposits localized by TEM mainly occurred at the sieve plates and rarely at the PPUs. According to our observations, in full-symptomatic *A. thaliana*, callose occlusion at the sieve pores could be sufficient to limit phytoplasma passage and their spread through the vascular system (Braun and Sinclair, 1976; Lherminier et al., 2003; Musetti et al., 2013). However, it would seem counterproductive to completely isolate the SEs from each other and from CCs, as previously reported by Froelich et al. (2011) in healthy-uninjured Arabidopsis tissues. It is worth noting that for phytoplasmas, as biotrophic pathogens, it would be important to ensure permanent metabolic and energetic support from the SE-CC complex.

In different species of wounded or pathogen-infected plants, P–proteins and callose masses are reported to stop or at least decrease the translocation of photosynthetic products (Braun and Sinclair, 1978; Ernst et al., 2012; Guthrie et al., 2001; Kartte and Seemüller, 1991; Lepka et al., 1999). As a consequence, photoassimilates accumulate in chloroplasts, mainly as starch deposits, and lead to a consistent disorganization of thylakoids (Braun and

Sinclair, 1978; Junqueira et al., 2004; Maust et al., 2003; Musetti et al., 2010). Dealing with phloem mass-flow reduction, it is not clear if the same principles are applicable to *A. thaliana* (Froelich et al., 2011; Knoblauch et al., 2014; Jekat et al., 2013). Nevertheless, TEM observations of infected *A. thaliana* plants revealed alteration in chloroplast ultrastructure due to starch accumulation, suggesting phloem impairment.

5. Conclusions

Our work demonstrated that *A. thaliana* is a reliable plant model for studying phytoplasma-plant interactions at macroscopical and ultramicroscopical level. Phytoplasma-infected *A. thaliana* exhibited characteristic symptoms of phytoplasma infection, presenting the main morphological and ultrastructural changes reported in various phytoplasma natural hosts. The high phytoplasma abundance in infected SEs allowed an easy detection and the minute study of phytoplasma interaction with diverse SE organelles. For the first time, a contact structure connecting phytoplasma membrane and SER cisternae has been described. The possible use of transformed Arabidopsis plants may enable quick progress in elucidating the molecular bases of plant-phytoplasma interactions.

Acknowledgments

Authors kindly thank Professor Domenico Bosco (University of Torino, Italy) for having provided the Chrysanthemum yellows (CY) phytoplasma strain and for his precious advice about insect rearing. The authors are grateful to Dr. Laurence Cantrill (Out of Site English, Sydney) for the English revision. This work was supported by the University of Udine.

References

Bacci, S., Pieri, L., Buccoliero, A.M., Bonelli, A., Taddei, G., Romagnoli, P., 2008. Smooth muscle cells, dendritic cells and mast cells are sources of TNFalpha and nitric oxide in human carotid artery atherosclerosis. Thromb. Res. 122 (5), 657–667, http://dx.doi.org/10.1016/j.thromres.2008.04.013.

Bai, X., Zhang, J., Ewing, A., Miller, S.A., Jancso Radek, A., Shevchenko, D.V., Tsukerman, K., Walunas, T., Lapidus, A., Campbell, J.W., Hogenhout, S.A., 2006. Living with genome instability: the adaptation of phytoplasmas to diverse environments of their insect and plant hosts. J. Bacteriol. 18, 3682–3696, http://dx.doi.org/10.1128/JB.188.10.3682-3696.2006.

Bai, X., Correa, V.R., Toruño, T.Y., Ammar, E.D., Kamoun, S., Hogenhout, S.A., 2009. AY-WB phytoplasma secretes a protein that targets plant cell nuclei. Mol. Plant Microbe Interact. 22, 18–30, http://dx.doi.org/10.1094/MPMI-22-1-0018.

Bamunusinghe, D., Sanderfoot, A.A., Ye, C.M., Silva, M.A., Payton, M., Verchot-Lubicz, J., 2009. Analysis of potato virus X replicase and TGBp3 subcellular locations. Virology 393, 272–285, http://dx.doi.org/10.1016/j.virol.2009.08.002.

Barratt, D.H., Kölling, K., Graf, A., Pike, M., Calder, G., Findlay, K., Zeeman, S.C., Smith, A.M., 2011. Callose synthase GSL7 is necessary for normal phloem transport and inflorescence growth in Arabidopsis. Plant Physiol. 155, 328–341, http://dx.doi.org/10.1104/pp.110.166330.

Batailler, B., Lemaitre, T., Vilaine, F., Sanchez, C., Renard, D., Cayla, T., Beneteau, J., Dinant, S., 2012. Soluble and filamentous proteins in Arabidopsis sieve elements. Plant Cell Environ. 35 (7), 1258–1273, http://dx.doi.org/10.1111/j.1365-3040.2012.02487.x.

Bertaccini, A., Duduk, B., 2010. Phytoplasma and phytoplasma diseases: a review of recent research. Phytopathol. Mediterr. 48 (3), 355–378, http://dx.doi.org/10.14601/Phytopathol_Mediterr-3300.

Bertaccini, A., Duduk, B., Paltrinieri, S., Contaldo, N., 2014. Phytoplasmas and phytoplasma diseases: a severe threat to agriculture. Am. J. Plant Sci. 5, 1763–1788, http://dx.doi.org/10.4236/ajps.2014.512191.

Bertamini, M., Nedunchezhian, N., Tomasi, F., Grando, M.S., 2002. Phytoplasma [Stolbur-subgroup (Bois Noir- BN)] infection inhibits photosynthetic pigments, ribulose-1,5-bisphosphate carboxylase and photosynthetic activities in field grown grapevine (*Vitis vinifera* L. cv Chardonnay) leaves. Physiol. Mol. Plant Pathol. 61, 357–366, http://dx.doi.org/10.1006/pmpp.2003.0449.

Bosco, D., Minucci, C., Boccardo, G., Conti, M., 1997. Differential acquisition of chrysanthemum yellows phytoplasma by three leafhopper species. Entomol. Exp. Appl. 83, 219–224, http://dx.doi.org/10.1046/j.1570-7458.1997.00175.x.

Boyes, D.C., Zayed, A.M., Ascenzi, R., McCaskill, A.J., Hoffman, N.E., Davis, K.R., Görlach, J., 2001. Growth stage—based phenotypic analysis of Arabidopsis a model for high throughput functional genomics in plants. Plant Cell 13 (7), 1499–1510, 10. 1105/ TPC.010011.

Braun, E.J., Sinclair, W.A., 1976. Histopathology of phloem necrosis in *Ulmus americana*. Phytopathology 66, 598–607, http://dx.doi.org/10.1094/Phyto-66-598.

Braun, E.J., Sinclair, W.A., 1978. Translocation in phloem necrosis-diseased American elm seedlings. Phytopathology 68, 1733–1737, http://dx.doi.org/10.1094/Phyto-68-1733.

Braun, E.J., Sinclair, W.A., 1979. Phloem necrosis of elms: symptoms and histopathological observations in tolerant hosts. Phytopathology 66, 598–607, http://dx.doi.org/10.1094/Phyto-69-354.

Bressan, A., Purcell, A.H., 2005. Effect of benzothiadiazole on transmission of X-disease phytoplasma by the vector *Colladonus montanus* to *Arabidopsis thaliana*, a new experimental host plant. Plant Dis. 89, 1121–1124, http://dx.doi.org/10.1094/PD-89-1121.

Buxa, S.V., Degola, F., Polizzotto, R., De Marco, F., Loschi, A., Kogel, K.-H., Sanità di Toppi, L., van Bel, A.J.E., Musetti, R., 2015. Phytoplasma infection in tomato is associated with re-organization of plasma membrane ER stacks, and actin filaments in sieve elements. Front. Plant Sci. 6, 650, http://dx.doi.org/10.3389/fpls.2015.00650.

Cettul, E., Firrao, G., 2011. Development of phytoplasma-induced flower symptoms in *Arabidopsis thaliana*. Physiol. Mol. Plant Pathol. 76, 204–211, http://dx.doi.org/10.1016/j.pmpp.2011.09.001.

Contaldo, N., Bertaccini, A., Paltrinieri, S., Windsor, H.M., Windsor, G.D., 2012. Axenic culture of plant pathogenic phytoplasmas. Phytopathol. Mediterr. 51, 607–617, http://dx.doi.org/10.14601/Phytopathol_Mediterr-11773.

De Marco, F., Pagliari, L., Degola, F., Buxa, S.V., Loschi, A., Dinant, S., Le Hir, R., Morin, H., Santi, S., Musetti, R., 2016. J. Microsc. Phloem occlusions and cell wall modifications in tomato leaves in response to 'Candidatus Phytoplasma solani', http://dx.doi.org/10.1111/jmi.12426, in press.

Doi, Y., Teranaka, M., Yora, K., Asuyama, H., 1967. Mycoplasma- or PLT group-like microorganisms found in the phloem elements of plants infected with mulberry dwarf, potato witches 'broom, aster yellows or paulownia witches' broom. Ann. Phytopathol. Soc. Jpn. 33, 259–266, http://dx.doi.org/10.3186/jjphytopath.33.259.

Doyle, J.J., Doyle, J.L., 1990. Isolation of plant DNA from fresh tissue. Focus 12, 13–15.

Ehlers, K., Knoblauch, M., van Bel, A.J.E., 2000. Ultrastructural features of well-preserved and injured sieve elements: minute clamps keep the phloem transport conduits free for mass flow. Protoplasma 214, 80–92, http://dx.doi.org/10.1007/BF02524265.

Ernst, A.M., Jekat, S.B., Zielonka, S., Muller, B., Neumann, U., Ruping, B., Twyman, R.M., Krzyzanek, V., Prufer, D., Noll, G.A., 2012. Sieve element occlusion (SEO) genes encode structural phloem proteins involved in wound sealing of the phloem. Proc. Natl. Acad. Sci. U. S. A. 109, E1980–E1989, http://dx.doi.org/10.1073/pnas.1202999109.

Froelich, D.R., Mullendore, D.L., Jensen, K.H., Ross-Elliott, T.J., Anstead, J.A., Thompson, G.A., Pélissier, H.C., Knoblauch, M., 2011. Phloem ultrastructure and pressure flow: sieve-element-occlusion-related agglomerations do not affect translocation. Plant Cell 23 (12), 4428–4445, http://dx.doi.org/10.1105/tpc.111.093179.

Gamalero, E., D'Amelio, R., Musso, C., Cantamessa, S., Pivato, B., D'Agostino, G., Duan, J., Bosco, D., Marzachì, C., Berta, G., 2010. Effects of Pseudomonas putida S1Pf1Rif against chrysanthemum yellows phytoplasma infection. Phytopathology 100 (8), 805–813, http://dx.doi.org/10.1094/PHYTO-100-8-0805.

Garcion, C., Eveillard, S., Renaudin, J., 2014. Characterisation of the tolerance to the beet leafhopper transmitted virescence agent phytoplasma in the PI128655 accession of Solanum peruvianum. Ann. Appl. Biol. 165 (2), 236–248, http://dx.doi.org/10.1111/aab.12131.

Gundersen, D.E., Lee, I.M., 1996. Ultrasensitive detection of phytoplasmas by nested-PCR assays using two universal primer pairs. Phytopathol. Mediterr. 35, 144–151.

Guthrie, J.N., Walsh, K.B., Scott, P.T., Rasmussen, T.S., 2001. The phytopathology of Australian papaya dieback: a proposed role for the phytoplasma. Physiol. Mol. Plant Pathol. 58, 23–30, http://dx.doi.org/10.1006/pmpp.2000.0311.

Hogenhout, S.A., Music, M., 2010. Phytoplasma genomics, from sequencing to comparative and functional genomics: what have we learnt? In: Weintraub, P.G., Jones, P. (Eds.), Phytoplasmas: Genomes, Plant Hosts and Vectors. CABI, Wallingford, UK, pp. 19–36.

Hogenhout, S.A., Oshima, K., Ammar, el-D., Kakizawa, S., Kingdom, H.N., Namba, S., 2008. Phytoplasmas: bacteria that manipulate plants and insects. Mol. Plant Pathol. 9 (4), 403–423, http://dx.doi.org/10.1111/j.1364-3703.2008.00472.x.

Hoshi, A., Oshima, K., Kakizawa, S., Ishii, Y., Ozeki, J., Hashimoto, M., Komatsu, K., Kagiwada, S., Yamaji, Y., Namba, S., 2009. A unique virulence factor for proliferation and dwarfism in plants identified from a phytopathogenic bacterium. Proc. Natl. Acad. Sci. U. S. A. 106, 6416–6421, http://dx.doi.org/10.1073/pnas.0813038106.

Iriti, M., Quaglino, F., Maffi, D., Casati, P., Bianco, P.A., Faoro, F., 2008. Solanum malacoxylon, a new natural host for Stolbur phytoplasma. J. Phytopathol. 156, 8–14, http://dx.doi.org/10.1111/j.1439-0434.2007.01311.x.

Jacobs, A.K., Lipka, V., Burton, R.A., Panstruga, R., Strizhov, N., Schulze-Lefert, P., Fincher, G.B., 2003. An Arabidopsis callose synthase GSL5, is required for wound and papillary callose formation. Plant Cell 15, 2503–2513, http://dx.doi.org/10.1105/tpc.016097.

Jekat, S.B., Ernst, A.M., von Bohl, A., Zielonka, S., Twyman, R.M., Noll, G.A., Prüfer, D., 2013. P-proteins in *Arabidopsis* are heteromeric structures involved in rapid sieve tube sealing. Front. Plant Sci. 4, 225, http://dx.doi.org/10.3389/fpls.2013.00225.

Junqueira, A., Bedendo, I., Pascholati, S., 2004. Biochemical changes in corn plants infected by the maize bushy stunt phytoplasma. Physiol. Mol. Plant Pathol. 65, 181–185, http://dx.doi.org/10.1016/j.pmpp.2005.01.005.

Kagan, J.C., Stein, M.P., Pypaert, M., Roy, C.R., 2004. Legionella subvert the functions of rab1 and sec22b to create a replicative organelle. J. Exp. Med. 199, 1201–1211, http://dx.doi.org/10.1084/jem.20031706.

Kaminska, M., Dziekanowska, D., Rudzinska-Langwald, A., 2001. Detection of phytoplasma infection in rose, with degeneration symptoms. J. Phytopathol. 149, 3–10, http://dx.doi.org/10.1046/j.1439-0434.2001.00554.x.

Kartte, S., Seemüller, E., 1991. Histopathology of apple proliferation in Malus taxa and hybrids of different susceptibility. J. Phytopathol. 131, 149–160, http://dx.doi.org/10.1111/j.1439-0434.1991.tb04740.x.

Knoblauch, M., van Bel, A.J.E., 1998. Sieve tubes in action. Plant Cell 13, 35–50, http://dx.doi.org/10.1105/tpc.10.1.35.

Knoblauch, M., Peters, W.S., Ehlers, K., van Bel, A.J.E., 2001. Reversible calcium-regulated stopcocks in legume sieve tubes. Plant Cell 13, 1221–1230, http://dx.doi.org/10.2307/3871375.

Knoblauch, M., Froelich, D.R., Pickard, W.F., Peters, W.S., 2014. SEORious business: structural proteins in sieve tubes and their involvement in sieve element occlusion. J. Exp. Bot. 65 (7), 1879–1893, http://dx.doi.org/10.1093/jxb/eru071.

Koornneef, M., Meinke, D., 2010. The development of Arabidopsis as a model plant. Plant J. 61, 909–921, http://dx.doi.org/10.1111/j.1365-313X.2009.04086.x.

Lee, I.M., Davis, R.E., Gundersen-Rindal, D.E., 2000. Phytoplasma: phytopathogenic mollicutes. Annu. Rev. Microbiol. 54, 221–255, http://dx.doi.org/10.1146/annurev.micro.54.1.221.

Lee, I.M., Gundersen-Rindal, D.E., Davis, R.E., Bottner, K.D., Marcone, C., Seemuller, E., 2004. 'Candidatus Phytoplasma asteris' a novel phytoplasma taxon associated with aster yellow and related disease. Int. J. Syst. Evol. Microbiol. 54, 1037–1048, http://dx.doi.org/10.1099/ijs.0.02843-0.

Lee, J.Y., Wang, X., Cui, W., Sager, R., Modla, S., Czymmek, K., Zybaliov, B., van Wijk, K., Zhang, C., Lu, H., Lakshmanan, V., 2011. A plasmodesmata-localized protein mediates crosstalk between cell-to-cell communication and innate immunity in Arabidopsis. Plant Cell 23 (9), 3353–3373, http://dx.doi.org/10.1105/tpc.111.087742.

Leljak-Levanić, D., Ježić, M., Cesar, V., Ludwig-Müller, J., Lepeduš, H., Mladinić, M., Katić, M., Ćurković-Perica, M., 2010. Biochemical and epigenetic changes in phytoplasmaćrecovered periwinkle after indole-3-butyric acid treatment. J. Appl. Microbiol. 109 (6), 2069–2078, http://dx.doi.org/10.1111/j.1365-2672.2010.04837.x.

Lepka, P., Stitt, M., Moll, E., Seemüller, E., 1999. Effect of phytoplasmal infection on concentration and translocation of carbohydrates and amino acids in periwinkle and tobacco. Physiol. Mol. Plant Pathol. 55, 59–68, http://dx.doi.org/10.1006/pmpp.1999.0202.

Lherminier, J., Benhamou, N., Larrue, J., Milat, M.L., Boudon-Padieu, E., Nicole, M., Blein, J.P., 2003. Cytological characterization of elicitin-induced protection in tobacco plants infected by *Phytophthora parasitica* or phytoplasma. Phytopathology 93 (10), 1308–1319, http://dx.doi.org/10.1094/PHYTO.2003.93.10.1308.

Luna, E., Pastor, V., Robert, J., Flors, V., Mauch-Mani, B., Ton, J., 2011. Callose deposition: a multifaceted plant defense response. Mol. Plant Microbe Interact. 24, 183–193, http://dx.doi.org/10.1094/MPMI-07-10-0149.

MacLean, A.M., Sugio, A., Kingdom, H.N., Grieve, V.M., Hogenhout, S.A., 2011. *Arabidopsis thaliana* as a model plant for understanding phytoplasma interactions with plant and insect hosts. Bull. Insectol. 64, 173–174.

Marcone, C., Lee, I.M., Davis, R.E., Ragozzino, A., Seemüller, E., 2000. Classification of aster yellows-group phytoplasmas based on combined analyses of rRNA and tuf gene sequences. Int. J. Syst. Evol. Microbiol. 50 (5), 1703–1713, http://dx.doi.org/10.1099/00207713-50-5-1703.

Marcone, C., Guerra, L.J., Uyemoto, J.K., 2014. Phytoplasmal diseases of peach and associated phytoplasma taxa. J. Plant Pathol. 96 (1), 15–28, http://dx.doi.org/10.4454/JPP.V96I1.004.

Martini, M., Musetti, R., Grisan, S., Poliziotto, R., Borselli, S., Pavan, F., Osler, R., 2009. DNA-dependent detection of the grapevine fungal endophytes aureobasidium pullulans and epicoccum nigrum. Plant Dis. 93, 993–998, http://dx.doi.org/10.1094/PDIS-93-10-0993.

Maust, B.E., Espadas, F., Talavera, C., Aguilar, M., Santamaria, J.M., Oropeza, C., 2003. Changes in carbohydrate metabolism in coconut palms infected with the lethal yellowing phytoplasma. Phytopathology 93, 976–981, http://dx.doi.org/10.1094/PHYTO.;1;2003.93.8.976.

Messiaen, J., Read, N.D., van Cutsem, P., Trewavas, A.J., 1993. Cell wall oligogalacturonides increase cytosolic free calcium in carrot protoplasts. J. Cell Sci. 104, 365–371.

Musetti, R., Paolacci, A., Ciaffi, M., Tanzarella, O.A., Polizzotto, R., Tubaro, F., Mizzau, M., Ermacora, P., Badiani, M., Osler, R., 2010. Phloem cytochemical modification and gene expression following the recovery of apple plants from apple proliferation disease. Phytopathology 100, 390–399, http://dx.doi.org/10.1094/PHYTO-100-4-0390.

Musetti, R., Grisan, S., Polizzotto, R., Martini, M., Paduano, C., Osler, R., 2011. Interactions between '*Candidatus* Phytoplasma mali' and the apple endophyte *Epicoccum nigrum* in *Catharanthus roseus* plants. J. Appl. Microbiol. 110, 746–756, http://dx.doi.org/10.1111/j.1365-2672.2011.04937.x.

Musetti, R., Buxa, S.V., De Marco, F., Loschi, A., Polizzotto, R., Kogel, K.H., van Bel, A.J.E., 2013. Phytoplasma-triggered Ca2+ influx is involved in sieve-tube blockage. Mol. Plant Microbe Interact. 26, 379–386, http://dx.doi.org/10.1094/MPMI-08-12-0207-R.

Musetti, R., Pagliari, L., Buxa, S.V., Degola, F., De Marco, F., Loschi, A., Kogel, K.H., van Bel, A.J.E., 2016. OHMS**: Phytoplasmas dictate changes in sieve-element ultrastructure to accommodate their requirements for nutrition, multiplication and translocation. Plant Signal. Behav. 11 (2), e1138191, http://dx.doi.org/10.1080/15592324.2016.1138191.

Musetti, R., 2010. Biochemical changes in plants infected by phytoplasmas. In: Weintraub, P.G., Jones, P. (Eds.), Phytoplasmas: Genomes, Plant Hosts and Vectors. CAB International, Wallingford, Oxfordshire, UK, pp. 114–131.

Nishimura, M.T., Stein, M., Hou, B.H., Vogel, J.P., Edwards, H., Somerville, S.C., 2003. Loss of a callose synthase results in salicylic acid-dependent disease resistance. Science 301, 969–972, http://dx.doi.org/10.1126/science.1086716.

Oshima, K., Shiomi, T., Kuboyama, T., Sawayanagi, T., Nishigawa, H., Kakizawa, S., Miyata, S., Ugaki, M., Namba, S., 2001. Isolation and characterization of derivative lines of the onion yellows phytoplasma that do not cause stunting or phloem hyperplasia. Phytopathology 91, 1024–1029, http://dx.doi.org/10.1094/PHYTO.2001.91.11.1024.

Oshima, K., Kakizawa, S., Nishigawa, H., Jung, H.Y., Wei, W., Suzuki, S., Arashida, R., Nakata, D., Miyata, S., Ugaki, M., Namba, S., 2004. Reductive evolution suggested from the complete genome sequence of a plant-pathogenic phytoplasma. Nat. Genet. 36, 27–29, http://dx.doi.org/10.1038/ng1277.

Read, S.M., Northcote, D.H., 1983. Chemical and immunological similarities between the phloem proteins of three genera of the Cucurbitaceae. Planta 158, 119–127, http://dx.doi.org/10.1007/BF00397704.

Reynolds, E.S., 1963. The use of lead citrate at high pH as an electronopaque stain for electron microscopy. J. Cell Biol. 17, 208, http://dx.doi.org/10.1083/jcb.17.1.208.

Rudzinska-Langwald, A., Kaminska, M., 2001. Ultrastructural change in aster yellows phytoplasma affected Limonium sinuatum Mill. Plants. I. Pathology of conducting tissues. Acta Soc. Bot. Pol. 70 (3), 173–180, http://dx.doi.org/10.5586/asbp.2001.022.

Sugio, A., MacLean, A.M., Grieve, V.M., Hogenhout, S.A., 2011. Phytoplasma protein effector SAP11 enhances insect vector reproduction by manipulating plant development and defense hormone biosynthesis. Proc. Nat. Acad. Sci. 108 (48), E1254–E1263, http://dx.doi.org/10.1073/pnas.1105664108.

Santi, S., Grisan, S., Pierasco, A., De Marco, F., Musetti, R., 2013. Laser microdissection of grapevine leaf phloem infected by stolbur reveals site-specific gene responses associated to sucrose transport and metabolism. Plant Cell Environ. 36 (2), 343–355, http://dx.doi.org/10.1111/j.1365-3040.2012.02577.x.

Schneider, H., 1977. Indicator hosts for pear decline: symptomatology, histopathology, and distribution of mycoplasma-like organisms in leaf veins. Phytopathology 67, 592–601, http://dx.doi.org/10.1094/Phyto-67-592.

Tilney, L.G., Harb, O.S., Connelly, P.S., Robinson, C.G., Roy, C.R., 2001. How the parasitic bacterium Legionella pneumophila modifies its phagosome and transforms it into rough ER: implications for conversion of plasma membrane to the ER membrane. J. Cell Sci. 114, 4637–4650.

Uehara, T., Tanaka, M., Shiomi, T., Namba, S., Tsuchizaki, T., Matsuda, I., 1999. Histopathological studies on two symptom types of phytoplasma associated with lettuce yellows. Ann. Phytopathol. Soc. Jpn. 65, 465–469, http://dx.doi.org/10.3186/jjphytopath.65.465.

van Bel, A.J.E., Furch, A.C.U., Will, T., Buxa, S.V., Musetti, R., Hafke, J.B., 2014. Spread the news: systemic dissemination and local impact of Ca2+ along the phloem pathway. J. Exp. Bot. 65 (7), 1761–1787, http://dx.doi.org/10.1093/jxb/ert425.

van Bel, A.J.E., 2003. The phloem, a miracle of ingenuity. Plant Cell Environ. 26, 125–149, http://dx.doi.org/10.1046/j.1365-3040.2003.00963.x.

Xie, B., Wang, X., Zhu, M., Zhan, Z., Hong, Z., 2011. CalS7 encodes a callose synthase responsible for callose deposition in the phloem. Plant J. 65, 1–14, http://dx.doi.org/10.1111/j.1365-313X.2010.04399.x.

4. SE-proteins role.

After having established that Arabidopsis is a reliable model for studying plant-phytoplasma interaction, it has been proceeded with the study of the role of SE filaments following phytoplasma infection. It has been hypothesised that filament agglutination could limit phloem flow and consequently pathogen spread (Gamalero *et al.*, 2010; Lherminier *et al.*, 2003; Musetti *et al.*, 2013). Nevertheless, these speculations were based on indirect evidences and, up to now, the information about the physiological role of the SE-protein filaments in non-Fabaceae are still fragmented even in physiological condition (Knoblauch *et al.*, 2014).

Manuscript submitted to Journal of Experimental Botany.

Phytoplasma infection provides novel information on the role of structural sieve-element proteins in phloem impairment and pathogen spread

Laura Pagliari[1], Sara Buoso[1], Simonetta Santi[1], Alexandra C. U. Furch[2], Marta Martini[1], Francesca Degola[3], Alberto Loschi[1], Michael Reichelt[4], Alex Mithöfer[5], Aart J. E. van Bel[6], Rita Musetti[1]*

1. Department of Agricultural, Food, Environmental and Animal Sciences, University of Udine, via delle Scienze, 206 I-33100 Udine, Italy

2. Institute of General Botany and Plant Physiology, Friedrich-Schiller-University of Jena, Dornburgerstrasse, 159 D-07743 Jena, Germany

3. Department of Life Sciences, University of Parma, via Usberti, 11/A I-43100 Parma, Italy

4. Department of Biochemistry, Max Planck Institute for Chemical Ecology, Hans-Knöll-Straße 8, D-07745 Jena, Germany

5. Department of Bioorganic Chemistry, Max Planck Institute for Chemical Ecology, Hans-Knöll-Straße, 8 D-07745 Jena, Germany

6. Department of Phytopathology and Applied Zoology, Justus Liebig University, Heinrich-Buff-Ring 26-32, D-35392 Giessen, Germany

***Corresponding author:** Phone: (39) 0432 558521. Fax: (39) 0432 558501.

E-mail: rita.musetti@uniud.it

Abstract

The understanding of the basic mechanisms of plant response to phytoplasma infection can contribute to the development of contrast strategies, limiting the huge impact of these pathogens on agricultural yield. In Fabaceae, dispersion of SE structural proteins, called forisomes, following phytoplasma infection has been hypothesised to limit phloem mass flow and, consequently, prevent pathogen spread. To elucidate the interaction between phytoplasma and sieve-element protein filaments, Arabidopsis mutant lines, lacking genes related to SE filament, were used both in healthy and in infected conditions. In the present work, various microscopic techniques were used, in order to combine fresh and embedded tissue observations, gaining information both on ultrastructural and physiological modifications in SEs. The analysis of both intact and infected plants suggested that SE protein filaments affect phloem flow only in case of a massive SE protein production, occurring only in stressed tissues. Moreover, even if filaments production also in mutant line was observed (indicating that in case of stressful condition SE protein filament formation can overcome *AtSEOR1* and *AtSEOR2* absence), the wild-type filament form is required for phloem impairment. No correlation between phloem impairment and pathogen concertation was found, indicating that plant activates other defence mechanism, probably related to JA and *cis*-OPDA pathway.

Keywords

Arabidopsis thaliana; phloem proteins; phloem mass flow; phytoplasmas; sieve-element occlusion

1) Introduction

Phytoplasmas are prokaryotic plant pathogens belonging to the class Mollicutes. They are transferred by insect vectors to the phloem tissue, where their pathogenicity is developed (Bertaccini and Duduk, 2009; Bertaccini *et al.*, 2014; Lee *et al.*, 2000). Phytoplasma-associated diseases have an enormous impact on agricultural yield, being associated with disorders affecting hundreds of plant species, including many economically important crops (Bertaccini *et al.*, 2014; Namba, 2011; Valiunas *et al.*, 2015). Phytoplasma outbreaks and spread can only be controlled thus far by using insecticides against vector populations or by eradicating infected plants. Alternative strategies, such as the individuation of resistant or tolerant plants (Osler *et al.*, 2014; 2016), require a thorough notion of the physiological mechanisms underlying the interactions between plant host and phytoplasmas.

Phytoplasmas are mostly confined to the sieve elements (SEs) in phloem tissue. Hardly anything is known about the cytological and molecular events at the phytoplasma-SE interface. Recently, the extensive ultrastructural re-organization of SEs following phytoplasma infection seems to represent changes that simultaneously serve the nutrition of phytoplasmas (Buxa *et al.*, 2015; Musetti *et al.*, 2016; Pagliari *et al.*, 2016) and the protection of the host plant against phytoplasma spread (De Marco *et al.*, 2016; Pagliari *et al.*, 2016). In infected *Vicia faba* plants, phytoplasmas also trigger structural modifications of forisomes in SEs (Musetti *et al.*, 2013). Forisomes are spindle-shaped, giant SE protein bodies, typical of SEs in Fabaceae. They can undergo a calcium-induced dispersion that leads to expansion and occlusion of the sieve pores (Knoblauch *et al.*, 2001; 2003; van Bel *et al.*, 2014). In this way, forisomes impair mass flow and probably limit pathogen invasion and spread (Srivastava *et al.*, 2015; Musetti *et al.*, 2013; van Bel, 2003).

Forisome components are encoded by members of the *Sieve-Element Occlusion* (*SEO*) gene family, first described in Fabaceae (Pélissier *et al.*, 2008) and subsequently found to be highly conserved among eudicotyledons (Ernst *et al.*, 2011; 2012; Froelich *et al.*, 2011; Pélissier *et al.*, 2008; Rüping *et al.*, 2010). In non-Fabaceae plants, *SEO* genes encode for filamentous proteins, called SE-proteins. SE protein filaments and forisomes may share several structural and functional features (Rüping *et al.*, 2010; Srivastava *et al.*, 2015), but instead of the well-ordered forisome structure, they form electron-dense, variously and irregularly branched, protein strands (Batailler *et al.*, 2012, Ernst *et al.*, 2012; Jekat *et al.*, 2012; Sjolund, 1997). In *Arabidopis thaliana*, SE-protein filament formation requires two so-called *Sieve-Element Occlusion Related (SEOR)* genes, *AtSEOR1* (At3g01680) and

AtSEOR2 (At3g01670) (Anstead *et al.*, 2012). These two contiguous genes, together with one pseudogene (At1g67790), are located on chromosome 3 and are the sole *AtSEOR* genes identified in Arabidopsis (Anstead *et al.*, 2012; Rüping *et al.*, 2010). No functional redundancy between these genes has been detected (Anstead *et al.*, 2012). The heterodimer formation mechanism is still unclear and AtSEOR1 and AtSEOR2 interaction seems to require one or more additional unknown proteins (Anstead *et al.*, 2012; Jekat *et al.*, 2013). Even if AtSEOR1 and AtSEOR2 are the sole proteins known to be necessary for SE-protein filament formation, the phloem protein 2, AtPP2-A1, encoded by the gene At4g19840, is associated with the SE-protein filaments in Arabidopsis (Batailler *et al.*, 2012).

In contrast to the solid information on forisome functioning (Furch *et al.*, 2007; 2009; Knoblauch et al, 2004; Srivastava *et al.*, 2015; Zimmermann *et al.*, 2013), the role of SE-protein filaments in non-Fabaceae is still a matter of debate (Ernst *et al.*, 2012; Froelich *et al.*, 2011; Jekat *et al.*, 2013; Knoblauch *et al.*, 2012; 2014). In Arabidopsis, SE-protein filament subunits are synthesized in immature SEs and assembled as large protein bodies, which disperse and relocate to the cell periphery along with the SE maturation (Evert *et al.*, 1972; Ehlers *et al.*, 2000; Ernst *et al.*, 2012; Froelich *et al.*, 2011). Under biotic and abiotic stress, SE-protein filaments displace from their parietal position and assemble in the SE lumen as strands or meshwork to plug the sieve plate (Achor *et al.*, 2010; Froelich *et al.*, 2011; Jekat *et al.*, 2013; Musetti *et al.*, 2010). Yet, different approaches led to conflicting conclusions with regard to actual occluding capabilities of SE proteins in Arabidopsis (Froelich *et al.*, 2011; Ernst *et al.*, 2012; Jekat *et al.*, 2013, Knoblauch *et al.*, 2014).

Considering the fact that SE-protein agglutination and plugging is a typical plant response to phytoplasma infection (Gamalero *et al.*, 2010; Lherminier *et al.*, 2003; Luna *et al.*, 2011; Musetti *et al.*, 2010; 2013), the potential SE occlusion by SEOR proteins in response to phytoplasma infection in Arabidopsis was investigated here. It was further studied, if sieve-tube occlusion and the associate phenotypic changes induced by phytoplasmas can be really considered defence mechanism and if they are related to biochemical responses, such us phytohormone signalling. In a multidisciplinary approach, the following questions were addressed:

a) Does phytoplasma-triggered SE-protein filament agglutination limit the phloem flow?
b) If so, can this strategy limit pathogen capability to proliferate in phloem tissue?

c) Is eventual SE-protein pathogen limitation simply related to a mechanical restriction mechanism or are SE-protein filaments associated to more complex mechanisms, in which phytohormones are involved?

To elucidate these aspects, wild-type and *AtSEOR* or *AtPP2-A1* Arabidopsis mutant lines were used, both in healthy and in phytoplasma-infected conditions.

2) Materials and methods

2.1) Arabidopsis mutant lines. Arabidopsis mutant lines, lacking one or both *AtSEOR* genes reported to be essential for SE protein filament formation (Anstead *et al.*, 2012), were used. Seeds for the single *AtSEOR* gene knockout lines, SALK_081968C (*AtSEOR1* knockout, hereafter called *Atseor1ko*) and SALK_148614C (*AtSEOR2* knockout, hereafter called *Atseor2ko*), were obtained from the European Arabidopsis Stock Centre (NASC). Two knockout/knockdown plant lines, obtained from the Institute of Plant Biology and Biotechnology of the University of Münster (Germany), were also used. These mutants, previously described from Jekat and co-authors (2013), have the *AtSEOR1* gene knockout and the *AtSEOR2* gene knockdown (*Atseor1ko/Atseor2kd*) or the *AtSEOR1* gene knockdown and *AtSEOR2* gene knockout (*Atseor1kd/Atseor2ko*), allowing the impairment of the expression of both genes (Jekat *et al.*, 2013). To study the role of PP2 protein in filament formation, the *AtPP2-A1* gene knockout line SALK_080914C was used. All mutants were in a Columbia (Col-0) background. In table 1, the main features of the Arabidopsis mutant lines we analysed, are summarized.

2.2) Plant materials and insect vectors. *A. thaliana* plants were infected with a phytoplasma strain related to '*Candidatus* Phytoplasma asteris' ('*Ca*. P. asteris', 16SrI-B subgroup), called Chrysanthemum yellows (CY) phytoplasma (Lee *et al.*, 2004). As extensively described by Pagliari and co-authors (2016), 4th and 5th instars of the insect vector *Euscelidius variegatus* (Bosco *et al.*, 1997; 2007) were transferred to CY-infected daisy plants (*Chrysanthemum carinatum* Schousboe), used as the source of inoculum, for a 7-day acquisition-feeding period. Thirty days after nymph transfer, 45-day-old *A. thaliana* plants were individually exposed to three infective insects. Healthy control plants were exposed to healthy insects. At the end of the 7-day inoculation-feeding period, insects were

manually removed. Both insect vectors and *A. thaliana* plants were grown at 20/22 °C, under short-day conditions (9hL/15hD period).

For every analysis, full-symptomatic and healthy control *A. thaliana* plants were tested 20 days after the end of the inoculation period. For rosette weight measurement, ultrastructural observations and phytoplasma titre analyses, ten healthy and ten infected plants from each line were used. Phloem mass flow experiment required three healthy and three infected plants *per* line. Finally, for gene expression and phytohormone investigation, at least five healthy and five infected plants were used.

2.3) Symptoms observation and rosette weight measurement. Symptom development was observed in ten healthy and ten infected plants *per* line, from the end of the inoculation period to the harvest for different analyses. For rosette weight, pots were saturated of water and, after 14 hours, plants were harvested, cutting them at ground level. Rosette weight was immediately measured. Statistical comparisons between healthy and infected plants and among the different Arabidopsis lines were performed by the Prism 7.02 software package (GraphPad Software, La Jolla, CA, USA), using, respectively, the unpaired *t*-test and the two- way ANOVA with a Dunnett's test as *post hoc* test for multiple comparisons.

2.4) Phytoplasma molecular detection. To check phytoplasma presence in Arabidopsis, each healthy and symptomatic plant was analysed by PCR. Total genomic DNA was extracted from 100 mg of leaf tissue according to Doyle and Doyle (1990), modified by Martini and co-authors (2009). DNA concentration and purity were checked using NanoDrop 1000 Spectrophotometer (Thermo Fisher Scientific, Wilmington, DE, USA). PCR amplifications were performed with primer pair R16F2n/R16R2 5'-GAAACGACTGCTAAGACTGG-3' / 5'-TGACGGGCGGTGTGTACAAACCCCG -3' (Gundersen and Lee, 1996; Lee *et al.*, 1995), using One Advanced thermocycler (Euroclone, Celbio, Milan, Italy) in 25-µl reactions containing 2.5 mM each of the four dNTPs, 20 µM of each primer, 25 mM MgCl2 5× polymerase buffer, 1 unit Taq polymerase (Promega, San Luis Obispo, CA, USA) and 1µl of sample nucleic acid (about 20 ng). Parameters used for 40-cycle PCR were: denaturation at 94°C for 1 min (2 min for the first cycle), annealing at 55°C for 1 min and extension at 72°C for 2 min (8 min for the last cycle). The amplified

products were analysed by electrophoresis in 1% agarose gel containing 1 µl Gel Red ™ (10000x, Biotium, Hayward, CA, USA) *per* ml.

2.5) Phloem mass flow. The phloem-mobile dye 5,6 carboxyfluoresceindiacetate (CFDA) (SIGMA Saint Louis, Missouri, USA) was used to investigate phloem flow. This dye, extensively used in plant research as a marker for symplastic transport, permeates the plasma membrane in acetate form and is cleaved by cytosolic enzymes producing membrane-impermeant carboxy- fluorescein (CF), which is transported by mass flow inside SEs (Froelich *et al.*, 2011; Furch *et al.*, 2010; Koh *et al.*, 2012; Knoblauch and van Bel., 1998).

As previously reported in *V. faba* (Musetti *et al.*, 2013), in healthy and infected *A. thaliana* plants a droplet of freshly prepared 1 µM CFDA solution was applied to the midrib after having removed the leaf tip. After a 1-hour incubation period at room temperature, 5 mm-long midrib samples were cut at a distance of approximately 3 cm from the CFDA application site. Sample pieces were included in 8% low melting point agarose. 100 µm-thick sections were cut by a HM560V vibratome (Microm Microtech, Brignais, France) and collected in phosphate-buffered saline solution. Sections were examined with a Leica TCS SP2 AOBS confocal laser scanning microscope (CLSM) (Leica, Wetzlar, Germany) with a 40 × water-immersion objective (HCX Apo 0.80), exciting CFDA with the blue argon ion laser (488 nm) and collecting emitted fluorescence from 500 to 545 nm. As control, unstained sections were observed at the same excitation wavelength used for the fluorochrome. For each *A. thaliana* line and condition, ten non-serial sections from three different plants were observed.

The fluorescence level in the phloem tissue was measured and compared in healthy and diseased samples by computerized image analysis in five non-serial sections *per* plant, using ImageJ 1.49m software (National Institutes of Health, Bethesda, MD, USA). The grey level (in arbitrary units; 0 = black, i.e. absence of signal; 255 = white) was measured on the tissue in an area devoid of signal at visual inspection and assumed as background (Bacci *et al.*, 2008). The threshold was then set at two times the background and fluorescence intensity were measured and divided for the analysed surface area. One-way analysis of variance (ANOVA) followed by a Dunnett's test was used to determine significance, with healthy wild-type values as control. Statistical analyses of fluorescence levels were performed with the Prism 7.02 software package (GraphPad Software).

2.6) Transmission electron microscopy (TEM). To preserve phloem tissue structure, a gentle preparation method was adopted, modifying the protocol by Ehlers and co-authors (2000), to adapt it to Arabidopsis leaves as recently reported by Pagliari and co-authors (2016). Briefly, from each plant, a 30 mm-long midrib portion was excised from three fully-expanded leaves of the rosette. The midrib segments were immediately submerged in a MES buffer for two hours at room temperature. A fixation solution of 3% paraformaldehyde and 4% glutaraldehyde was used and substituted every 30 minutes for 6 hours. Samples were rinsed for 1 h and postfixed overnight with 2% (w/v) OsO_4. Samples were dehydrated in a graded ethanol series and then transferred into propylene oxide. From the central part of each midrib, a 6-7 mm long piece was finally excised and embedded in Epon/Araldite epoxy resin (Electron Microscopy Sciences, Fort Washington, PA, USA). Ultrathin sections (60-70 nm in thickness) were cut using an ultramicrotome (Reichert Leica Ultracut E ultramicrotome, Leica Microsystems, Wetzlar, Germany), collected on uncoated copper grids, stained with uranyl acetate and lead citrate (Reynolds, 1963), and then observed under a PHILIPS CM 10 TEM (FEI, Eindhoven, The Netherlands), operating at 80 kV. Five non-serial cross sections from each sample were analysed.

2.7) RNA extraction and gene expression analyses. Total RNA was extracted from approximately 1 g of leaves, ground into fine powder and homogenized in 5 ml of lysis buffer (MacKenzie *et al.*, 1997). Homogenate (1.5 ml) was collected and centrifuged for 6 minutes at 12.000 rpm. One milliliter of supernatant was mixed with 100 µl of 20% (wt/vol) sarkosyl buffer and incubated 15 minutes at 70°C. Samples were then transferred to a QIAshredder spin column (lilac) and RNA purified with RNeasy Plant Mini Kit (Qiagen GmbH, Hilden, Germany) according to the manufacturer's instructions. Extracted RNAs were DNAse-treated and reverse-transcribed into complementary DNA (cDNA) with the QuantiTect Reverse Transcription Kit (Qiagen GmbH) following the manufacturer's instructions. The expression of *AtSEOR1*, *AtSEOR2* and *AtPP2-A1* genes was analysed in healthy and infected plants by real time experiments performed on a CFX96 instrument (Bio-Rad Laboratories, Richmond, CA, USA). Reference gene was individuated comparing *UBC9* (ubiquitin conjugating enzyme 9), *TIP41* (TIP41-like family protein), *SAND* (SAND family protein) and *UBQ10* (polyubiquitin 10) genes (Table 2). The gene stability measures (M value) were calculated according to the geNorm program (Vandesompele *et al.*, 2002) (Table 2). *UBC9* gene was found to be the most stably expressed gene and so the most suitable as reference gene.

SsoFast EvaGreen Supermix (Bio-Rad Laboratories Inc., Hercules, CA, USA), cDNA obtained from 5 ng of RNA and specific primers were used in a total volume of 10 µL for *AtSEOR1* and *AtPP2-A1* genes. *AtSEOR2* gene expression analyses were carried out with cDNA from 10 ng of RNA in a total volume of 20 µL. Every reaction was performed at 95°C for 3 min, 40 cycles of 95°C for 5 sec and 58°C for 5 sec, followed by a melting curve analysis from 65°C to 95°C to check primer specificity. Primers were designed using Primer3 software (http://bioinfo.ut.ee/primer3-0.4.0/primer3/) and primer specificity evaluated with the BLASTN (Nucleotide Basic Local Alignment Search Tool) algorithm (Altschul *et al.,*1997). Primer pair efficiency (E) was evaluated as described by Pfaffl (2001) on the standard curves of different dilutions of pooled cDNA. Gene and primer sequences for expression analysis are reported in Table 3. A mean normalized expression (MNE) for each gene of interest (Muller *et al.,* 2002) was calculated by normalizing its mean expression level to the level of the UBC9 gene. Three technical repeats and at least five individuals concurred to gene MNE determination.

Statistical analyses of gene expression levels were performed with the Prism 7.02 software package (GraphPad Software) using an unpaired *t*-test and two-way ANOVA test and a Dunnett's test as *post hoc* test for multiple comparisons.

2.8) Phytoplasma quantification. Total genomic DNA was extracted from 1 g of leaf tissue as described above for phytoplasma molecular detection. Ribosomal protein (rp) gene *rplV* (*rpl22*) was chosen as target for the amplification of CY phytoplasma DNA using the primer pairs rp(I-B)F2/rp(I-B)R2 5'- CGTTTGGGTGGTGCTGAAAT-3'/5'-GAGGGCGTCTGTTAGGAGTG-3' (this study; Lee *et al*., 2003) and producing an amplicon of 232 bp. To quantify CY phytoplasma DNA, a 1260 bp ribosomal protein fragment from CY phytoplasma, amplified with primer pair rpF1C/rp(I)R1A (Martini *et al*., 2007), was cloned in pGem®T-Easy vector (Promega). Plasmid DNA was first quantified by using Qubit® 2.0 Fluorometer (Invitrogen, Carlsbad, CA, USA); then a standard curve was established by 10-fold serial dilutions of plasmid DNA corresponding to ca. 10^9 to 10^1 target genomes. Standards and 1 ng of each DNA sample (run in three replicates) were added to a mixture containing 0.3 µM each primer, 7.5 µl 2x SsoFast EvaGreen Supermix (Bio-Rad Laboratories) in a 15 µl total volume. Cycling conditions were as follows: initial denaturation at 98 °C for 2 min; 44 cycles of 5 sec at 98 °C and 5 sec at 60 °C, and a final extension at 95 °C for 1 min. A melting curve analysis (ramp from 65 °C to 95 °C at 0.5 °C/sec) was programmed at the end of the cycling reaction to evaluate the purity of the amplification

product. CY phytoplasma concentration was expressed as the number of CY phytoplasma genome units (GU)/1 mg of leaf sample to normalize the data.

The comparisons of phytoplasma population size were performed analysing the quantification results from three technical repeats of ten plants *per* line with the Prism 7.02 software package (GraphPad Software), using one-way ANOVA and a Dunnett's test as *post hoc* test for multiple comparisons, with wild-type line as control.

2.9) Phytohormone analysis of midrib and laminar tissue. The stress-related phytohormones, abscisic acid (ABA), salicylic acid (SA) and the jasmonates, jasmonic acid (JA), *cis*-12-oxo-phytodienoic acid (*cis*-OPDA), and (+)-7-iso-jasmonoyl-l-isoleucine (JA-Ile), and the jasmonate degradation products 12-hydroxy jasmonic acid (OH-JA), as well the 12-hydroxy (OH-JA-Ile) and 12-carboxy (COOH-JA-Ile) form of (+)-7-iso-jasmonoyl-l-isoleucine were investigated in leaves.

In each plant, leaf midrib was separated from the other part of the lamina and roughly 250 mg of fresh material from both leaf parts was collected in two different vials and immediately frozen in liquid nitrogen. After freeze-drying, samples were weighted and homogenized in a Geno/Grinder 2000 (SPEX Certiprep, London, UK) at 1000 rpm for 60 sec. Plant material was extracted with 1.5 ml methanol containing 60 ng of 9,10-D_2-9,10-dihydrojasmonic acid, 60 ng of D_4-salicylic acid, 60 ng of D_6-ABA (Santa Cruz Biotechnology, Santa Cruz, CA, USA), and 15 ng of JA-[$^{13}C_6$] Ile conjugate as internal standards (Vadassery *et al.*, 2012). The suspension was centrifuged at 13000 g for 20 min. Then, the supernatant removed to a fresh tube and the pellet was extracted again with 500 µl of methanol, mixed, and centrifuged. Supernatants were combined, evaporated in a Speed Vac at 30°C and finally dissolved in 500 µl of methanol.

For chromatography, an Agilent 1200 HPLC system (Agilent Technologies, Böblingen, Germany) equipped with a Zorbax Eclipse XDB-C18 column (50 × 4.6 mm, 1.8 m, Agilent) was employed and eluates were analysed according to Vadassery and co-authors (2012).

Statistical comparisons between healthy and infected plants and among the different Arabidopsis lines were performed by the Prism 7.02 software package (GraphPad Software) using, respectively, the unpaired *t*-test and two- way ANOVA with a Dunnett's test as *post hoc* test for multiple comparisons.

3) Results

3.1) Macroscopic phenotypes of heathy and full-symptomatic plants. Ten healthy and ten infected plants from each line were observed and weighted. Healthy plants of all lines grew at similar rates (Fig.1, 2). Within 20 days of inoculation, common phytoplasma disease symptoms appeared in every plant exposed to three infective insects. Infected plants showed yellowing, reduced growth and general stunting (Fig. 1). Leaves having emerged after phytoplasma inoculation were shorter, with a thick main vein and a smaller petiolar area. Wild-type and mutant lines did not differ in symptom development or plant phenotype due to infection (Fig. 1). A decrease of roughly 40 % in growth was observed in all infected plant lines compared to the healthy ones, but no differences in rosette fresh weights among the lines were measured (Fig. 2).

3.2) Phytoplasma molecular detection. Phytoplasma detection and quantification was performed in healthy and symptomatic plants. Direct PCR analysis allowed the amplification of a 1250-bp fragment, confirming the presence of phytoplasmas only in the symptomatic plants (not shown).

3.3) Phloem mass flow analysis with CFDA dye. To examine alterations of SE mass flow due to infection in diverse SE-protein mutants, phloem-mass flow was observed under CLSM using leaf cross-sections and CFDA. For each *A. thaliana* line, ten non-serial sections from three different plants were observed at about 3 cm remote from the site of CFDA application. Unstained sections were observed at the same excitation wavelength used for the fluorochrome and no fluorescent signals were detected (Fig. 3). In healthy plants of each line investigated, the phloem-mobile CF emitted strong signals from the phloem area (Fig. 4). Colorless CFDA must have entered the SEs via the plasma membrane and, following de-esterification, the membrane-impermeant CF was translocated by mass flow through the sieve tubes. From there, CF has probably moved to companion cells (CCs) and phloem parenchyma cells (cf. Knoblauch and van Bel, 1998). In the latter cells, CF may have accumulated in the vacuoles, enhancing fluorescence signal (Fig. 4). Due to the high hydration and the softness of Arabidopsis tissue, cross-sectioning by vibratome caused CF contamination in correspondence to xylem area. No significant differences between the

aggregate fluorescence levels in the phloem were detected among the various lines (Fig. 4).

In infected plants, the phloem areas were larger than in healthy plants due to phloem hyperplasia, the excessive production of new phloem tissue due to procambial or cambial hyperactivity following phytoplasma infection. Infected wild-type plants were characterized by reduced CF signals (Fig. 5 A). In infected mutant lines, the CF emitted signals from the phloem area, comparable in strength to the ones detected in wild-type plants (Fig. 5). The interpretation of the observations was corroborated by a fluorescence quantification analysis that revealed a strong reduction of fluorescence in the infected wild-type line in comparison to all other specimens (Fig. 6).

3.4) SE changes in ultrastructural organization following infection. To visualize changes in SE ultrastructure due to mutation or pathogen presence, and eventually correlate them with phloem impairment, phloem tissue was observed by TEM. For each condition, five non-serial sections from ten different plants were analysed. Observations of healthy samples showed a well-preserved sieve-tube ultrastructure, with a regular shape and no signs of necrosis or subcellular aberrations, also in case of transformed plants (Fig. 7). In the latter lines, the SE plasma membrane had a regular profile, appressed to the cell wall. Mitochondria and thin stacks of sieve-element reticulum (SER) adhered to the plasma membrane. In wild-type plants, SE protein filaments were rarely observed and only tiny filaments were detected (Fig. 7 A). Sieve-plate pores appeared unobstructed and free from filament plugs or callose deposition (not shown). In mutant plants lacking one or both *AtSEOR* genes, SE lumina were fully devoid of filaments (Fig 7 B-E). By contrast, SE lumina of *Atpp2-a1ko* plants showed filaments that did not appear to morphologically differ from wild-type protein filaments (Fig. 7 F).

In all infected lines, phytoplasmas were present exclusively in SEs (Fig. 8), with a disparate distribution over the SEs (data not shown, cf Pagliari *et al.*, 2016). The phytoplasmas exhibited a well-preserved structure, with their typical pleomorphic profile, delimited by an electron-dense membrane, enclosing dispersed DNA strands and ribosome granules (Fig. 8). Pleomorphic phytoplasmas were observed to float freely in the SE lumen or to be linked to the SE plasma membrane or SER stacks (Fig. 8 A, B). In infected wild-type plants, SEs were characterized by various alterations, such as callose accumulation around the sieve pores (Fig. 8 C, D), condensation of protein filaments, or traces of necrosis or plasmolysis. Protein filaments appeared to be organized in simple or branched strands,

or thin networks (Fig. 8 A). In other cases, the protein filaments formed a dense meshwork filling the SE lumen that surrounded phytoplasmas and plugged sieve-plate pores (Fig. 8 B, D).

In every infected section of Arabidopsis lines lacking one or both *AtSEOR* genes, SEs showed electron-dense strands that could be straight, branched or even organized into thin networks, with morphology and organization similar to those observed in infected wild-type plants (Fig. 9 B-E). Filaments were also observed in the infected SEs of *Atpp2-a1ko* plants (Fig. 9 F).

3.5) *AtSEOR1*, *AtSEOR2* and *AtPP2-A1* gene expression analyses. To check if *AtSEOR1*, *AtSEOR2* and *AtPP2-A1* genes are involved in infection response, their expression was analysed in healthy and infected plants by real-time RT-PCR experiments. For each condition, three technical repeats in at least five individuals were investigated. For all samples, gene-expression analyses are presented in Fig. 10, where the mean normalised expression of each gene is plotted as the transcript abundance compared to the *UBC9* expression level (set at 100). The expression level of the *AtSEOR1* and *AtSEOR2* genes was low, with MNE values fluctuating from 0.07 to 1.59 and from 0.08 to 2.10, respectively. *AtPP2-A1* presented a higher gene transcription level compared to *AtSEOR* genes, ranging from 2.77 to 19.84.

The unpaired *t*-test on MNE values showed that each gene analysed was significantly up-regulated in infected plants (Fig. 10). To compare the expression level of each single gene in respective Arabidopsis lines, a two-way ANOVA and a Dunnett's test as *post hoc* test were performed using the wild-type MNE values as negative controls. No significant differences were detected among expression levels in healthy plants, except for *AtSEOR2*, which was significantly up-regulated in healthy *Atpp2-a1ko* plants. On the other hand, in infected plants, each gene showed a significant increase in gene transcription levels in the mutant lines in comparison to the wild-type ones (Fig. 10).

3.6) Phytoplasma titre quantification. To correlate phloem impairment with pathogen replication capability and spread, phytoplasma titre was quantified in ten infected plants from each line, performing every time three technical replicates. Molecular analyses confirmed the presence of phytoplasmas in every symptomatic plant. Wild-type, *Atseor2ko*, *Atseor1ko/Atseor2kd* and *Atpp2-a1ko* plants were characterized by phytoplasma titres

ranging from 440.75E+06 to 724.68E+06 phytoplasma genome units (GU)/1 mg of leaf sample. One-way ANOVA and a Dunnett's *post hoc* tests revealed significantly lower phytoplasma concentrations in *Atseor1ko* and *Atseor1ko/Atseor2kd* plants (95.55E+06 and 248.61E+06 phytoplasma GU/1 mg of leaf sample, respectively) than in wild-type plants (601.68E+06 phytoplasma GU/1 mg of leaf sample) (Fig. 11).

3.7) Phytohormone analysis of midrib and laminar tissue. The fact that widely different phytoplasma titres did not coincide with phloem mass flow condition in the various Arabidopsis lines (cf. Figs 4, 5 and 11) suggested an alternative defence mechanism for pathogen limitation. To see if and how defence mechanisms were activated, analyses of phytohormones, central regulators of plant immunity, were carried out. The phytohormones ABA, SA, JA and some of their derivatives were analysed separately in the leaf midrib and the remaining lamina, in each healthy and infected plant lines under examination. For each condition, five different plants were studied. In healthy plants, the ABA concentrations were consistently higher in lamina tissue (Fig. 12 A, for specific amounts see supplementary Fig. S1) than in the midribs. Phytoplasma infection caused a significant increase to the same level in ABA levels in both tissues (Fig. 12 A). Thus, the relative response to infection is higher in the midribs (Fig. 12 A). While the SA concentrations in midrib and lamina tissue were similar in healthy plants, the SA levels in infected plants significantly dropped in the midribs and remained stable in the laminae (Fig. 12 B, Fig. S1). The opposite held for the JA concentrations which were similar in midribs and laminae of intact plants of all lines (except of *Atpp2-a1ko* plants), but were significantly higher in the midribs of all plant lines (Fig. 12 C). The JA active form, JA-Ile, showed an even more explicit effect of infection. Ja-Ile occurred in higher concentrations in the laminae than in the midribs of intact plants, but generally decreased in the laminae and significantly increased in the midribs of infected plants (Fig. 12 D, Fig. S1).

In healthy plants, the JA-precursor *cis*-OPDA levels were almost identical (Fig. 12 E). Phytoplasma infection effected a considerable and significant increment of the *cis*-OPDA concentration in both tissues of every line, but the effect was stronger in laminae (Fig. 12 E, Fig. S1). The infection did not cause a distinct result on the JA degradation form, OH-JA, with exception of a rise in infected *Atpp2-a1ko* plants (Fig. 12 F, Fig. S1). Both in healthy and in infected plants, OH-JA-Ile had a lower concentration in midribs than in lamina tissue. The difference was statistically significant in infected plants (Fig. 12 G, Fig. S1). Despite the variability, it was concluded that COOH-JA-Ile was present in lower concentrations in the

midribs than in the laminae of healthy plants. The difference was more distinct in infected plants, where the COOH-JA-Ile level rose to a higher extent (Fig. 12 H, Fig. S1).

4) Discussion

4.1) Phytoplasma infection induces SE-protein filament formation in *AtSEOR* mutant lines. In Arabidopsis two non-redundant *SEO* genes, *AtSEOR1* and *AtSEOR2* (Anstead *et al.*, 2012; Rüping *et al.*, 2010), are regarded to be necessary for SE-protein filament formation (Anstead *et al.*, 2012). TEM pictures reveal the presence of SE protein filaments only in healthy wild-type and *Atpp2-a1*ko plants (Fig 7), in line with what previously reported in literature (Anstead *et al.*, 2012). By contrast, infected plants of every line show a significant presence of SE-protein filaments (Fig 9). These findings lead to hypothesize that under stressful conditions SE-protein filament formation becomes independent of *AtSEOR1* and *AtSEOR2* expression. Up to date, most of the proteins that take part to SE-filament formation are unknown and *AtSEOR1* and *AtSEOR2* interaction mechanism seems to require one or more unknown components (Anstead *et al.*, 2012; Jekat *et al.*, 2013). In infected plants, statistical analyses underline the overexpression of SE-protein genes in mutant lines in comparison to wild-type lines (Fig. 10), suggesting that plants try to compensate the lack of one SE-protein by enhanced production of the others to overcome the deficits in mutant lines, as already observed in other systems (Gierth and Mäser, 2007; Kawakatsu *et al.*, 2009; Ramundo *et al.*, 2014; Schneider *et al.*, 2002). The upregulation of genes under stress conditions, may sustain the production of SE-protein filaments in an alternative way.

4.2) Wild-type SE-protein filaments restrict phloem flow. The question now arises if occlusion by protein filaments restricts mass flow. Phytoplasma-infected plants show stunted growth and a diversity of alterations like yellowing, leaf-size reduction and vein enlargement (Fig 1). Such symptoms have commonly been attributed to impairment of phloem activities following phytoplasma infection (Braun and Sinclair, 1978; Kartte and Seemüller, 1991; Lepka *et al.*, 1999; Maust *et al.*, 2003). However, yellowing could also be due to downregulation of photosynthetic proteins (Ji *et al.*, 2009; Hren *et al.*, 2009; Taheri *et al.*, 2011), accompanied by a reduction of total chlorophyll content (Bertamini *et al.*, 2002a; 2002b; Junqueira *et al.*, 2004; Zafari *et al.*, 2011).

The identical sieve-tube conductance for CF in healthy wild-type and mutant lines (Fig. 4) is in line with the identical mass flow velocities found in wild-type and AtSEOR1 mutants (Froelich *et al.*, 2011). The latter study seemingly conflicts with involvement of SE-protein filaments in sieve-tube occlusion. However, sieve-tube occlusion in infected wild-type plants (Fig. 5) indicates that SE-filament proteins are engaged in sieve-plate plugging, as seen in phytoplasma-infected *V. faba* (Musetti *et al.*, 2013) and as concluded from exudation experiments in Arabidopsis (Ernst *et al.*, 2012; Jekat *et al.* 2013). The reason for the contradictory results may lie in the fact that the SE-proteins do not aggregate in intact wild-type plants, whereas the SE-proteins coagulate in stressed wild-type plants, likely owing to Ca^{2+} influx mediated by stress-activated Ca^{2+}-permeable channels (Hafke *et al.*, 2010; van Bel *et al.*, 2014). Lack of one of the SEOR proteins may explain the inability to seal sieve tubes in infected mutants (Fig. 5) despite the phytoplasma-imposed stress. Masses of SE-protein filaments showing up in TEM-pictures of phytoplasma-infected mutant plants (Fig. 9) may result from compensatory expression of other genes (Fig. 10). Like in forisomes a structural arrangement of filamentous SEOR-proteins may provide the spatial conditions for Ca^{2+}-binding to attain plug formation. If one of the proteins is lacking, effective occlusion structures will not be reached. Another explanation for the lack of occlusion may be that the porosity of the material is critical (Froelich *et al.*, 2011). Proteins, especially if they contain a high percentage of charged amino acids, are surrounded by viscous hydration shells, which increase the effective filament diameter significantly (Bánó and Marek, 2006).

4.3) Phloem impairment does not effectively affect pathogen spread. Phytoplasma-triggered phloem impairment has been postulated to be a plant strategy to limit pathogen spread (Gamalero *et al.*, 2010; Lherminier *et al.*, 2003; Musetti *et al.*, 2013). Remarkably, the phytoplasma titre in wild-type plants equals that in some mutants (Fig. 11), excluding a possible connection between phloem impairment and pathogen spread limitation. This phenomenon is consistent with the view that phytoplasma spread is not only dependent on phloem mass flow (Garcia-Chapa *et al.*, 2003; Wei *et al.*, 2004; Buxa *et al.*, 2015). Moreover, the lower phytoplasma titre found in *Atseor1ko* and *Atseor1ko*/*Atseor2kd* plants indicate other defence mechanisms being associated with the filamentous SE-proteins. In view of the putative involvement of AtSEOR2 protein in plant immune signalling (Afzal *et al.*, 2013), phytohormone analyses were carried out.

4.4) *S*ite-specific JA increase to phytoplasma infection. Plants have evolved sophisticated survival strategies, including phytohormones as major actors in response to a range of biotic and abiotic stresses (Peleg and Blumwald. 2011; Vidhyasekaran, 2015). Primary defence hormones are jasmonates (JAs), salicylates (SAs), ethylene (ET) and abscisic acid (ABA), but several other hormones, reputed for their role in plant growth and development, participate in defence responses (Pieterse *et al.*, 2009; Robert-Seilaniantz *et al.*, 2011). The involvement of so many regulators in plant immunity suggests that defence mechanisms cross-communicate in complex signalling networks with interactive effects (Foyer *et al.*, 2016; Kazan and Lyons, 2014; Koornneef and Pieterse, 2008; Robert-Seilaniantz *et al.*, 2011).

ABA is regarded as a broad-spectrum phytohormone, engaged in general defence mechanisms (Dar *et al.*, 2015; Robert-Seilaniantz *et al.*, 2011; Vidhyasekaran, 2015). As observed in this study (Fig. 12 A), the ABA concentration -or the expression of ABA-related genes- rises in case of phytoplasma infection (Janik *et al.*, 2016; Leon *et al.*, 1996; Mou *et al.*, 2013; Punelli *et al.*, 2016; Zimmermann *et al.*, 2015). The ABA burst could retard stem elongation and shoot growth, being the main cause of smaller leaves and shorter internodes as result of phytoplasma infection (Mou *et al.*, 2013).

SA and JA are plant hormones required for signal transduction leading to plant resistance. JA and SA-mediated signalling pathways are mutually antagonistic (Koornneef and Pieterse, 2008; Loake and Grant, 2007; Vidhyasekaran, 2015). Traditionally, SA signalling is deemed to activate resistance against biotrophic and hemibiotrophic pathogens, while JA is mainly though to induce resistance against necrotrophic pathogens and wounding (Kazan and Lyons, 2014; Pieterse *et al.*, 2009; Robert-Seilaniantz *et al.*, 2011). Phytoplasmas are biotrophic pathogens (Bertaccini *et al.*, 2014) and the expected increase in SA level and decrease of JA level were demonstrated (Minato *et al.*, 2014; Musetti *et al.*, 2013; Patui *et al.*, 2013; Sugio *et al.*, 2011; Zimmermann *et al.*, 2015). In this study (Fig. 12 B, D) and in other analyses, in which main-vein and lamina tissues were separately measured, an increase in JA was detected or expected by expression analysis (Luge *et al.*, 2014; Punelli *et al.*, 2016). The veins are the sites where the direct interaction between phytoplasma and host occurs and the midribs, being rich in vascular tissue, express the vein responses most clearly. In conclusion, it seems vascular tissue reacts to the infection by a boost in JA production.

To better understand the processes responsible for the JA burst, JA metabolites were analysed in lamina and vein tissues. JA is synthesised via the oxylipin pathway, that starts in chloroplasts, where *cis*-OPDA is produced and transported into peroxisomes, to be converted to JA. JA is then translocated to the cytosol where it can be methylated or conjugated to amino acids (Dar *et al.*, 2015; Vidhyasekaran, 2015; Wasternack and Hause, 2013). Several JA metabolites act as signal molecules in triggering plant immunity. Among them, JA-Ile is the major bioactive form (Dar *et al.*, 2015; Vidhyasekaran, 2015). Investigation on midribs and leaf lamina tissue is compatible with the pattern observed for JA, with an increase in JA-Ile in the main veins (Fig. 12 D). *Cis*-OPDA is not just an intermediate in the JA pathway, but triggers innate immune responses having signalling properties distinct of JA (Dave and Graham, 2012; Park *et al.*, 2013; Wasternack and Hause, 2013). In case of phytoplasma infection, it has been observed that *cis*-OPDA level can both rise (Janik *et al.*, 2016) or fall (Janik *et al.*, 2016; Zimmermann *et al.*, 2015). Its boost following infection (Fig. 12 E) suggests an important role of *cis*-OPDA in restriction of phytoplasma spread and/or multiplication. *cis*-OPDA accumulation leads to glutathione synthesis (Park *et al.*, 2013) and to the consequent changes of the cellular redox homeostasis. Since redox homeostasis is a key issue in transcriptional regulation (Foyer and Noctor, 2005), *cis*-OPDA contributes to the operational control of nuclear gene expression (Park *et al.*, 2013). Higher *cis*-OPDA levels found in mutant lines (*Atseor1ko* and *Atseor1ko/Atseor2kd*) with the low phytoplasma titres could indicate a better regulation of the defence genes expression in these lines.

JA and JA-Ile can be hydroxylated at C-12 or C-11, or carboxylated at C-12 (Wasternack and Hause, 2013). The role of these compounds is still matter of debate (Nakamura *et al.*, 2011) and up to know, no information is reported about a possible role in phytoplasma infection. Nevertheless, the increase of JA hydroxylated forms in infected tissue suggests that an intense activity and regulation of the JA pathway as response to phytoplasma infection is occurring (Miersch *et al.*, 2008).

5) Conclusions

With this survey, it has been attempted to give an insight about the relationship between phytoplasma infection and SE protein filament agglutination, as plant response to pathogen invasion. It was observed that, in case of stressful condition, SE-protein filament formation can overcome *AtSEOR1* and *AtSEOR2* absence, corroborating the previous hypothesis

about a wider protein composition of the SE protein filament (Ansteadt *et al.*, 2012; Jekat *et al.*, 2013). Phloem flow analysis on both intact and infected plants suggested that SE protein filaments cause phloem impairment only in case of a massive SE protein production in its wild-type form. This result nicely matches with previous records (Ernst *et al.*, 2012; Froelich *et al.*, 2011; Jekat *et al.*, 2013). Moreover, no correlation between phloem impairment and pathogen multiplication was found, indicating that plant activate other defence mechanism, probably related to JA and *cis*-OPDA pathway. Phytohormone analysis establishes an inspected correlation between *cis*-OPDA and pathogen presence and spread, confirming the recent data about a specific role of *cis*-OPDA in plant defence response and signalling (Dave and Graham, 2012; Park *et al.*, 2013; Wasternack and Hause, 2013). However, further experiments are necessary, to confirm the possible relation between *cis*-OPDA, phytoplasma infection and their ability to multiply, for example comparing wild-type and *opr* Arabidopsis mutant lines, lacking the 12-oxophytodienoic acid reductase required for jasmonate synthesis (Stintzi and Browse, 2000).

6) Acknowledgments

Authors kindly thank Professor Domenico Bosco (University of Torino, Italy) for having provided the Chrysanthemum yellows (CY) phytoplasma strain and for his precious advice about insect rearing, Dr. Stefanie Vera Buxa (Justus Liebig University, Giessen, Germany) for her precious advices for phloem mass flow experiment, Dr. Andrea Genre (University of Torino, Italy) for his willingness and his help in phloem mass flow experiment, Dr. Gundula A. Noll (University of Münster, Münster, Germany) for giving them seeds of *Atseor1ko/Atseor2kd* and *Atseor1kd/Atseor2ko* mutant lines. This work was supported by the University of Udine.

Tables

Table 1. List of Arabidopsis mutant lines used for the experiments.

Line	*Atseor1ko*	*Atseor2ko*	*Atseor1ko Atseor2kd*	*Atseor1kd Atseor2ko*	*Atpp2-a1*ko
Gene	At3g01680.1	At3g01670.1	At3g01680.1 At3g01670.1	At3g01680.1 At3g01670.1	At4g19840.1
Source	SALK_081968C (NASC)	SALK_148614C (NASC)	Jekat *et al.*, 2013	Jekat *et al.*, 2013	SALK_080914C (NASC)
Transformation	t-dna insertion	t-dna insertion	At3g01680.1 t-dna insertion At3g01670.1 hpRNA cassettes	At3g01680.1 hpRNA cassettes At3g01670.1 t-dna insertion	t-dna insertion

Table 2. List of primers and accession number of sequences used housekeeping individuation.

Gene	Forward primer 5'-3'	Reverse primer 5'-3'	nM	M value	NCBI accession no.
UBC9	TCACAATTTCCAAGGTGCTGC	CGAGCAGTGGACTCGTACTT	300	0.43	NM_179131.3 NM_118934.3
TIP41	CCTCTTGCGATTTTGGCTGAG	ACGAAGAACAGTTGGTGCCT	400	0.52	NM_119592.5
SAND	AGATCAATCGCGGAAGGTGG	TATGTCGGGACCAGGTGAGT	400	0.74	NM_128399.4
UBQ10	CGTCTTCGTGGTGGTTTCTAA	ACAAGGCCCCAAAACACAAAC	300	0.59	NM_178968.5* NM_001084884.5* NM_001340546.1* NM_116771.5* NM_202787.4* NM_001340547.1* NM_178969.6* NM_178970.5*

*This primer pair amplifies every gene transcript variant.

Table 3. List of primers and accession number of sequences used in real-time PCRs.

Gene	Forward primer 5'-3'	Reverse primer 5'-3'	nM	E (%)	NCBI accession n.
AtSEOR1	ACCATCTCGCTGAGACCTTGAGG (Anstead *et al.*, 2012)	GGCCGTGAGAATCTTCATGTTATCA (Anstead *et al.*, 2012)	500	97,8	NM_111034.3
AtSEOR2	TTCAAAGAGACGCGTCGGG	GCTGCCATGCTTCTGTGTAG	500	104	NM_111033.3
AtPP2-A1	GGTGGACGAGAGAAACAGCA	GCTTCCACATTCTCGTTTGGT	400	96,3	NM_118104.5
UBC9	TCACAATTTCCAAGGTGCTGC	CGAGCAGTGGACTCGTACTT	300	97,1	NM_179131.3* NM_118934.3*

*This primer pair amplifies both gene transcript variants.

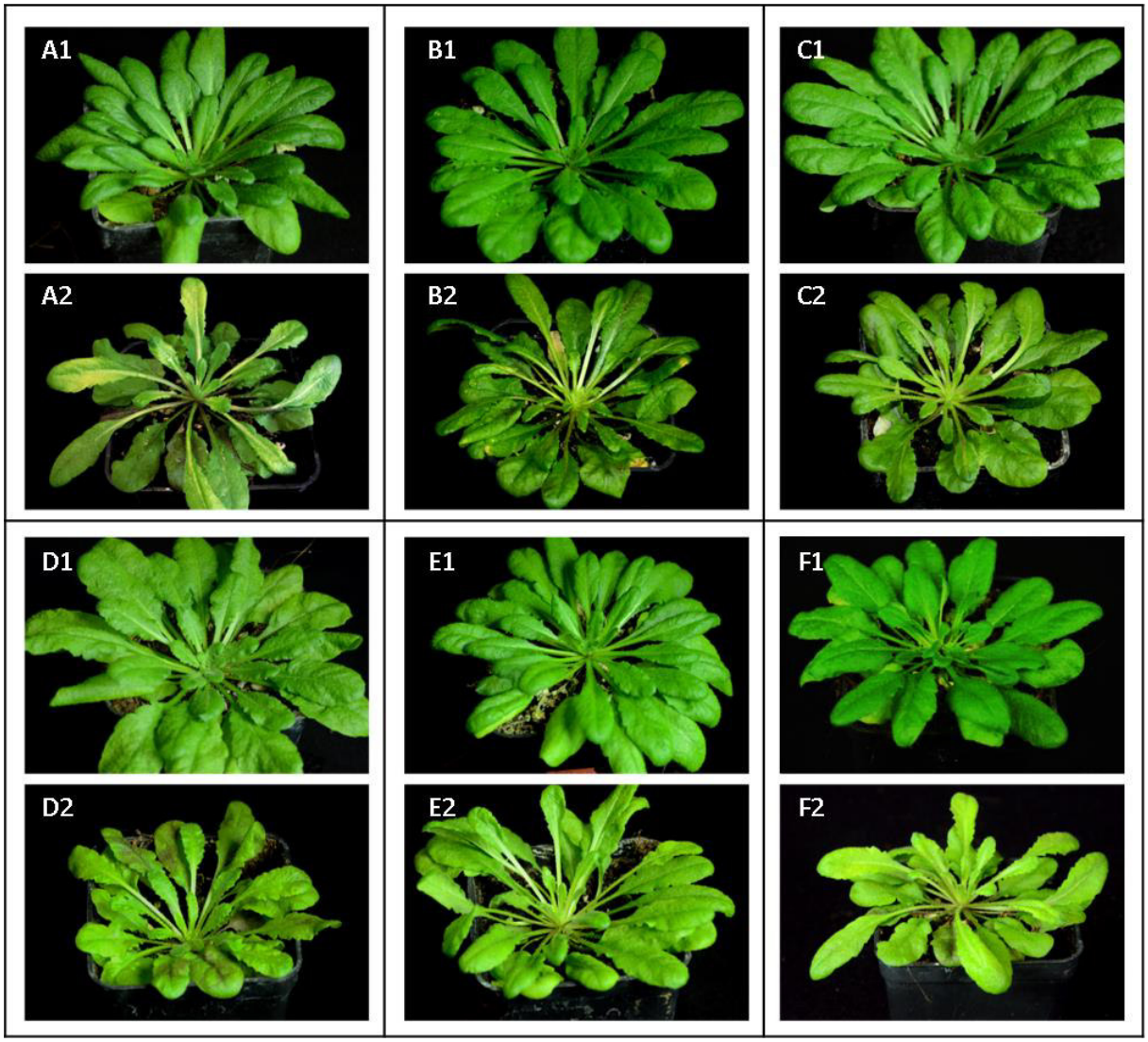

Figure 1. Macroscopic phenotypes of representative heathy and full-symptomatic plants at 70 days. Different *A. thaliana* lines were indicated as follows: A. wild-type, B. *Atseor1ko*, C. *Atseor2ko*, D. *Atseor1ko/Atseor2kd*, E. *Atseor1kd/Atseor2ko*, F. *Atpp2-a1ko*. Phytoplasma infection altered the phenotype of *A. thaliana*, producing classic phytoplasmosis symptoms. Healthy plants (1) showed regular growth, while infected plants (2) were characterized by reduced growth and shorter, yellowish leaves, with a thick main vein. No obvious difference was recorded among the different plant lines. For each condition, 10 different plants were analyzed.

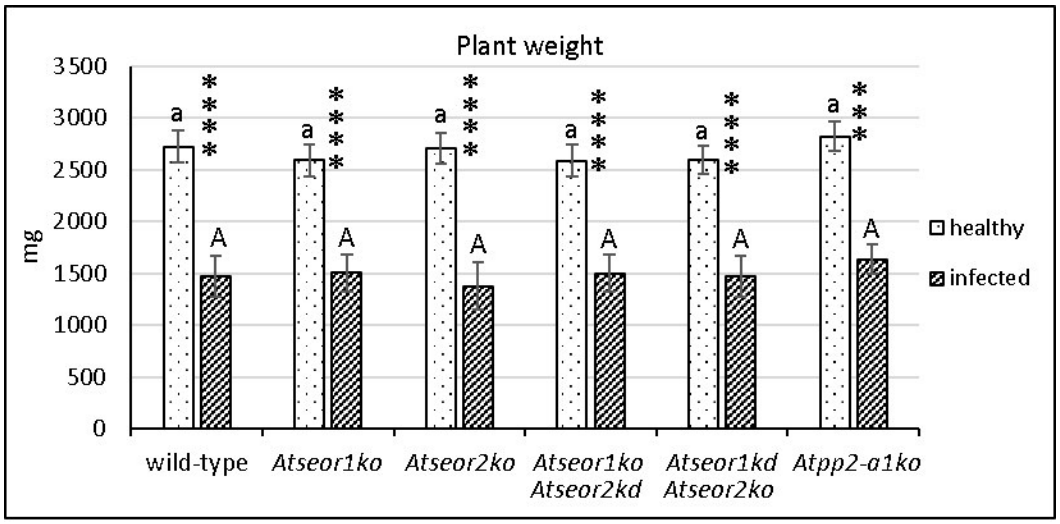

Figure 2. Fresh rosette weight of healthy and infected wild-type and mutant *A. thaliana* lines. The results are expressed as mean ± SD. Infected plants were characterized by reduced growth in every line considered. No difference between wild-type and mutant lines was recorded, nor in healthy or in infected plants. For each condition, 10 different plants were analyzed. Differences between healthy and infected conditions in each line were calculated using unpaired *t*-test. Family-wise significance and confidence level: 0.05. **** P<0.0001. For comparisons among the different lines, two-way ANOVA followed by a Dunnett's test was used, with wild-type values as control. Family-wise significance and confidence level: 0.05. A, a: no significant difference with wild-type values.

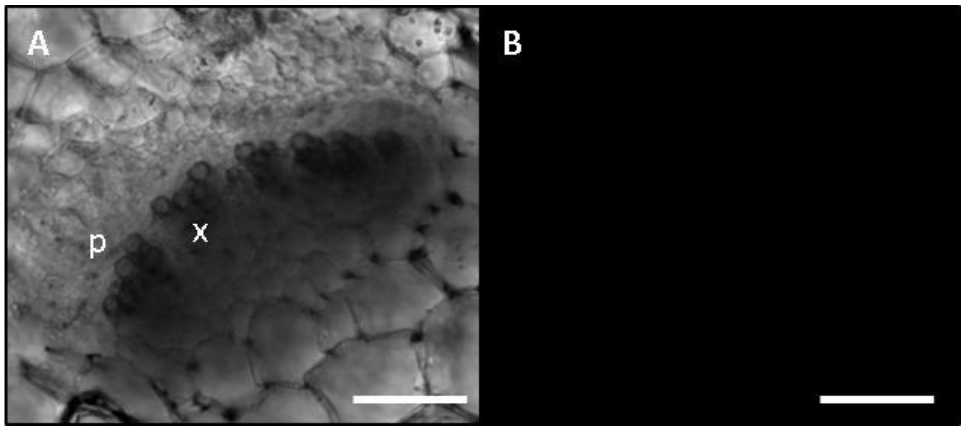

Figure 3. Unstained vibratome section of fresh tissue as staining control. CLSM images of unstained section from healthy wild-type A. *thaliana* midribs were excited at the same wavelength used for the fluorochrome (excitation: 488 nm, emission: 500-545 nm). No autofluorescence signal was detected (B). p: phloem, x: xylem. Bars: 75 µm

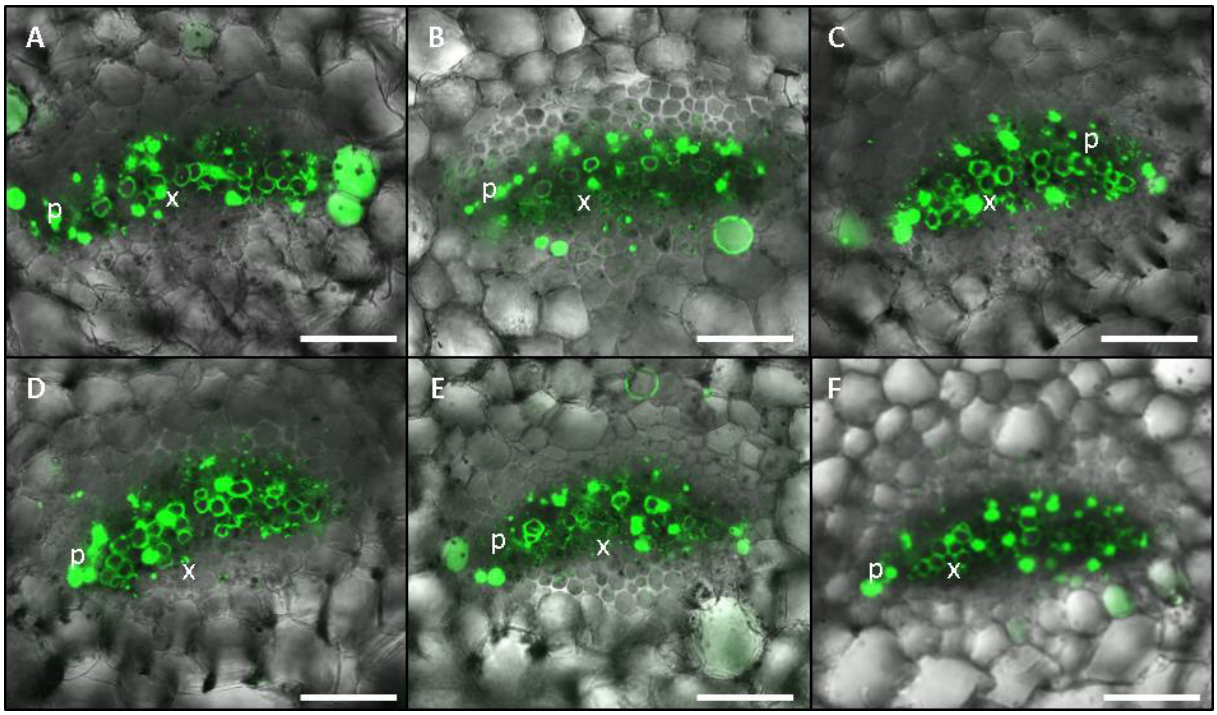

Figure 4. CF fluorescence signal in vibratome sections of fresh tissue of healthy wild-type and mutant *A. thaliana* lines. The fluorescence of CF in the sieve elements of wild type and mutant plants was observed in cross-sections, approximately 3 cm far from the dye application site. In healthy plants, CF emitted a strong signal in correspondence to phloem area in every line considered. For each *A. thaliana* line, 10 non-serial sections from 3 different plants were observed. A. wild-type, B. *Atseor1ko*, C. *Atseor2ko*, D. *Atseor1ko/Atseor2kd*, E. *Atseor1kd/Atseor2ko*, F. *Atpp2-a1ko*. p: phloem, x: xylem. Bars: 75 µm.

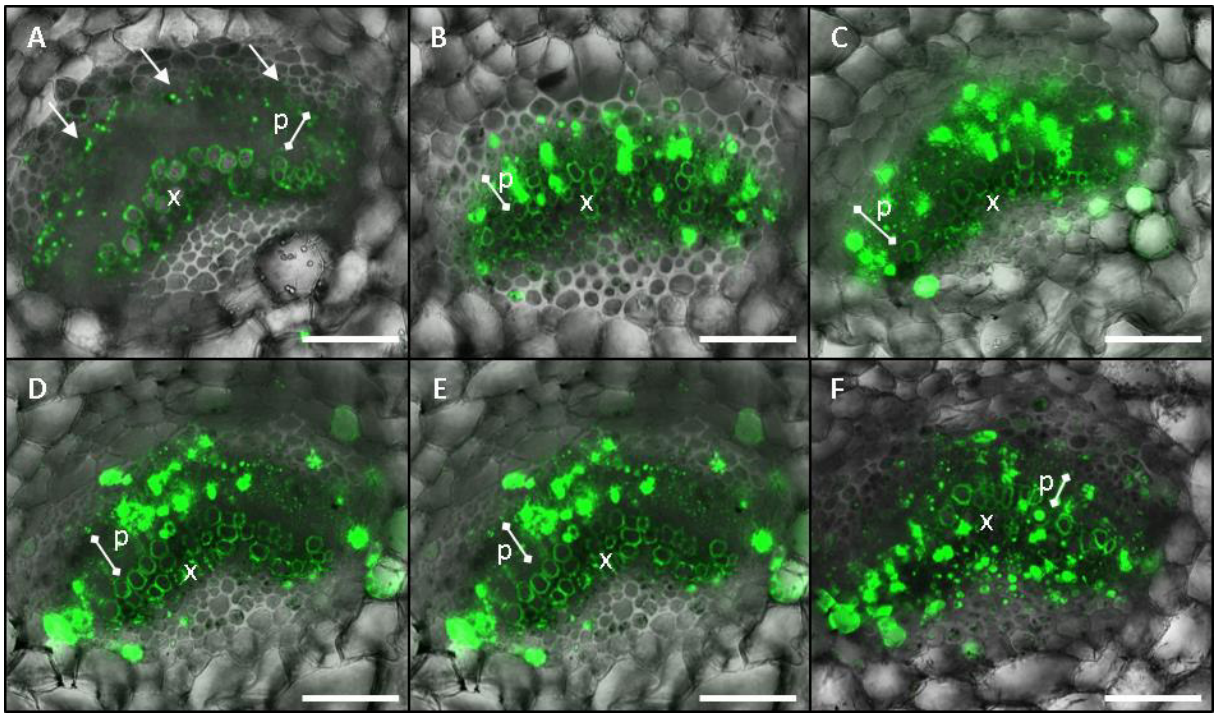

Figure 5. CF fluorescence signal in vibratome sections of fresh tissue of infected wild-type and mutant *A. thaliana* lines. In infected plants, the phloem tissue was larger than one observed in healthy plants (phloem area is indicated by white bar). While in wild-type plants (A) phytoplasma infection drove to a modest CF signal, mutant lines (B-F) showed high fluorescence level and dye accumulation in phloem cells. For each *A. thaliana* line, 10 non-serial sections from 3 different plants were observed A. wild-type, B. *Atseor1ko*, C. *Atseor2ko*, D. *Atseor1ko/Atseor2kd*, E. *Atseor1kd/Atseor2ko*, F. *Atpp2-a1ko*. p: phloem, x: xylem. Bars: 75 µm.

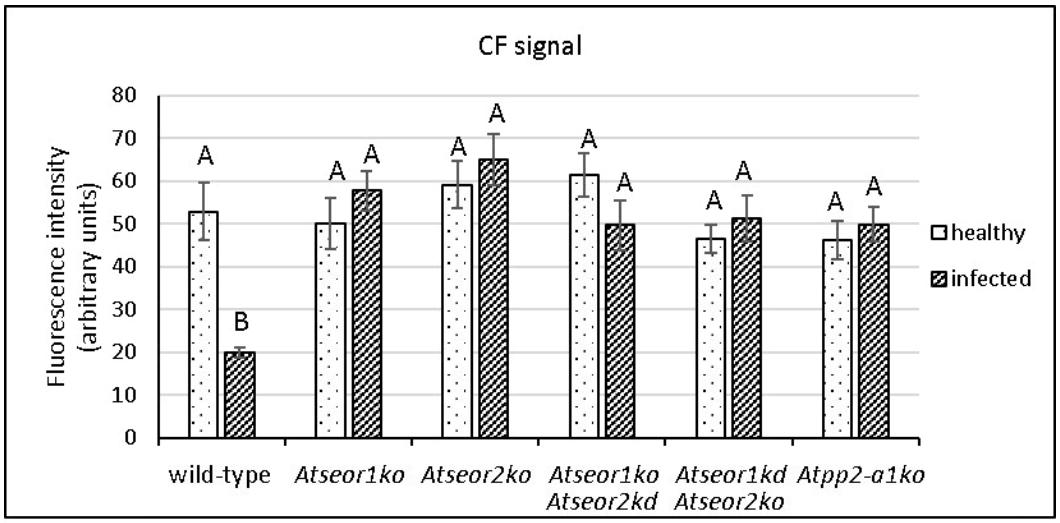

Figure 6. CF fluorescence quantification sections of fresh tissue of healthy and infected wild-type and mutant *A. thaliana* lines. The fluorescence level in the phloem tissue were measured and divided for the analysed surface area. The results are expressed as mean ± SD. While in healthy plants no significant difference was detected, in infected plants wild-type line showed a dramatic drop in CF signal. For each condition, 5 non-serial sections from 5 different plants were analyzed. One-way ANOVA followed by a Dunnett's test was used to determine significance, with healthy wild-type values as control. Family-wise significance and confidence level: 0.05. Different letters indicate different significance levels: A: no significant difference with wild-type values, B: $P < 0.01$.

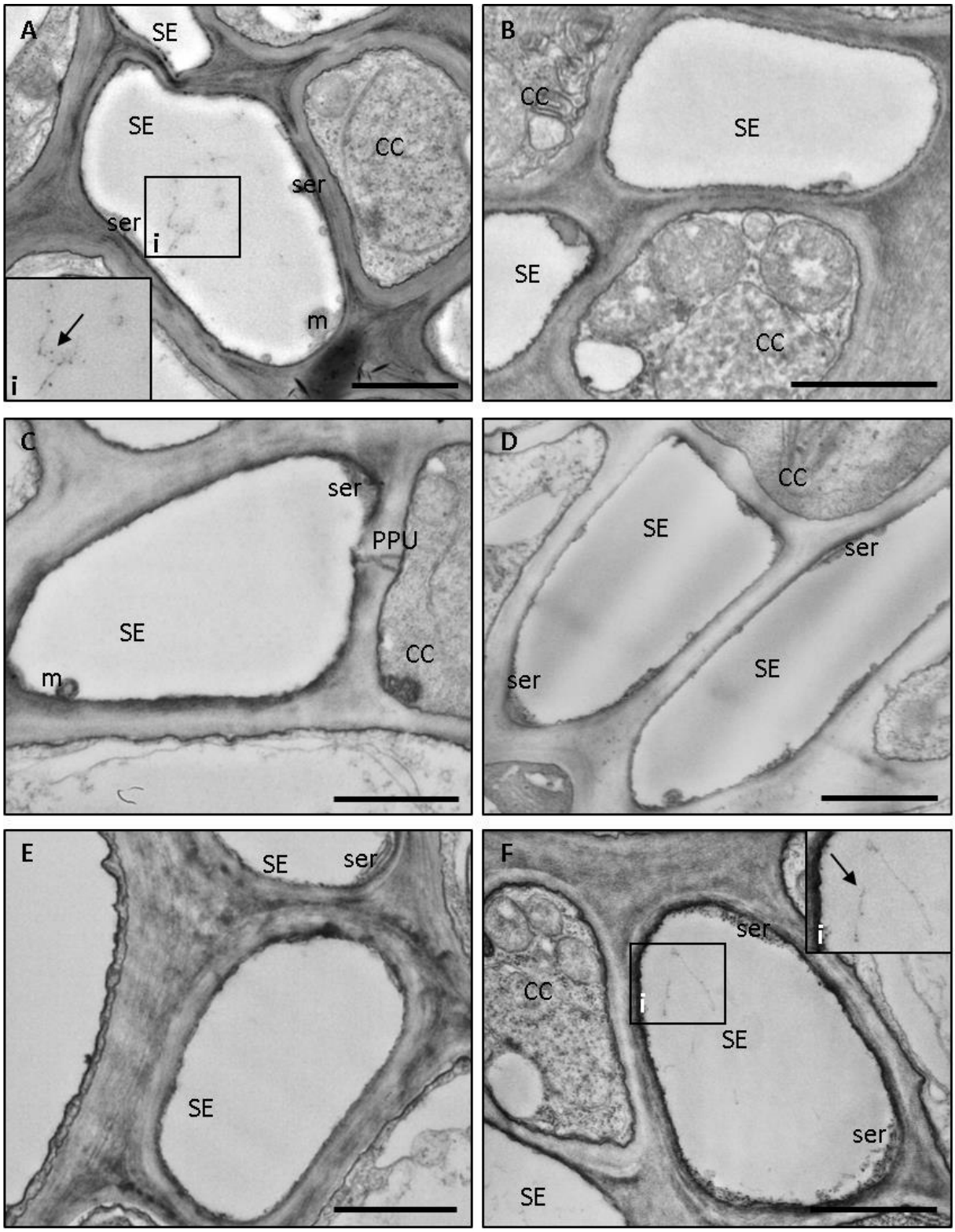

Figure 7. TEM micrographs of sieve elements in different healthy *A. thaliana* lines. Different *A. thaliana* lines were indicated as follows: A. wild-type, B. *Atseor1ko*, C. *Atseor2ko*, D. *Atseor1ko/Atseor2kd*, E. *Atseor1kd/Atseor2ko*, F. *Atpp2-a1ko*. Healthy samples presented unaltered phloem tissue, also in case of transformed plants (B-F). In wild-type (A) and in *Atpp2-a1ko* plants (F), some protein filaments were observed (arrows, insets). On the other hand, lumina of mutants lacking one or both *AtSEOR* genes (B-E) appeared empty, without any sign of filament formation. For each condition, 5 non-serial sections from 10 different plants were analyzed. CC: companion cell; m: mitochondrion; PPU: pore plasmodesma unit; SE: sieve element; ser: sieve-element reticulum. Bars: 1 µm.

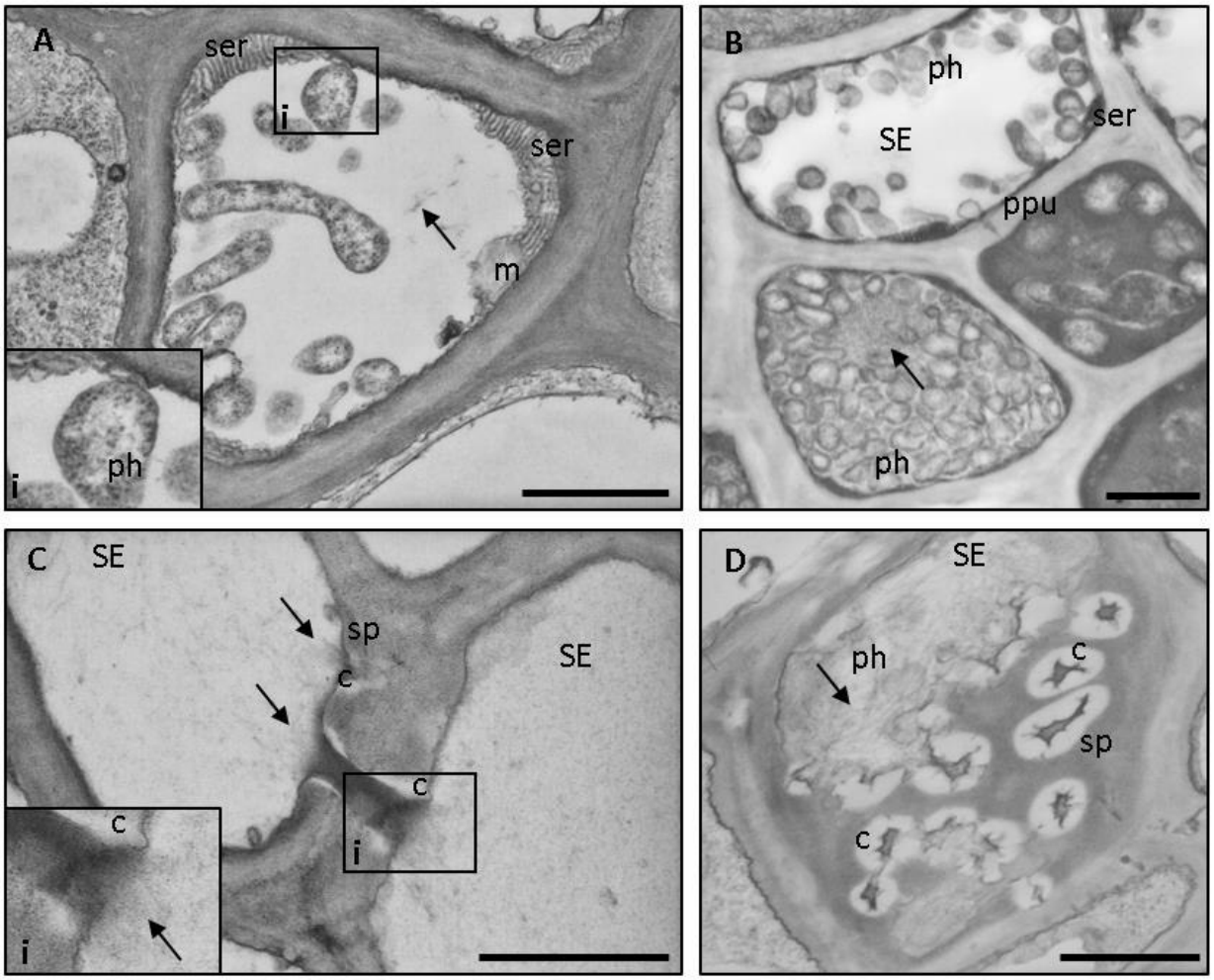

Figure 8. Phytoplasma distribution and ultrastructural responses in sieve tubes of wild-type *A. thaliana* plants. Phytoplasmas presented their typical pleomorphic profile, delimited by an electron-dense membrane, holding dispersed DNA strands and ribosome granules (A, inset). While some phytoplasmas were observed free-floating in the SE lumen (A, B), others established a connection with the host cell at plasma membrane or sieve-element reticulum (SER) stack level (A, B). Plants responded to the infection with alterations at ultrastructural level, such as callose accumulation at sieve pores level (C, D), and SE-protein filament condensation (arrows). SE-protein filaments formed networks with different organization and density (B), that can plug pores at the sieve plates (C, inset). 5 non-serial sections from 10 different plants were analyzed. c: callose; CC: companion cell; m: mitochondrion; ph: phytoplasma; PPU: pore plasmodesma unit; SE: sieve element; ser: sieve-element reticulum; sp: sieve plate. Bars: 1 µm.

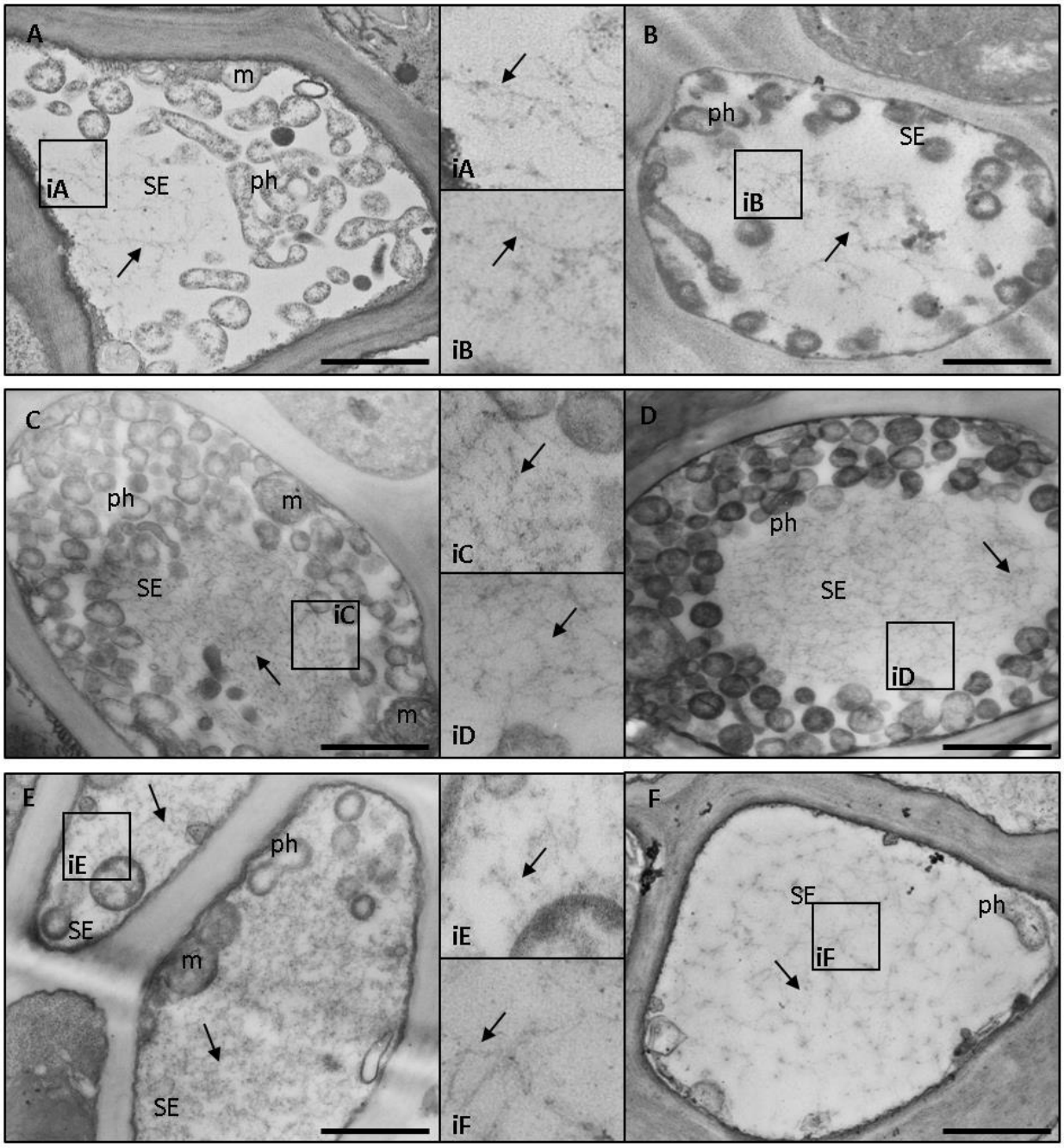

Figure 9. TEM micrographs of sieve elements in different infected *A. thaliana* lines. Different *A. thaliana* lines were indicated as follows: A. wild-type, B. *Atseor1ko*, C. *Atseor2ko*, D. *Atseor1ko/Atseor2kd*, E. *Atseor1kd/Atseor2ko*, F. *Atpp2-a1ko*. In infected tissue, wild-type (A) and *Atpp2-a1ko* (F). SEs showed a massive presence of agglutinated SE-protein filaments (arrows, insets). Also in *A. thaliana* lines lacking one or both *AtSEOR* genes (B-E), infected SEs showed filaments with morphology and organization similar to those observed in wild-type plants (arrows, insets). For each condition, 5 non-serial sections from 10 different plants were analyzed. CC: companion cell; m: mitochondrion; ph: phytoplasma; SE: sieve element. Bars: 1 µm.

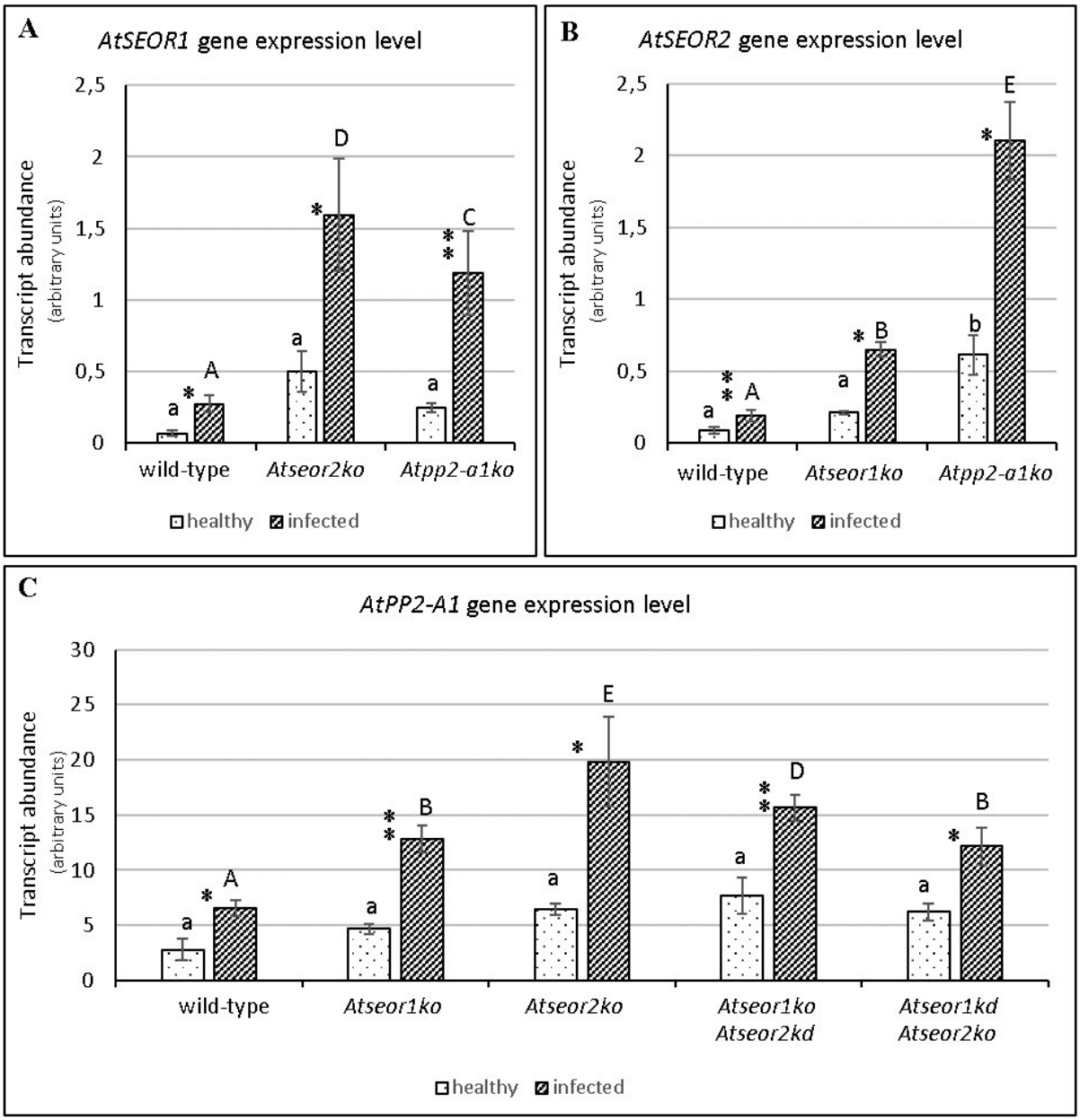

Figure 10. Gene expression level of healthy and infected wild-type and mutant *A. thaliana* lines. The expression of *AtSEOR1* (A), *AtSEOR2* (B) and *AtPP2-A1* (C) genes was analysed in healthy and infected plants of both wild-type and mutant lines by real time RT-PCR experiments. Expression values were normalized to *UBC9* expression level, arbitrarily fixed at 100, then expressed as mean normalized expression ± SD and indicated as transcript abundance. Every gene was significantly up-regulated in infected plants compared to healthy plants. No significant differences were detected among expression levels in healthy plants, except for *AtSEOR2* in *Atpp2-a1ko* plants. In infected plants, each gene showed a significant increase in gene transcription levels in the mutant lines in comparison to the wild-type ones. For each condition, 3 technical repeats from 5 different plants were carried out. Differences between healthy and infected conditions in each line were calculated using unpaired *t*-test. Family-wise significance and confidence level: 0.05. * = P<0.05, ** = P<0.01. For comparisons among the different lines, two-way ANOVA followed by a Dunnett's test was used, with wild-type values as control. Family-wise significance and confidence level: 0.05. Different letters indicate different significance levels. Healthy plants: a: wild-type level, b: P<0.05. Infected plants: A: no significant difference with wild-type values, B: P<0.05, C: P<0.01, D: P< 0.001, E: P<0.0001.

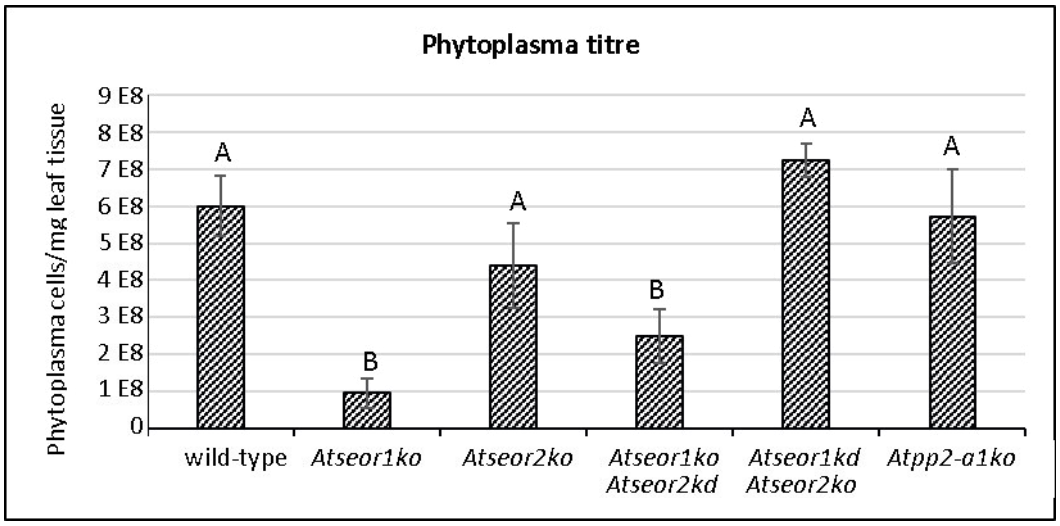

Figure 11. Phytoplasma titre in infected leaves of various sieve-element protein *A. thaliana* mutants. Phytoplasma quantification in the different *A. thaliana* lines was detected by qPCR and expressed as the number of CY phytoplasma genome units (GU)/1 mg of leaf sample. The results are expressed as mean ± SD. Wild-type, *Atseor2ko*, *Atseor1ko/Atseor2k*d and *Atpp2-a1ko* plants were characterized by similar phytoplasma titres, while *Atseor1ko* and *Atseor1ko/Atseor2kd* plants showed lower mean phytoplasma concentrations. In every line, 3 technical repeats from 10 different plants were carried out. One-way ANOVA followed by a Dunnett's test was used to determine significance, with wild-type values as control. Family-wise significance and confidence level: 0.05. Different letters indicate different significance levels: A: no significant difference with wild-type values, B: $P < 0.0001$

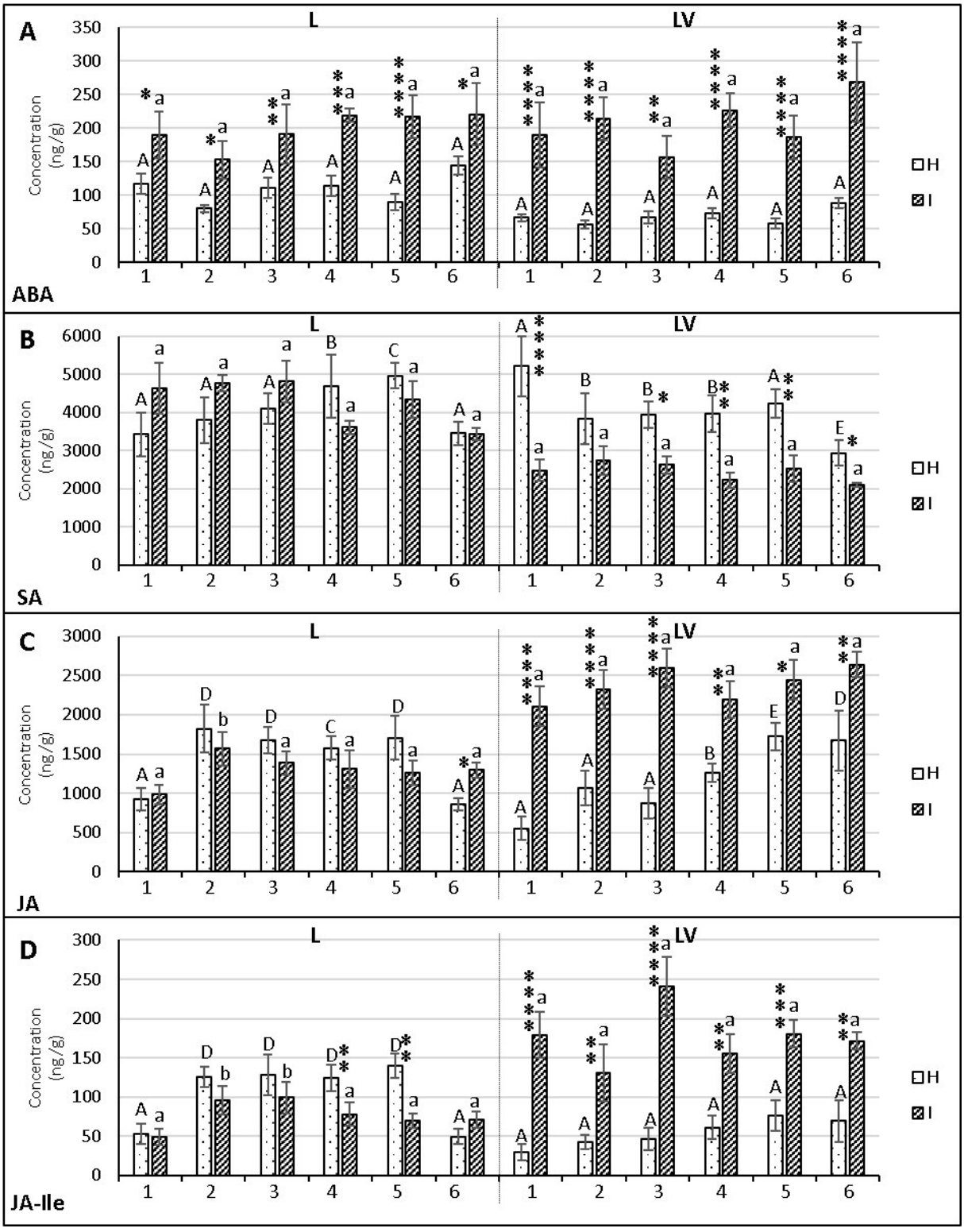

Figure 12. Phytohormone analysis of midrib and laminar tissue. The phytohormones were analysed in the leaves deprived of the midrib (L) and in leaf veins (LV), each in healthy (H) and infected (I) condition. The results are expressed as mean ± SD, calculated as ng phytohormone per g of dried plant tissue. Different *A. thaliana* lines were indicated as follows: 1. wild-type, 2. *Atseor1ko*, 3. *Atseor2ko*, 4. *Atseor1ko/Atseor2kd*, 5. *Atseor1kd/Atseor2ko*, 6. *Atpp2-a1ko.* Following infection, ABA level increased in both tissue types and every *A. thaliana* line (A). SA concentration decreased in leaf vein tissue (B), while JA (C) and JA-Ile (D) levels rose. On the other hand, the level of these three hormones remained unaltered in leaf tissue deprived of main veins.

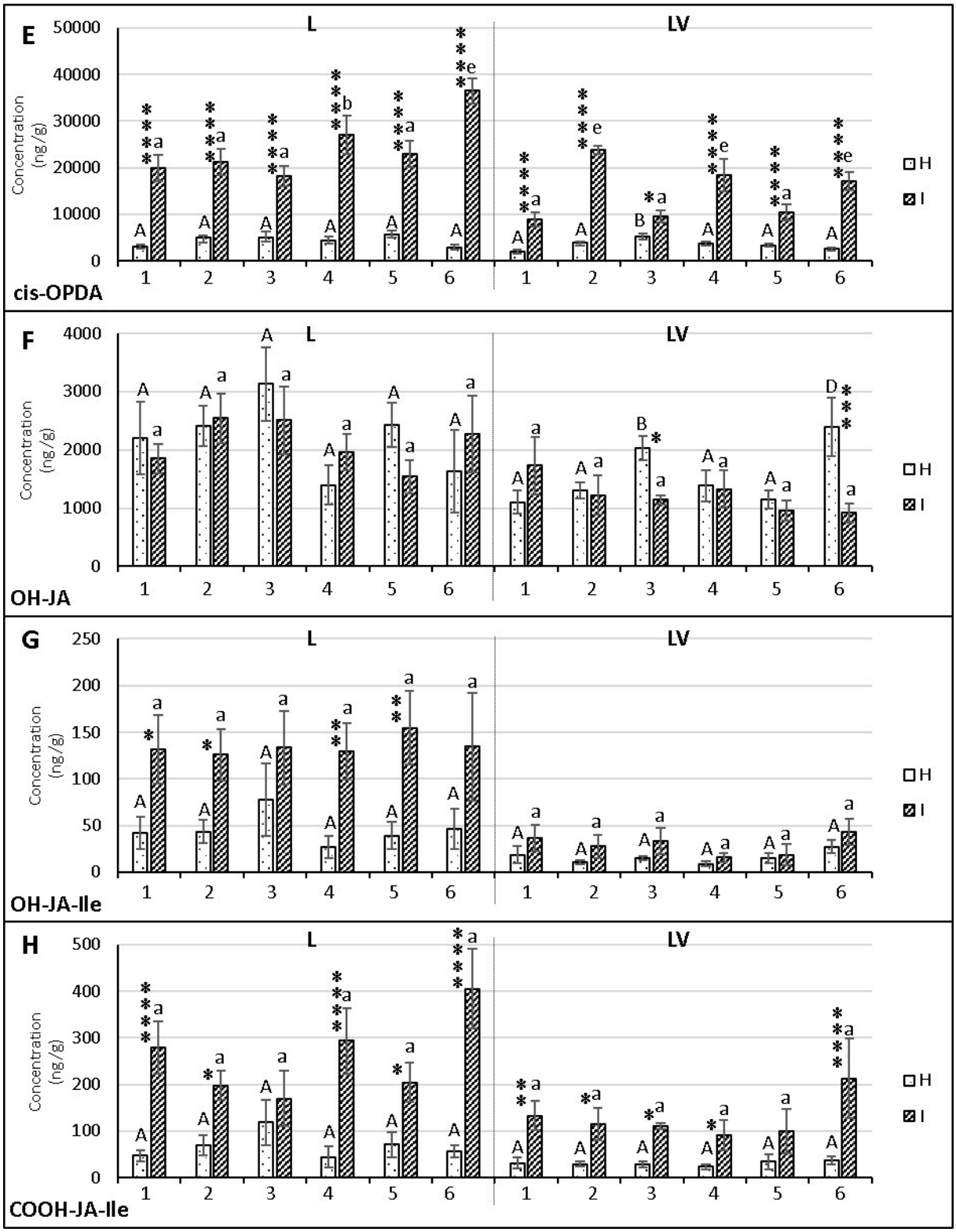

Figure 12. Phytohormone analysis (continued). *cis*-OPDA levels oscillated without a clear pattern, increasing following phytoplasma infection (E). OH-JA concentration values were characterized by a considerable oscillation (F). Both in healthy and in infected plants, OH-JA-Ile (G) and COOH-JA-Ile (H) presented a lower concentration in midribs than in other part of the leaf. Following phytoplasma infection a considerable raise occurred only in leaf deprived of main vein (OH-JA-Ile) or in the whole tissue (COOH-JA-Ile). For each condition, 5 different plants were analyzed. Differences between healthy and infected conditions in each line were calculated using unpaired *t*-test (results were marked with *). For comparisons among the different lines, two-way ANOVA followed by a Dunnett's test was used, with wild-type values as control (results are marked with different letters). Family-wise significance and confidence level (in both tests): 0.05. a, A: no

significant difference with wild-type values; b, B,*: P<0.05; c, C, **: P<0.01; d, D, ***: P< 0.001; e, E, ****: P<0.0001.

			mean (ng/g dried tissue)								standard deviation (ng/g dried tissue)							
			ABA	SA	JA	JA-Ile	cis-OPDA	OH-JA	OH-JA-Ile	COOH-JA-Ile	ABA	SA	JA	JA-Ile	cis-OPDA	OH-JA	OH-JA-Ile	COOH-JA-Ile
wild-type	L	H	117,02	3426,40	918,96	53,14	3017,00	2202,83	42,36	46,92	30,02	1154,21	284,85	26,43	951,82	1242,73	34,43	22,01
		I	190,31	4630,45	982,31	49,56	19945,64	1856,45	131,81	279,46	69,54	1345,85	240,76	20,69	5536,69	500,40	73,90	112,34
	LV	H	66,57	5215,54	551,49	29,72	1956,78	1102,33	18,69	31,74	10,80	1585,90	301,71	19,65	701,07	393,83	17,42	24,04
		I	189,56	2487,03	2105,40	178,89	8936,49	1731,87	37,00	133,31	97,92	557,04	503,20	58,11	2921,31	975,64	28,19	62,70
Atseor1ko	L	H	80,20	3802,13	1822,27	125,62	5053,63	2413,08	43,26	69,27	10,38	1203,52	610,23	26,24	2437,99	688,81	24,48	41,78
		I	152,87	4775,81	1568,43	96,03	21215,95	2544,12	125,79	197,19	55,59	432,78	432,08	36,60	5498,64	853,17	55,20	62,59
	LV	H	56,48	3845,77	1066,17	42,94	3865,97	1311,15	10,66	29,55	11,28	1339,36	430,62	18,72	1154,47	280,18	3,64	9,66
		I	214,36	2754,25	2323,06	131,19	23738,22	1223,11	27,46	115,17	63,22	743,66	491,47	72,72	1783,64	675,20	24,64	69,54
Atseor2ko	L	H	111,53	4105,96	1678,75	128,38	4972,06	3132,86	77,65	119,25	30,23	787,16	332,02	52,62	1580,85	1260,78	76,78	97,16
		I	191,33	4814,45	1385,08	99,04	18218,12	2506,41	133,54	169,80	87,93	1109,86	295,39	40,01	4379,43	1154,86	78,44	118,74
	LV	H	66,95	3947,04	869,28	46,39	5209,60	2025,36	15,14	28,75	18,99	703,10	387,03	27,56	1231,15	414,19	3,80	13,83
		I	156,51	2625,05	2593,28	240,75	9606,20	1142,11	33,61	110,89	63,57	439,66	497,28	76,00	2638,54	166,83	28,40	13,97
Atseor1ko Atseor2kd	L	H	114,11	4696,65	1577,77	124,23	4406,28	1397,01	27,20	44,68	29,57	1656,37	287,24	33,02	1551,83	685,67	23,64	44,38
		I	219,09	3615,02	1307,06	78,18	27123,93	1956,86	129,11	293,72	19,65	334,27	479,36	28,88	8231,41	618,08	60,67	140,81
	LV	H	73,34	3968,82	1260,50	61,33	3594,79	1385,32	8,86	23,82	15,43	945,82	220,80	29,55	848,64	533,47	5,42	10,99
		I	226,75	2230,30	2195,56	154,93	18380,55	1325,28	15,72	91,20	50,69	388,85	460,35	49,17	6983,47	633,68	9,32	64,81
Atseor1kd Atseor2ko	L	H	90,51	4968,84	1705,98	139,49	5707,36	2429,08	39,10	70,75	23,95	674,53	557,20	31,11	1418,68	753,16	28,66	54,97
		I	217,15	4352,60	1262,17	69,70	22933,79	1540,16	154,67	204,05	64,03	964,81	318,10	17,96	5779,23	575,58	78,96	83,43
	LV	H	58,13	4233,36	1723,75	76,00	3305,28	1145,42	15,04	34,02	16,58	729,07	354,61	38,88	629,54	302,75	10,23	30,85
		I	186,49	2534,38	2441,07	180,65	10352,77	962,46	18,46	99,64	65,03	706,03	505,84	34,78	3495,53	345,93	22,82	96,12
Atpp2-a1ko	L	H	144,96	3452,33	859,16	49,73	2791,00	1628,85	45,94	56,62	26,97	630,11	154,03	18,20	798,23	1412,56	42,98	26,85
		I	220,62	3446,18	1294,85	71,39	36450,35	2270,34	134,48	405,22	92,38	328,27	193,71	21,17	5496,34	1317,76	116,27	169,90
	LV	H	88,28	2940,54	1673,19	69,43	2569,11	2390,12	27,24	36,84	14,82	678,13	763,34	53,70	749,98	1008,42	13,66	16,32
		I	268,51	2099,98	2638,09	171,59	17111,75	919,79	43,43	212,60	118,49	113,57	327,28	23,27	4031,35	332,40	28,09	171,31

Figure S1. Phytohormone analysis. The phytohormones were analysed in the leaves deprived of the midrib (L) and in leaf veins (LV), in healthy (H) and infected (I) conditions. Mean and SD were calculated as ng phytohormone per g of dried plant tissue. For each condition, 5 different plants were analyzed.

Literature

Achor, D. S., Etxeberria, E., Wang, N., Folimonova, S. Y., Chung, K. R., & Albrigo, L. G. (2010). Citrus affected with huanglongbing disease. *Plant Pathol J*, *9*, 56-64.

Afzal, A. J., Kim, J. H., & Mackey, D. (2013). The role of NOI-domain containing proteins in plant immune signaling. *BMC genomics*, *14*(1), 1.

Altschul, S. F., Madden, T. L., Schäffer, A. A., Zhang, J., Zhang, Z., Miller, W., & Lipman, D. J. (1997). Gapped BLAST and PSI-BLAST: a new generation of protein database search programs. *Nucleic acids research*, *25*(17), 3389-3402.

Anstead, J. A., Froelich, D. R., Knoblauch, M., & Thompson, G. A. (2012). Arabidopsis SE protein filament formation requires both AtSEOR1 and AtSEOR2. *Plant and Cell Physiology*, *53*(6), 1033-1042.

Bacci, S., Pieri, L., Buccoliero, A. M., Bonelli, A., Taddei, G., & Romagnoli, P. (2008). Smooth muscle cells, dendritic cells and mast cells are sources of TNFalpha and nitric oxide in human carotid artery atherosclerosis. *Thrombosis research*, *122*(5), 657-667.

Bánó, M., & Marek, J. (2006). How thick is the layer of thermal volume surrounding the protein?. *Biophysical chemistry*, *120*(1), 44-54.

Batailler, B., Lemaitre, T., Vilaine, F., Sanchez, C., Renard, D., Cayla, T., ... & Dinant, S. (2012). Soluble and filamentous proteins in Arabidopsis sieve elements. *Plant, cell & environment*, *35*(7), 1258-1273.

Bertaccini, A., & Duduk, B. (2009). Phytoplasma and phytoplasma diseases: a review of recent research. *Phytopathologia mediterranea*, *48*(3), 355-378.

Bertaccini, A., Duduk, B., Paltrinieri, S., & Contaldo, N. (2014). Phytoplasmas and phytoplasma diseases: a severe threat to agriculture. *American Journal of Plant Sciences*, *5*:1763–1788.

Bertamini, M., Grando, M. S., Muthuchelian, K., & Nedunchezhian, N. (2002a). Effect of phytoplasmal infection on photosystem II efficiency and thylakoid membrane protein changes in field grown apple (Malus pumila) leaves. *Physiological and molecular plant pathology*, *61*(6), 349-356.

Bertamini, M., Nedunchezhian, N., Tomasi, F., & Grando, M. S. (2002b). Phytoplasma [Stolbur-subgroup (Bois Noir-BN)] infection inhibits photosynthetic pigments, ribulose-1, 5-bisphosphate carboxylase and photosynthetic activities in field grown grapevine (Vitis vinifera L. cv. Chardonnay) leaves. *Physiological and Molecular Plant Pathology*, *61*(6), 357-366.

Bosco, D., Galetto, L., Leoncini, P., Saracco, P., Raccah, B., & Marzachì, C. (2007). Interrelationships between “Candidatus Phytoplasma asteris” and its leafhopper vectors (Homoptera: Cicadellidae). *Journal of economic entomology*, *100*(5), 1504-1511.

Bosco, D., Minucci, C., Boccardo, G., & Conti, M. (1997). Differential acquisition of chrysanthemum yellows phytoplasma by three leafhopper species. *Entomologia Experimentalis et Applicata*, *83*(2), 219-224.

Bradford, M. M. (1976). A rapid and sensitive method for the quantitation of microgram quantities of protein utilizing the principle of protein-dye binding. *Analytical biochemistry*, *72*(1-2), 248-254.

Braun, E. J., & Sinclair, W. A. (1978). Translocation in phloem necrosis-diseased American elm seedlings. *Phytopathology*, *68*(12), 1733-1737.

Buxa, S. V., Degola, F., Polizzotto, R., De Marco, F., Loschi, A., Kogel, K. H., ... & Musetti, R. (2015). Phytoplasma infection in tomato is associated with re-organization of plasma membrane, ER stacks, and actin filaments in sieve elements. *Frontiers in plant science*, *6*, 650-660.

Dar, T. A., Uddin, M., Khan, M. M. A., Hakeem, K. R., & Jaleel, H. (2015). Jasmonates counter plant stress: a review. *Environmental and Experimental Botany*, *115*, 49-57.

Dave, A., & Graham, I. A. (2012). Oxylipin signaling: a distinct role for the jasmonic acid precursor *cis*-(+)-12-oxo-phytodienoic acid (*cis*-OPDA). *Lipid signaling in plants*, *3*(42), 140.

De Marco, F., Pagliari, L., Degola, F., Buxa, S. V., Loschi, A., Dinant, S., ... & Musetti, R. (2016). Combined microscopy and molecular analyses show phloem occlusions and cell wall modifications in tomato leaves in response to 'Candidatus Phytoplasma solani'. *Journal of Microscopy, 263* (2), 212-225.

Doyle, J. J., & Doyle, J. L. (1990). DNA extraction from Arabidopsis. *Focus*, *12*, 13-15.

Ehlers, K., Knoblauch, M., & Van Bel, A. J. E. (2000). Ultrastructural features of well-preserved and injured sieve elements: minute clamps keep the phloem transport conduits free for mass flow. *Protoplasma*, *214*(1-2), 80-92.

Ernst, A. M., Jekat, S. B., Zielonka, S., Müller, B., Neumann, U., Rüping, B., ... & Noll, G. A. (2012). Sieve element occlusion (SEO) genes encode structural phloem proteins involved in wound sealing of the phloem. *Proceedings of the National Academy of Sciences*, *109*(28), E1980-E1989.

Ernst, A. M., Rüping, B., Jekat, S. B., Nordzieke, S., Reineke, A. R., Müller, B., ... & Noll, G. A. (2011). The sieve element occlusion gene family in dicotyledonous plants. *Plant signaling & behavior*, *6*(1), 151-153.

Evert, R. F., Eschrich, W., & Eichhorn, S. E. (1972). SE protein distribution in mature sieve elements of Cucurbita maxima. *Planta*, *109*(3), 193-210.

Foyer, C. H., & Noctor, G. (2005). Redox homeostasis and antioxidant signaling: a metabolic interface between stress perception and physiological responses. *The Plant Cell*, *17*(7), 1866-1875.

Foyer, C. H., Rasool, B., Davey, J. W., & Hancock, R. D. (2016). Cross-tolerance to biotic and abiotic stresses in plants: a focus on resistance to aphid infestation. *Journal of experimental botany*, *67*(7), 2025-2037.

Froelich, D. R., Mullendore, D. L., Jensen, K. H., Ross-Elliott, T. J., Anstead, J. A., Thompson, G. A., ... & Knoblauch, M. (2011). Phloem ultrastructure and pressure flow: sieve-element-occlusion-related agglomerations do not affect translocation. *The Plant Cell*, *23*(12), 4428-4445.

Furch, A. C., Hafke, J. B., Schulz, A., & van Bel, A. J. (2007). Ca2+-mediated remote control of reversible sieve tube occlusion in Vicia faba. *Journal of Experimental Botany*, *58*(11), 2827-2838.

Furch, A. C., van Bel, A. J., Fricker, M. D., Felle, H. H., Fuchs, M., & Hafke, J. B. (2009). Sieve element Ca2+ channels as relay stations between remote stimuli and sieve tube occlusion in Vicia faba. *The Plant Cell*, *21*(7), 2118-2132.

Furch, A. C., Zimmermann, M. R., Will, T., Hafke, J. B., & Van Bel, A. J. (2010). Remote-controlled stop of phloem mass flow by biphasic occlusion in Cucurbita maxima. *Journal of experimental botany*, *61*(13), 3697-3708.

Gamalero, E., D'Amelio, R., Musso, C., Cantamessa, S., Pivato, B., D'Agostino, G., ... & Berta, G. (2010). Effects of Pseudomonas putida S1Pf1Rif against chrysanthemum yellows phytoplasma infection. *Phytopathology*, *100*(8), 805-813.

Garcia-Chapa, M., Medina, V., Viruel, M. A., Lavina, A., & Batlle, A. (2003). Seasonal detection of pear decline phytoplasma by nested-PCR in different pear cultivars. *Plant pathology*, *52*(4), 513-520.

Gierth, M., & Mäser, P. (2007). Potassium transporters in plants–involvement in K+ acquisition, redistribution and homeostasis. *FEBS letters*, *581*(12), 2348-2356.

Gundersen, D. E., & Lee, I. M. (1996). Ultrasensitive detection of phytoplasmas by nested-PCR assays using two universal primer pairs. *Phytopathologia mediterranea*, *35*, 144-151.

Hafke, J. B., Ehlers, K., Föller, J., Höll, S. R., Becker, S., & van Bel, A. J. (2013). Involvement of the sieve element cytoskeleton in electrical responses to cold shocks. *Plant physiology*, *162*(2), 707-719.

Hren, M., Nikolić, P., Rotter, A., Blejec, A., Terrier, N., Ravnikar, M., ... & Gruden, K. (2009). 'Bois noir'phytoplasma induces significant reprogramming of the leaf transcriptome in the field grown grapevine. *BMC genomics*, *10*(1), 1.

Janik, K., Mithöfer, A., Raffeiner, M., Stellmach, H., Hause, B., & Schlink, K. (2016). An effector of apple proliferation phytoplasma targets TCP transcription factors—a generalized virulence strategy of phytoplasma?. *Molecular plant pathology*. doi:10.1111/mpp.12409

Jekat, S. B., Ernst, A. M., von Bohl, A., Zielonka, S., Twyman, R. M., Noll, G. A., & Prüfer, D. (2013). P-proteins in Arabidopsis are heteromeric structures involved in rapid sieve tube sealing. *Frontiers in plant science*, *4*, 225.

Ji, X., Gai, Y., Zheng, C., & Mu, Z. (2009). Comparative proteomic analysis provides new insights into mulberry dwarf responses in mulberry (Morus alba L.). *Proteomics*, *9*(23), 5328-5339.

Junqueira, A., Bedendo, I., & Pascholati, S. (2004). Biochemical changes in corn plants infected by the maize bushy stunt phytoplasma. *Physiological and Molecular Plant Pathology*, *65*(4), 181-185.

Kartte, S., & Seemüller, E. (1991). Susceptibility of grafted Malus taxa and hybrids to apple proliferation disease. *Journal of Phytopathology*, *131*(2), 137-148.

Kawakatsu, T., Yamamoto, M. P., Touno, S. M., Yasuda, H., & Takaiwa, F. (2009). Compensation and interaction between RISBZ1 and RPBF during grain filling in rice. *The Plant Journal*, *59*(6), 908-920.

Kazan, K., & Lyons, R. (2014). Intervention of phytohormone pathways by pathogen effectors. *The Plant Cell*, *26*(6), 2285-2309.

Knoblauch, M., & van Bel, A. J. (1998). Sieve tubes in action. *The Plant Cell*, *10*(1), 35-50.

Knoblauch, M., Froelich, D. R., Pickard, W. F., & Peters, W. S. (2014). SEORious business: structural proteins in sieve tubes and their involvement in sieve element occlusion. *Journal of experimental botany*, *65*(7), 1879-1893.

Knoblauch, M., Noll, G. A., Müller, T., Prüfer, D., Schneider-Hüther, I., Scharner, D., ... & Peters, W. S. (2003). ATP-independent contractile proteins from plants. *Nature materials*, *2*(9), 600-603.

Knoblauch, M., Peters, W. S., Ehlers, K., & van Bel, A. J. (2001). Reversible calcium-regulated stopcocks in legume sieve tubes. *The Plant Cell*, *13*(5), 1221-1230.

Knoblauch, M., Stubenrauch, M., Van Bel, A. J., & Peters, W. S. (2012). Forisome performance in artificial sieve tubes. *Plant, cell & environment*, *35*(8), 1419-1427.

Koh, E. J., Zhou, L., Williams, D. S., Park, J., Ding, N., Duan, Y. P., & Kang, B. H. (2012). Callose deposition in the phloem plasmodesmata and inhibition of phloem transport in citrus leaves infected with “Candidatus Liberibacter asiaticus”. *Protoplasma*, *249*(3), 687-697.

Koornneef, A., & Pieterse, C. M. (2008). Cross talk in defense signaling. *Plant physiology*, *146*(3), 839-844.

Lee, I. M., Bertaccini, A., Vibio, M., & Gundersen, D. E. (1995). Detection of multiple phytoplasmas in perennial fruit trees with decline symptoms in Italy. *Phytopathology*, *85*(6), 728-735.

Lee, I. M., Davis, R. E., & Gundersen-Rindal, D. E. (2000). Phytoplasma: Phytopathogenic Mollicutes 1. *Annual Reviews in Microbiology*, *54*(1), 221-255.

Lee, I. M., Gundersen-Rindal, D. E., Davis, R. E., Bottner, K. D., Marcone, C., & Seemüller, E. (2004). ‘Candidatus Phytoplasma asteris’, a novel phytoplasma taxon associated with aster yellows and related diseases. *International journal of systematic and evolutionary microbiology*, *54*(4), 1037-1048.

Lee, I. M., Martini, M., Bottner, K. D., Dane, R. A., Black, M. C., & Troxclair, N. (2003). Ecological implications from a molecular analysis of phytoplasmas involved in an aster yellows epidemic in various crops in Texas. *Phytopathology*, *93*(11), 1368-1377.

Leon, R., Santamaria, J. M., Alpizar, L., Escamilla, J. A., & Oropeza, C. (1996). Physiological and biochemical changes in shoots of coconut palms affected by lethal yellowing. *New Phytologist*, *134*(2), 227-234.

Lepka, P., Stitt, M., Moll, E., & Seemüller, E. (1999). Effect of phytoplasmal infection on concentration and translocation of carbohydrates and amino acids in periwinkle and tobacco. *Physiological and Molecular Plant Pathology*, *55*(1), 59-68.

Lherminier, J., Benhamou, N., Larrue, J., Milat, M. L., Boudon-Padieu, E., Nicole, M., & Blein, J. P. (2003). Cytological characterization of elicitin-induced protection in tobacco plants infected by Phytophthora parasitica or phytoplasma. *Phytopathology*, *93*(10), 1308-1319.

Loake, G., & Grant, M. (2007). Salicylic acid in plant defence—the players and protagonists. *Current opinion in plant biology*, *10*(5), 466-472.

Luge, T., Kube, M., Freiwald, A., Meierhofer, D., Seemüller, E., & Sauer, S. (2014). Transcriptomics assisted proteomic analysis of Nicotiana occidentalis infected by Candidatus Phytoplasma mali strain AT. *Proteomics*, *14*(16), 1882-1889.

MacKenzie, D. J., McLean, M. A., Mukerji, S., & Green, M. (1997). Improved RNA extraction from woody plants for the detection of viral pathogens by reverse transcription-polymerase chain reaction. *Plant Disease*, *81*(2), 222-226.

Martini, M., Lee, I. M., Bottner, K. D., Zhao, Y., Botti, S., Bertaccini, A., ... & Osler, R. (2007). Ribosomal protein gene-based phylogeny for finer differentiation and classification of phytoplasmas. *International Journal of Systematic and Evolutionary Microbiology*, *57*(9), 2037-2051.

Martini, M., Musetti, R., Grisan, S., Polizzotto, R., Borselli, S., Pavan, F., & Osler, R. (2009). DNA-dependent detection of the grapevine fungal endophytes Aureobasidium pullulans and Epicoccum nigrum. *Plant Disease*, *93*(10), 993-998.

Maust, B. E., Espadas, F., Talavera, C., Aguilar, M., Santamaría, J. M., & Oropeza, C. (2003). Changes in carbohydrate metabolism in coconut palms infected with the lethal yellowing phytoplasma. *Phytopathology*, *93*(8), 976-981.

Miersch, O., Neumerkel, J., Dippe, M., Stenzel, I., & Wasternack, C. (2008). Hydroxylated jasmonates are commonly occurring metabolites of jasmonic acid and contribute to a partial switch-off in jasmonate signaling. *New Phytologist*, *177*(1), 114-127.

Minato, N., Himeno, M., Hoshi, A., Maejima, K., Komatsu, K., Takebayashi, Y., ... & Kamiya, Y. (2014). The phytoplasmal virulence factor TENGU causes plant sterility by downregulating of the jasmonic acid and auxin pathways. *Scientific reports*, *4*, 1399

Mou, H. Q., Lu, J., Zhu, S. F., Lin, C. L., Tian, G. Z., Xu, X., & Zhao, W. J. (2013). Transcriptomic analysis of paulownia infected by paulownia witches'-broom phytoplasma. *PLoS One*, *8*(10), e77217.

Muller, P. Y., Janovjak, H., Miserez, A. R., & Dobbie, Z. (2002). Short technical report processing of gene expression data generated by quantitative Real-Time RT-PCR. *Biotechniques*, *32*(6), 1372-1379.

Musetti, R., Buxa, S. V., De Marco, F., Loschi, A., Polizzotto, R., Kogel, K. H., & van Bel, A. J. (2013). Phytoplasma-triggered Ca2+ influx is involved in sieve-tube blockage. *Molecular Plant-Microbe Interactions*, *26*(4), 379-386.

Musetti, R., Pagliari, L., Buxa, S. V., Degola, F., De Marco, F., Loschi, A., ... & van Bel, A. J. (2016). OHMS**: Phytoplasmas dictate changes in sieve-element ultrastructure to accommodate their requirements for nutrition, multiplication and translocation. *Plant signaling & behavior*, *11*(2), e1138191.

Musetti, R., Paolacci, A., Ciaffi, M., Tanzarella, O. A., Polizzotto, R., Tubaro, F., ... & Osler, R. (2010). Phloem cytochemical modification and gene expression following the recovery of apple plants from apple proliferation disease. *Phytopathology*, *100*(4), 390-399.

Nakamura, Y., Mithöfer, A., Kombrink, E., Boland, W., Hamamoto, S., Uozumi, N., ... & Ueda, M. (2011). 12-Hydroxyjasmonic acid glucoside is a COI1-JAZ-independent activator of leaf-closing movement in Samanea saman. *Plant physiology*, *155*(3), 1226-1236.

Namba, S. (2011). Phytoplasmas: a century of pioneering research. *Journal of General Plant Pathology*, *77*(6), 345-349.

Osler, R., Borselli, S., Ermacora, P., Ferrini, F., Loschi, A., Martini, M., ... & Loi, N. (2016). Transmissible tolerance to European stone fruit yellows (ESFY) in apricot: cross-protection or a plant mediated process?. *Phytoparasitica*, *44,* 203-211.

Osler, R., Borselli, S., Ermacora, P., Loschi, A., Martini, M., Musetti, R., & Loi, N. (2014). Acquired tolerance in apricot plants that stably recovered from European stone fruit yellows. *Plant Disease*, *98*(4), 492-496.

Pagliari, L., Martini, M., Loschi, A., & Musetti, R. (2016). Looking inside phytoplasma-infected sieve elements: A combined microscopy approach using Arabidopsis thaliana as a model plant. *Micron*, *89*, 87-97.

Park, S. W., Li, W., Viehhauser, A., He, B., Kim, S., Nilsson, A. K., ... & Esker, A. R. (2013). Cyclophilin 20-3 relays a 12-oxo-phytodienoic acid signal during stress responsive regulation of cellular redox homeostasis. *Proceedings of the National Academy of Sciences*, *110*(23), 9559-9564.

Patui, S., Bertolini, A., Clincon, L., Ermacora, P., Braidot, E., Vianello, A., & Zancani, M. (2013). Involvement of plasma membrane peroxidases and oxylipin pathway in the recovery from phytoplasma disease in apple (Malus domestica). *Physiologia plantarum*, *148*(2), 200-213.

Peleg, Z., & Blumwald, E. (2011). Hormone balance and abiotic stress tolerance in crop plants. *Current opinion in plant biology*, *14*(3), 290-295.

Pelissier, H. C., Peters, W. S., Collier, R., van Bel, A. J., & Knoblauch, M. (2008). GFP tagging of sieve element occlusion (SEO) proteins results in green fluorescent forisomes. *Plant and Cell Physiology*, *49*(11), 1699-1710.

Pfaffl, M. W. (2001). A new mathematical model for relative quantification in real-time RT–PCR. *Nucleic acids research*, *29*(9), e45-e45.

Pieterse, C. M., Leon-Reyes, A., Van der Ent, S., & Van Wees, S. C. (2009). Networking by small-molecule hormones in plant immunity. *Nature chemical biology*, *5*(5), 308-316.

Punelli, F., Al Hassan, M., Fileccia, V., Uva, P., Pasquini, G., & Martinelli, F. (2016). A microarray analysis highlights the role of tetrapyrrole pathways in grapevine responses to “stolbur” phytoplasma, phloem virus infections and recovered status. *Physiological and Molecular Plant Pathology*, *93*, 129-137.

Ramundo, S., Casero, D., Mühlhaus, T., Hemme, D., Sommer, F., Crèvecoeur, M., ... & Pellegrini, M. (2014). Conditional depletion of the Chlamydomonas chloroplast ClpP protease activates nuclear genes involved in autophagy and plastid protein quality control. *The Plant Cell*, *26*(5), 2201-2222.

Robert-Seilaniantz, A., Grant, M., & Jones, J. D. (2011). Hormone crosstalk in plant disease and defense: more than just jasmonate-salicylate antagonism. *Annual review of phytopathology*, *49*, 317-343.

Rüping, B., Ernst, A. M., Jekat, S. B., Nordzieke, S., Reineke, A. R., Müller, B., ... & Noll, G. A. (2010). Molecular and phylogenetic characterization of the sieve element occlusion gene family in Fabaceae and non-Fabaceae plants. *BMC plant biology*, *10*(1), 219.

Schneider, A., Häusler, R. E., Kolukisaoglu, Ü., Kunze, R., Van Der Graaff, E., Schwacke, R., ... & Flügge, U. I. (2002). An Arabidopsis thaliana knock-out mutant of the chloroplast triose phosphate/phosphate translocator is severely compromised only when starch synthesis, but not starch mobilisation is abolished. *The Plant Journal*, *32*(5), 685-699.

Sjolund, R. D. (1997). The phloem sieve element: a river runs through it. *The Plant Cell*, *9*(7), 1137.

Srivastava, V. K., Tuteja, R., & Tuteja, N. (2015). Calcium-energized motor protein forisome controls damage in phloem: potential applications as biomimetic “smart” material. *Critical reviews in biotechnology*, *35*(2), 173-183.

Stintzi, A. & Browse, J. (2000). The Arabidopsis male-sterile mutant, opr3, lacks the 12-oxophytodienoic acid reductase required for jasmonate synthesis. *Proceedings of the National Academy of Sciences*, *97*(19), 10625-10630.

Sugio, A., MacLean, A. M., Grieve, V. M., & Hogenhout, S. A. (2011). Phytoplasma protein effector SAP11 enhances insect vector reproduction by manipulating plant development and defense hormone biosynthesis. *Proceedings of the National Academy of Sciences*, *108*(48), E1254-E1263.

Taheri, F., Nematzadeh, G., Zamharir, M. G., Nekouei, M. K., Naghavi, M., Mardi, M., & Salekdeh, G. H. (2011). Proteomic analysis of the Mexican lime tree response to “Candidatus Phytoplasma aurantifolia” infection. *Molecular BioSystems*, *7*(11), 3028-3035.

Vadassery, J., Reichelt, M., Hause, B., Gershenzon, J., Boland, W., & Mithöfer, A. (2012). CML42-mediated calcium signaling coordinates responses to Spodoptera herbivory and abiotic stresses in Arabidopsis. *Plant physiology*, *159*(3), 1159-1175.

Valiunas, V., Wang, H. Z., Li, L., Gordon, C., Valiuniene, L., Cohen, I. S., & Brink, P. R. (2015). A comparison of two cellular delivery mechanisms for small interfering RNA. *Physiological reports*, *3*(2), e12286.

Van Bel, A. J. (2003). The phloem, a miracle of ingenuity. *Plant, Cell & Environment*, *26*(1), 125-149.

Van Bel, A. J., Furch, A. C., Will, T., Buxa, S. V., Musetti, R., & Hafke, J. B. (2014). Spread the news: systemic dissemination and local impact of Ca2+ signals along the phloem pathway. *Journal of experimental botany*, *65*, 1761-1787.

Vandesompele, J., De Preter, K., Pattyn, F., Poppe, B., Van Roy, N., De Paepe, A., & Speleman, F. (2002). Accurate normalization of real-time quantitative RT-PCR data by geometric averaging of multiple internal control genes. *Genome biology*, *3*(7), 1.

Vidhyasekaran, P. (2015). *Plant hormone signaling systems in plant innate immunity* (pp. 27-244). Springer.

Wasternack, C., & Hause, B. (2013). Jasmonates: biosynthesis, perception, signal transduction and action in plant stress response, growth and development. An update to the 2007 review in Annals of Botany. *Annals of botany*, *111*(6), 1021-1058.

Wei, W., Kakizawa, S., Suzuki, S., Jung, H. Y., Nishigawa, H., Miyata, S. I., ... & Namba, S. (2004). In planta dynamic analysis of onion yellows phytoplasma using localized inoculation by insect transmission. *Phytopathology*, *94*(3), 244-250.

Zafari, S., Niknam, V., Musetti, R., & Noorbakhsh, S. N. (2012). Effect of phytoplasma infection on metabolite content and antioxidant enzyme activity in lime (Citrus aurantifolia). *Acta physiologiae plantarum*, *34*(2), 561-568.

Zimmermann, M. R., Schneider, B., Mithöfer, A., Reichelt, M., Seemüller, E., & Furch, A. C. (2015). Implications of Candidatus Phytoplasma mali infection on phloem function of apple trees. *Endocytobiosis and cell research: journal of the International Society of Endocytobiology*, *26*, 67-75.

5. Discussion and conclusions.

Phytoplasmas are unique bacteria that can efficiently colonize and replicate intracellularly in hosts belonging to two different kingdoms. This capability implies the pathogen capability to intimately adapt to host cells and the evolution of mechanisms for manipulation of host cellular processes (Christensen *et al.*, 2005). In plants, phytoplasmas are confined into the phloem tissue, in SEs, specialised enucleated living cells responsible for the phloem flow and the photosynthate translocation (Bertaccini and Duduk., 2009). In infected plants, macroscopic symptoms suggest a strong alteration of phloem functionality (Himeno *et al.*, 2014; Loebenstein *et al.*, 2009), but no specific analyses were carried out to explain this phenomenon and its consequence on phytoplasma fitness. The most promising candidates as cause of phloem impairment are callose deposition and SE-protein filament agglutination (Musetti *et al.*, 2010). While TEM observations clearly documented a clear reduction of the sieve pore lumen by callose deposition (De Marco *et al.*, 2016; Musetti *et al.*, 2010), the role of SE-protein filaments in sieve pore plugging have been remained uncertain, even in physiological conditions (Knoblauch *et al.*, 2014). So, investigating the interaction between phytoplasmas and their host could help in understanding not only the biology of phytoplasmas but also that of the most specialized cells of the phloem.

In the present work, various microscopic techniques, such as Light- (LM), Epifluorescence- (EFM) and Confocal Laser Scanning Microscopy (CLSM) and TEM, were used. The combination of observations from fresh and embedded tissue provides information both on ultrastructural and physiological modifications in SEs following phytoplasma infection.

TEM observations allowed a detailed analysis of site-specific interaction between pathogen and host. While many phytoplasmas were in the SE lumen free-floating or dividing, other phytoplasmas adhered to SE plasma membrane and SER stacks. Even if TEM micrographs represent just fixed shots and no consequential order can be inferred, further information has been gained, confirming what reported and speculated previously (Buxa *et al.*, 2015; Musetti *et al.*, 2016) and individuating another linking site between the two organisms at SER level. The connection structure resulted in a continuity layer between phytoplasma membrane and SER stacks. Even if it was not possible to understand if this structure consists in an open channel or not, SER is considered an important source of proteins and metabolites available for intracellular pathogens (Swanson and Isberg, 1995) and thus represents a convincing candidate for phytoplasma nutrition stores. At the same time, mechanisms different from bulk flow could be supposed considering the fact that phytoplasmas probably rely strongly on the uptake of nutrients by membrane transport processes and in general it is still unclear how

phytoplasmas catch resources from the host for their metabolism, growth and multiplication (Christensen *et al.*, 2005; Saigo *et al.*, 2014; Siewert *et al.*, 2014).

LM and EFM observations completed the symptom examination, demonstrating that *A. thaliana* is a reliable model plant for studying phytoplasma-plant interaction (Pagliari *et al.*, 2016).

A. thaliana has emerged in the last thirty years as model system for research in plant biology and mutant lines are available by request to stock centres (Koornneef and Meinke, 2010). For this project, 5 mutant lines were used, lacking one or two genes related to SE-protein filament (*AtSEOR1* -At3g01680-, *AtSEOR2* -At3g01670- and *AtPP2-A1* -At4g19840-), both in healthy and infected condition.

CLSM observations gave the opportunity to move from a fixed and descriptive point of view to a physiological approach, investigating alleged phytoplasma affection to phloem mass flow. The protocol used didn't alter phloem physiology (Knoblauch *et al.*, 2014), so an effective comparison between healthy (intact) and infected (stressed) plants was possible. On the other hand, mutant lines offered the chance to study the involvement of SE-protein in phloem impairment mechanism. The combined results from CLSM and TEM observations suggested that SE-protein filaments cause phloem impairment only in case of a massive SE-protein production in its wild-type form. The use of both intact and stressed conditions finally matches with previous and opposite records on the topic (Ernst *et al.*, 2012; Froelich *et al.*, 2011; Jekat *et al.*, 2013), confirming SE-protein as a structural protein activated in defence mechanisms. Moreover, comparison between wild-type and mutant lines indicated that SE-protein filaments don't perform a simple mechanical function, but they interact with the surrounding environment. Besides fitting with CSLM images, TEM images also raised another interesting question, showing that that in case of stressful condition SE-protein filament formation can overawed *AtSEOR1* and *AtSEOR2* absence, corroborating the previous hypothesis about a wider protein composition of the SE-protein filament (Ansteadt *et al.*, 2012; Jekat *et al.*, 2013). Even if results obtained by gene expression analysis suggested a possible compensation attempt by the plant, extensive expression analyses, such as mRNA sequencing, are necessary.

In order to study if and how SE-proteins may affect phytoplasmas, molecular and biochemical analyses were also carried out. Gene expression analyses confirmed the SE-protein involvement in phytoplasma infection. Phytoplasma quantification established that does not exist any correlation between phloem impairment and pathogen replication and spread capability, indicating that plant activate other defence mechanisms. For this reason, phytohormone investigation was carried out.

The separation of midrib and the remaining tissue allowed a site-specific study and revealed an increased JA concentration at midrib level in case of infection. Even if it is not possible to exclude

that JA rise is limited to '*Candidatus* Phytoplasma asteris'- *A. thaliana* interaction, the specific analysis of the main veins in other phytoplasma-plant pathosystems confirmed that midrib-specific JA burst is not an isolated phenomenon (Luge *et al.*, 2014; Punelli *et al.*, 2016). The correlation that might intervene between phytoplasma infection and JA defence response is reinforced by the fact that increase in *cis*-OPDA level, the JA precursor, seems to be related to lower phytoplasma titre. However, further experiments are necessary, to confirm the possible relation between JA, *cis*-OPDA, phytoplasma infection and their ability to multiply. Many ways could be followed, but the extensive screening on the expression of JA- and *cis*-OPDA-related defence genes (Jimenez-Aleman *et al.*, 2015) and the use *opr* Arabidopsis mutant lines, lacking the 12-oxophytodienoic acid reductase required for jasmonate synthesis (Stintzi and Browse, 2000), seem to be promising.

Nevertheless, the data obtained with this survey confirm again the infinite complexity of plant-pathogen interaction and how long is still the way for a good comprehension of both phloem and phytoplasma physiology.

6. Acknowledgments.

The multidisciplinary approach adopted in this work required various expertise and different backgrounds and it wouldn't be possible without the support of many people belonging to the scientific community.

Dr. Gundula A. Noll (University of Münster, Münster, Germany) donated seeds of *Atseor1ko/Atseor2kd* and *Atseor1kd/Atseor2ko A. thaliana* mutant lines. The Nottingham Arabidopsis Stock Centre (NASC) community furnished the seeds of the remaining *A. thaliana* lines I used.

Professor Domenico Bosco (University of Torino, Italy) provided the Chrysanthemum yellows (CY) phytoplasma strain and precious advices about insect rearing.

Alberto Loschi (University of Udine, Italy) taught me many greenhouse techniques and supported me in rearing plants and insects, taking care of them with professionality, regardless of holidays and personal commitments, continuously for three years.

Dr. Stefanie Vera Buxa (Justus Liebig University, Giessen, Germany) and Dr. Alexandra Furch (Friedrich Schiller University, Jena, Germany) gave me precious advices for phloem mass flow experiment. Thanks to Dr. Alexandra Furch and Dr. Alex Mithöfer (Max Planck Institute for Chemical Ecology, Jena, Germany), phytohormone investigations were carried out.

Dr. Andrea Genre (University of Torino, Italy) taught me to use confocal laser scanner microscope and hosted me several times in his laboratory for phloem mass flow experiment, demonstrating infinite willingness and patience.

Dr. Simonetta Santi (University of Udine, Italy) introduced and guided me in gene expression study, teaching techniques and supervising the analyses. Sara Buoso (University of Udine, Italy) helped me in setting gene expression experiments, doing part of the analyses and overcoming every trouble we met.

Dr. Marta Martini (University of Udine, Italy) taught me how to perform phytoplasma diagnosis and quantification, supervising the analyses.

Dr. Paolo Ermacora (University of Udine, Italy) economically supported my project, giving to me the possibility to join congresses and courses and to carry out every experiment I considered necessary.

Prof. Aart J. E. van Bel (Justus Liebig University, Giessen, Germany) enriched the project with a critical point of view, allowing me to overwhelm technical and theoretical weaknesses. Moreover, he

carefully read and commented the manuscript of my paper about SE-protein role in case of phytoplasma infection.

I would also like to thank Dr. Alexandra Furch (Friedrich Schiller University, Jena, Germany) and Dr. Sabrina Palmano (Institute of Plant Virology, CNR, Torino, Italy) for serving as my committee members and generously giving their time toward checking and improving my manuscript.

Finally, Dr. Rita Musetti (University of Udine, Italy) not only trained me in electron microscopy methods but supervised my whole Phd project. She has been an affectionate supervisor, present whenever I needed an advice, a critical opinion or some help to overcome crisis situations. At the same time, she encouraged my research, my intuitions and my independence, allowing me to grow as scientist.

I would like to thank each mentioned person, for supporting me in such enthusiastic and unconditional way, sharing with me their time and their knowledge, without underlining my unpreparedness but on the contrary stimulating me to learn and improve my skills.

Considering the fact that this work has involved me not only as a scientist but firstly as a human being, I'm grateful to my colleagues and my family that donated me time, confidence and encouragement, allowing me to take up with serenity this path.

7. Literature.

Ahmad, J. N., Renaudin, J., & Eveillard, S. (2014). Expression of defence genes in stolbur phytoplasma infected tomatoes, and effect of defence stimulators on disease development. *European journal of plant pathology*, *139*(1), 39-51.

Albertazzi, G., Milc, J., Caffagni, A., Francia, E., Roncaglia, E., Ferrari, F., ... & Pecchioni, N. (2009). Gene expression in grapevine cultivars in response to Bois Noir phytoplasma infection. *Plant Science*, *176*(6), 792-804.

Allen, A. K. (1979). A lectin from the exudate of the fruit of the vegetable marrow (Cucurbita pepo) that has a specificity for β-1, 4-linked N-acetylglucosamine oligosaccharides. *Biochemical journal*, *183*(1), 133-137.

Alosi, M. C., Melroy, D. L., & Park, R. B. (1988). The regulation of gelation of phloem exudate from Cucurbita fruit by dilution, glutathione, and glutathione reductase. *Plant Physiology*, *86*(4), 1089-1094.

Anstead, J. A., Froelich, D. R., Knoblauch, M., & Thompson, G. A. (2012). Arabidopsis P-protein filament formation requires both AtSEOR1 and AtSEOR2. *Plant and Cell Physiology*, *53*(6), 1033-1042.

Apel, K., & Hirt, H. (2004). Reactive oxygen species: metabolism, oxidative stress, and signal transduction. *Annu. Rev. Plant Biol.*, *55*, 373-399.

Bai, X., Correa, V. R., Toruño, T. Y., Ammar, E. D., Kamoun, S., & Hogenhout, S. A. (2009). AY-WB phytoplasma secretes a protein that targets plant cell nuclei. *Molecular plant-microbe interactions*, *22*(1), 18-30.

Bai, X., Zhang, J., Ewing, A., Miller, S. A., Radek, A. J., Shevchenko, D. V., ... & Hogenhout, S. A. (2006). Living with genome instability: the adaptation of phytoplasmas to diverse environments of their insect and plant hosts. *Journal of bacteriology*, *188*(10), 3682-3696.

Barratt, D. P., Kölling, K., Graf, A., Pike, M., Calder, G., Findlay, K., ... & Smith, A. M. (2011). Callose synthase GSL7 is necessary for normal phloem transport and inflorescence growth in Arabidopsis. *Plant physiology*, *155*(1), 328-341.

Batailler, B., Lemaitre, T., Vilaine, F., Sanchez, C., Renard, D., Cayla, T., ... & Dinant, S. (2012). Soluble and filamentous proteins in Arabidopsis sieve elements. *Plant, cell & environment*, *35*(7), 1258-1273.

Baxter, A., Mittler, R., & Suzuki, N. (2014). ROS as key players in plant stress signalling. *Journal of experimental botany*, *65*(5), 1229-1240.

Bencharki, B., Boissinot, S., Revollon, S., Ziegler-Graff, V., Erdinger, M., Wiss, L., ... & Brault, V. (2010). Phloem protein partners of Cucurbit aphid borne yellows virus: possible involvement of phloem proteins in virus transmission by aphids. *Molecular plant-microbe interactions*, *23*(6), 799-810.

Beneteau, J., Renard, D., Marché, L., Douville, E., Lavenant, L., Rahbé, Y., ... & Dinant, S. (2010). Binding properties of the N-acetylglucosamine and high-mannose N-glycan PP2-A1 phloem lectin in Arabidopsis. *Plant physiology*, *153*(3), 1345-1361.

Bent, A. F., & Mackey, D. (2007). Elicitors, effectors, and R genes: the new paradigm and a lifetime supply of questions. *Annu. Rev. Phytopathol.*, *45*, 399-436.

Berg, M., Davies, D. L., Clark, M. F., Vetten, H. J., Maie, G., Marcone, C., & Seemüller, E. (1999). Isolation of the gene encoding an immunodominant membrane protein of the apple proliferation phytoplasma, and expression and characterization of the gene product. *Microbiology*, *145*(8), 1937-1943.

Bertaccini, A., & Duduk, B. (2009). Phytoplasma and phytoplasma diseases: a review of recent research. *Phytopathologia mediterranea*, *48*(3), 355-378.

Bertaccini, A., Duduk, B., Paltrinieri, S., & Contaldo, N. (2014). Phytoplasmas and phytoplasma diseases: a severe threat to agriculture. *American Journal of Plant Sciences*, *5*, 763–1788.

Bertamini, M., & Nedunchezhian, N. (2001). Effects of phytoplasma [stolbur-subgroup (Bois noir-BN)] on photosynthetic pigments, saccharides, ribulose 1, 5-bisphosphate carboxylase, nitrate and nitrite reductases, and photosynthetic activities in field-grown grapevine (Vitis vinifera L. cv. Chardonnay) leaves. *Photosynthetica*, *39*(1), 119-122.

Bertamini, M., Grando, M. S., & Nedunchezhian, N. (2003). Effects of phytoplasma infection on pigments, chlorophyll-protein complex and photosynthetic activities in field grown apple leaves. *Biologia plantarum*, *47*(2), 237-242.

Bertamini, M., Grando, M. S., Muthuchelian, K., & Nedunchezhian, N. (2002a). Effect of phytoplasmal infection on photosystem II efficiency and thylakoid membrane protein changes in field grown apple (Malus pumila) leaves. *Physiological and molecular plant pathology*, *61*(6), 349-356.

Bertamini, M., Nedunchezhian, N., Tomasi, F., & Grando, M. S. (2002b). Phytoplasma [Stolbur-subgroup (Bois Noir-BN)] infection inhibits photosynthetic pigments, ribulose-1, 5-bisphosphate carboxylase and photosynthetic activities in field grown grapevine (Vitis vinifera L. cv. Chardonnay) leaves. *Physiological and Molecular Plant Pathology*, *61*(6), 357-366.

Boonrod, K., Munteanu, B., Jarausch, B., Jarausch, W., & Krczal, G. (2012). An immunodominant membrane protein (Imp) of 'Candidatus Phytoplasma mali' binds to plant actin. *Molecular Plant-Microbe Interactions*, *25*(7), 889-895.

Borisy, G. G., & Svitkina, T. M. (2000). Actin machinery: pushing the envelope. *Current opinion in cell biology*, *12*(1), 104-112.

Bosco, D., Galetto, L., Leoncini, P., Saracco, P., Raccah, B., & Marzachì, C. (2007). Interrelationships between "Candidatus Phytoplasma asteris" and its leafhopper vectors (Homoptera: Cicadellidae). *Journal of economic entomology*, *100*(5), 1504-1511.

Bové, J. M., & Garnier, M. (2003). Phloem-and xylem-restricted plant pathogenic bacteria. *Plant Science*, *164*(3), 423-438.

Bowman, J. L. (2013). Walkabout on the long branches of plant evolution. *Current opinion in plant biology, 16*(1), 70-77.

Boyes, D. C., Zayed, A. M., Ascenzi, R., McCaskill, A. J., Hoffman, N. E., Davis, K. R., & Görlach, J. (2001). Growth stage–based phenotypic analysis of Arabidopsis a model for high throughput functional genomics in plants. *The Plant Cell*, *13*(7), 1499-1510.

Braun, E. J., & Sinclair, W. A. (1978). Translocation in phloem necrosis-diseased American elm seedlings. *Phytopathology*, *68*(12), 1733-1737.

Braun, E. J., & Sinclair, W. A. (1979). Phloem necrosis of elms: symptoms and histopathological observations in tolerant hosts. *Phytopathology*, *69*(4), 354-358.

Bressan, A., & Purcell, A. H. (2005). Effect of benzothiadiazole on transmission of X-disease phytoplasma by the vector Colladonus montanus to Arabidopsis thaliana, a new experimental host plant. *Plant Disease*, *89*(10), 1121-1124.

Buxa, S. V., Degola, F., Polizzotto, R., De Marco, F., Loschi, A., Kogel, K. H., ... & Musetti, R. (2015). Phytoplasma infection in tomato is associated with re-organization of plasma membrane, ER stacks, and actin filaments in sieve elements. *Frontiers in plant science*, *6*, 650-660.

Cettul, E., & Firrao, G. (2011). Development of phytoplasma-induced flower symptoms in Arabidopsis thaliana. *Physiological and molecular plant pathology*, *76*(3), 204-211.

Chang, C. J. (1998). Pathogenicity of aster yellows phytoplasma and Spiroplasma citri on periwinkle. *Phytopathology*, *88*(12), 1347-1350.

Chen, X. Y., & Kim, J. Y. (2009). Callose synthesis in higher plants. *Plant signaling & behavior*, *4*(6), 489-492.

Choi, Y. H., Tapias, E. C., Kim, H. K., Lefeber, A. W., Erkelens, C., Verhoeven, J. T. J., ... & Verpoorte, R. (2004). Metabolic discrimination of Catharanthus roseus leaves infected by phytoplasma using 1H-NMR spectroscopy and multivariate data analysis. *Plant Physiology*, *135*(4), 2398-2410.

Christensen, N. M., Axelsen, K. B., Nicolaisen, M., & Schulz, A. (2005). Phytoplasmas and their interactions with hosts. *Trends in plant science*, *10*(11), 526-535.

Clark, A. M., Jacobsen, K. R., Bostwick, D. E., Dannenhoffer, J. M., Skaggs, M. I., & Thompson, G. A. (1997). Molecular characterization of a phloem-specific gene encoding the filament protein, Phloem Protein 1 (PP1), from Cucurbita maxima. *The Plant Journal*, *12*(1), 49-61.

Contaldo, N., Bertaccini, A., Paltrinieri, S., Windsor, H. M., & Windsor, G. D. (2012). Axenic culture of plant pathogenic phytoplasmas. *Phytopathologia Mediterranea*, *51*(3), 607-617.

Cordova, I., Jones, P., Harrison, N. A., & Oropeza, C. (2003). In situ PCR detection of phytoplasma DNA in embryos from coconut palms with lethal yellowing disease. *Molecular Plant Pathology*, *4*(2), 99-108.

Cosgrove, D. J. (2005). Growth of the plant cell wall. *Nature reviews molecular cell biology*, *6*(11), 850-861.

Cronshaw, J., & Esau, K. (1967). Tubular and fibrillar components of mature and differentiating sieve elements. *The Journal of cell biology, 34*(3), 801-815.

Cronshaw, J., & Sabnis, D.D. (1990). Phloem proteins. In *Sieve Elements. Comparative Structure, Induction and Development* (eds H.-D.Behnke & R.D.Sjolund), Springer, Berlin, Germany. 257–283.

Dannenhoffer, J. M., Suhr, R. C., & Thompson, G. A. (2001). Phloem-specific expression of the pumpkin fruit trypsin inhibitor. *Planta*, *212*(2), 155-162.

De Marco, F., Pagliari, L., Degola, F., Buxa, S. V., Loschi, A., Dinant, S., ... & Musetti, R. (2016). Combined microscopy and molecular analyses show phloem occlusions and cell wall modifications in tomato leaves in response to 'Candidatus Phytoplasma solani'. *Journal of Microscopy, 263* (2), 212-225.

Delwiche, C. F., & Cooper, E. D. (2015). The evolutionary origin of a terrestrial flora. *Current Biology*, *25*(19), R899-R910.

Deslandes, L., & Rivas, S. (2012). Catch me if you can: bacterial effectors and plant targets. *Trends in plant science*, *17*(11), 644-655.

Desneux, N., Decourtye, A., & Delpuech, J. M. (2007). The sublethal effects of pesticides on beneficial arthropods. *Annu. Rev. Entomol.*, *52*, 81-106.

Dinant, S., Bonnemain, J. L., Girousse, C., & Kehr, J. (2010). Phloem sap intricacy and interplay with aphid feeding. *Comptes rendus biologies*, *333*(6), 504-515.

Dinant, S., Clark, A. M., Zhu, Y., Vilaine, F., Palauqui, J. C., Kusiak, C., & Thompson, G. A. (2003). Diversity of the superfamily of phloem lectins (phloem protein 2) in angiosperms. *Plant Physiology*, *131*(1), 114-128.

Doi, Y., Terenaka, M., Yora, K., & Asuyama, H. (1967). Mycoplasma or PLTgroup-like microorganisms found in the phloem elements of plants infected with mulberry dwarf, potato witches' broom, aster yellows, or paulownia witches' broom.- *Annals Phytopathological Society Japan, 33*: 259-266.

Douglas, A. E. (2006). Phloem-sap feeding by animals: problems and solutions. *Journal of Experimental Botany*, *57*(4), 747-754.

Doyle, J. J., & Doyle, J. L. (1990). Isolation of plant DNA from fresh tissue. *Focus (Life Technol. Inc.) 12*, 13-15.

Durrant, W. E., & Dong, X. (2004). Systemic acquired resistance. *Annu. Rev. Phytopathol.*, *42*, 185-209.

Ebrahim, S., Usha, K., & Singh, B. (2011). Pathogenesis related (PR) proteins in plant defense mechanism. *Sci Against Microb Pathog*, *2*, 1043-1054.

Ehlers, K., Knoblauch, M., & Van Bel, A. J. E. (2000). Ultrastructural features of well-preserved and injured sieve elements: minute clamps keep the phloem transport conduits free for mass flow. *Protoplasma*, *214*(1-2), 80-92.

Ehya, F., Monavarfeshani, A., Fard, E. M., Farsad, L. K., Nekouei, M. K., Mardi, M., & Salekdeh, G. H. (2013). Phytoplasma-responsive microRNAs modulate hormonal, nutritional, and stress signalling pathways in Mexican lime trees. *PloS one*, *8*(6), e66372.

Ernst, A. M., Jekat, S. B., Zielonka, S., Müller, B., Neumann, U., Rüping, B., ... & Noll, G. A. (2012). Sieve element occlusion (SEO) genes encode structural phloem proteins involved in wound sealing of the phloem. *Proceedings of the National Academy of Sciences*, *109*(28), E1980-E1989.

Ernst, A. M., Rüping, B., Jekat, S. B., Nordzieke, S., Reineke, A. R., Müller, B., ... & Noll, G. A. (2011). The sieve element occlusion gene family in dicotyledonous plants. *Plant signaling & behavior*, *6*(1), 151-153.

Esau, K. (1969). The phloem. Encyclopedia of plant anatomy. *Gebrüder Borntraegger, Berlin-Stuttgart*.

Evert, R. F., Eschrich, W., & Eichhorn, S. E. (1972). P-protein distribution in mature sieve elements of Cucurbita maxima. *Planta*, *109*(3), 193-210.

Favali, M.A., di Toppi, L. S., Vestena, C., Fossati, F., & Musetti R. (2001) Phytoplasmas associated with tomato stolbur disease. *Acta Hortic 551*:93–99.

Fisher, D. B. (1975). Structure of functional soybean sieve elements. *Plant Physiology*, 56(5), 555-569.

Froelich, D. R., Mullendore, D. L., Jensen, K. H., Ross-Elliott, T. J., Anstead, J. A., Thompson, G. A., ... & Knoblauch, M. (2011). Phloem ultrastructure and pressure flow: sieve-element-occlusion-related agglomerations do not affect translocation. *The Plant Cell*, *23*(12), 4428-4445.

Fu, Z. Q., & Dong, X. (2013). Systemic acquired resistance: turning local infection into global defense. *Annual review of plant biology*, *64*, 839-863.

Fukumorita, T., & Chino, M. (1982). Sugar, amino acid and inorganic contents in rice phloem sap. *Plant and Cell Physiology*, *23*(2), 273-283.

Furch, A. C., Hafke, J. B., & van Bel, A. J. (2008). Plant-and stimulus-specific variations in remote-controlled sieve-tube occlusion. *Plant signaling & behavior*, *3*(10), 858-861.

Furch, A. C., Hafke, J. B., Schulz, A., & van Bel, A. J. (2007). Ca2+-mediated remote control of reversible sieve tube occlusion in Vicia faba. *Journal of Experimental Botany*, *58*(11), 2827-2838.

Furch, A. C., Zimmermann, M. R., Kogel, K. H., Reichelt, M., & Mithöfer, A. (2014). Direct and individual analysis of stress-related phytohormone dispersion in the vascular system of Cucurbita maxima after flagellin 22 treatment. *New Phytologist*, *201*(4), 1176-1182.

Furch, A. C., Zimmermann, M. R., Will, T., Hafke, J. B., & van Bel, A. J. (2010). Remote-controlled stop of phloem mass flow by biphasic occlusion in Cucurbita maxima. *Journal of experimental botany*, *61*(13), 3697-3708.

Gai, Y. P., Li, Y. Q., Guo, F. Y., Yuan, C. Z., Mo, Y. Y., Zhang, H. L., ... & Ji, X. L. (2014). Analysis of phytoplasma-responsive sRNAs provide insight into the pathogenic mechanisms of mulberry yellow dwarf disease. *Scientific reports*, *4*.

Galetto, L., Bosco, D., Balestrini, R., Genre, A., Fletcher, J., & Marzachì, C. (2011). The major antigenic membrane protein of "Candidatus Phytoplasma asteris" selectively interacts with ATP synthase and actin of leafhopper vectors. *PLoS One*, *6*(7), e22571.

Gamalero, E., D'Amelio, R., Musso, C., Cantamessa, S., Pivato, B., D'Agostino, G., ... & Berta, G. (2010). Effects of Pseudomonas putida S1Pf1Rif against chrysanthemum yellows phytoplasma infection. *Phytopathology*, *100*(8), 805-813.

Garcia-Chapa, M., Medina, V., Viruel, M. A., Lavina, A., & Batlle, A. (2003). Seasonal detection of pear decline phytoplasma by nested-PCR in different pear cultivars. *Plant pathology*, *52*(4), 513-520.

Garcion, C., Eveillard, S., & Renaudin, J. (2014). Characterisation of the tolerance to the beet leafhopper transmitted virescence agent phytoplasma in the PI128655 accession of Solanum peruvianum. *Annals of Applied Biology*, *165*(2), 236-248.

Giorno, F., Guerriero, G., Biagetti, M., Ciccotti, A. M., & Baric, S. (2013). Gene expression and biochemical changes of carbohydrate metabolism in in vitro micro-propagated apple plantlets infected by 'Candidatus Phytoplasma mali'. *Plant physiology and biochemistry*, *70*, 311-317.

Gundersen, D. E., & Lee, I. M. (1996). Ultrasensitive detection of phytoplasmas by nested-PCR assays using two universal primer pairs. *Phytopathologia mediterranea, 35*, 144-151.

Hafke, J. B., Ehlers, K., Föller, J., Höll, S. R., Becker, S., & van Bel, A. J. (2013). Involvement of the sieve element cytoskeleton in electrical responses to cold shocks. *Plant physiology*, *162*(2), 707-719.

Haglund, C. M., & Welch, M. D. (2011). Pathogens and polymers: microbe–host interactions illuminate the cytoskeleton. *The Journal of cell biology*, *195*(1), 7-17.

Heo, J. O., Roszak, P., Furuta, K. M., & Helariutta, Y. (2014). Phloem development: current knowledge and future perspectives. *American journal of botany*, *101*(9), 1393-1402.

Hijaz, F., & Killiny, N. (2014). Collection and chemical composition of phloem sap from Citrus sinensis L. Osbeck (sweet orange). *PloS one*, *9*(7), e101830.

Himeno, M., Kitazawa, Y., Yoshida, T., Maejima, K., Yamaji, Y., Oshima, K., & Namba, S. (2014). Purple top symptoms are associated with reduction of leaf cell death in phytoplasma-infected plants. *Scientific reports*, *4*. 4111.

Hoffmann, M. H. (2002). Biogeography of Arabidopsis thaliana (l.) heynh. (Brassicaceae). *Journal of Biogeography*, *29*(1), 125-134.

Hogenhout, S. A., & Loria, R. (2008). Virulence mechanisms of Gram-positive plant pathogenic bacteria. *Current opinion in plant biology*, *11*(4), 449-456.

Hogenhout, S. A., & Segura, M. (2010). Phytoplasma genomics, from sequencing to comparative and functional genomics-What have we learnt. *Phytoplasmas: genomes, plant hosts and vectors*, 19-36.

Hogenhout, S. A., Oshima, K., Ammar, E. D., Kakizawa, S., Kingdom, H. N., & Namba, S. (2008). Phytoplasmas: bacteria that manipulate plants and insects. *Molecular Plant Pathology*, *9*(4), 403-423.

Hogenhout, S.A., & Music, M. (2010). Phytoplasma genomics, from sequencing to comparative and functional genomics: what have we learnt? In: Weintraub, P.G., Jones, P. (Eds.), Phytoplasmas: Genomes, Plant Hosts and Vectors. CABI, Wallingford, UK, 19–36.

Hoshi, A., Oshima, K., Kakizawa, S., Ishii, Y., Ozeki, J., Hashimoto, M., ... & Namba, S. (2009). A unique virulence factor for proliferation and dwarfism in plants identified from a phytopathogenic bacterium. *Proceedings of the National Academy of Sciences*, *106*(15), 6416-6421.

Hren, M., Nikolić, P., Rotter, A., Blejec, A., Terrier, N., Ravnikar, M., ... & Gruden, K. (2009). 'Bois noir'phytoplasma induces significant reprogramming of the leaf transcriptome in the field grown grapevine. *BMC genomics*, *10*(1), 1.

Huala, E., Dickerman, A. W., Garcia-Hernandez, M., Weems, D., Reiser, L., LaFond, F., ... & Mueller, L. A. (2001). The Arabidopsis Information Resource (TAIR): a comprehensive database and web-based information retrieval, analysis, and visualization system for a model plant. *Nucleic acids research*, *29*(1), 102-105.

Iriti, M., Quaglino, F., Maffi, D., Casati, P., Bianco, P. A., & Faoro, F. (2008). Solanum malacoxylon, a new natural host of stolbur phytoplasma. *Journal of phytopathology*, *156*(1), 8-14.

IRPCM, P., & Spiroplasma, W. T. P. T. G. (2004). 'Candidatus Phytoplasma', a taxon for the wall-less, non-helical prokaryotes that colonize plant phloem and insects. *International Journal of Systematic and Evolutionary Microbiology*, *54*(Pt 4), 1243.

Janik, K., Mithöfer, A., Raffeiner, M., Stellmach, H., Hause, B., & Schlink, K. (2016). An effector of apple proliferation phytoplasma targets TCP transcription factors—a generalized virulence strategy of phytoplasma?. *Molecular plant pathology*. doi:10.1111/mpp.12409

Jekat, S. B., Ernst, A. M., von Bohl, A., Zielonka, S., Twyman, R. M., Noll, G. A., & Prüfer, D. (2013). P-proteins in Arabidopsis are heteromeric structures involved in rapid sieve tube sealing. *Frontiers in plant science*, *4*, 225.

Ji, X., Gai, Y., Zheng, C., & Mu, Z. (2009). Comparative proteomic analysis provides new insights into mulberry dwarf responses in mulberry (Morus alba L.). *Proteomics*, *9*(23), 5328-5339.

Jimenez-Aleman, G. H., Scholz, S. S., Heyer, M., Reichelt, M., Mithöfer, A., & Boland, W. (2015). Synthesis, metabolism and systemic transport of a fluorinated mimic of the endogenous jasmonate precursor OPC-8: 0. *Biochimica et Biophysica Acta (BBA)-Molecular and Cell Biology of Lipids*, *1851*(12), 1545-1553.

Jomantiene, R., Zhao, Y., Lee, M., & Davis, R. E. (2011). Phytoplasmas infecting sour cherry and lilac represent two distinct lineages having close evolutionary affinities with clover phyllody phytoplasma. *European Journal of Plant Pathology*, *130*(1), 97-107.

Jones, J. D., & Dangl, J. L. (2006). The plant immune system. *Nature*, *444*(7117), 323-329.

Junqueira, A., Bedendo, I., & Pascholati, S. (2004). Biochemical changes in corn plants infected by the maize bushy stunt phytoplasma. *Physiological and Molecular Plant Pathology*, *65*(4), 181-185.

Kakizawa, S., Oshima, K., & Namba, S. (2006). Diversity and functional importance of phytoplasma membrane proteins. *Trends in microbiology*, *14*(6), 254-256.

Katagiri, F., & Tsuda, K. (2010). Understanding the plant immune system. *Molecular plant-microbe interactions*, *23*(12), 1531-1536.

Kaul, S., Koo, H. L., Jenkins, J., Rizzo, M., Rooney, T., Tallon, L. J., ... & Town, C. D. (2000). Analysis of the genome sequence of the flowering plant Arabidopsis thaliana. *nature*, *408*(6814), 796-815.

Kazan, K., & Lyons, R. (2014). Intervention of phytohormone pathways by pathogen effectors. *The Plant Cell*, *26*(6), 2285-2309.

Kempers, R., & van Bel, A. J. (1997). Symplasmic connections between sieve element and companion cell in the stem phloem of Vicia faba L. have a molecular exclusion limit of at least 10 kDa. *Planta*, *201*(2), 195-201.

Knoblauch, M., & Oparka, K. (2012). The structure of the phloem–still more questions than answers. *The Plant Journal*, *70*(1), 147-156.

Knoblauch, M., & Peters, W. S. (2004). Forisomes, a novel type of Ca2+-dependent contractile protein motor. *Cell motility and the cytoskeleton*, *58*(3), 137-142.

Knoblauch, M., & van Bel, A. J. (1998). Sieve tubes in action. *The Plant Cell*, *10*(1), 35-50.

Knoblauch, M., Froelich, D. R., Pickard, W. F., & Peters, W. S. (2014). SEORious business: structural proteins in sieve tubes and their involvement in sieve element occlusion. *Journal of experimental botany*, *65*(7), 1879-1893.

Knoblauch, M., Noll, G. A., Müller, T., Prüfer, D., Schneider-Hüther, I., Scharner, D., ... & Peters, W. S. (2003). ATP-independent contractile proteins from plants. *Nature materials*, *2*(9), 600-603.

Knoblauch, M., Peters, W. S., Ehlers, K., & van Bel, A. J. (2001). Reversible calcium-regulated stopcocks in legume sieve tubes. *The Plant Cell*, *13*(5), 1221-1230.

Komor, E., Orlich, G., Weig, A., & Köckenberger, W. (1996). Phloem loading—not metaphysical, only complex: towards a unified model of phloem loading. *Journal of experimental botany*, *47*(Special Issue), 1155-1164.

Koornneef, M., & Meinke, D. (2010). The development of Arabidopsis as a model plant. *The Plant Journal*, *61*(6), 909-921.

Kudla, J., Batistič, O., & Hashimoto, K. (2010). Calcium signals: the lead currency of plant information processing. *The Plant Cell*, *22*(3), 541-563.

Lamb, C., & Dixon, R. A. (1997). The oxidative burst in plant disease resistance. *Annual review of plant biology*, *48*(1), 251-275.

Lee, I. M., Davis, R. E., & Gundersen-Rindal, D. E. (2000). Phytoplasma: Phytopathogenic Mollicutes 1. *Annual Reviews in Microbiology*, *54*(1), 221-255.

Lee, I. M., Gundersen-Rindal, D. E., & Bertaccini, A. (1998). Phytoplasma: ecology and genomic diversity. *Phytopathology*, *88*(12), 1359-1366.

Lee, I. M., Gundersen-Rindal, D. E., Davis, R. E., Bottner, K. D., Marcone, C., & Seemüller, E. (2004a). 'Candidatus Phytoplasma asteris', a novel phytoplasma taxon associated with aster yellows and related diseases. *International journal of systematic and evolutionary microbiology*, *54*(4), 1037-1048.

Lee, I. M., Klopmeyer, M., Bartoszyk, I. M., Gundersen-Rindal, D. E., Chou, T. S., Thomson, K. L., & Eisenreich, R. (1997). Phytoplasma induced free-branching in commercial poinsettia cultivars. *Nature biotechnology*, *15*(2), 178-182.

Lee, I. M., Zhao, Y., Davis, R. E., Wei, W., Martini, M., Bertaccini, A., & Maini, S. (2007). Prospects of DNA-based systems for differentiation and classification of phytoplasmas. *Bulletin of Insectology*, *60*(2), 239-244.

Lee, I.M., Martini, M., Marcone, C., & Zhu, S. F. (2004b). Classification of phytoplasma strains in the elm yellows group (16SrV) and proposal of 'Candidatus Phytoplasma ulmi' for the phytoplasma associated with elm yellows. *International Journal of Systematic and Evolutionary Microbiology*, *54*(2), 337-347.

Lee, J. R., Boltz, K. A., & Lee, S. Y. (2014). Molecular chaperone function of Arabidopsis thaliana phloem protein 2-A1, encodes a protein similar to phloem lectin. *Biochemical and biophysical research communications*, *443*(1), 18-21.

Lepka, P., Stitt, M., Moll, E., & Seemüller, E. (1999). Effect of phytoplasmal infection on concentration and translocation of carbohydrates and amino acids in periwinkle and tobacco. *Physiological and Molecular Plant Pathology*, *55*(1), 59-68.

Lherminier, J., Benhamou, N., Larrue, J., Milat, M. L., Boudon-Padieu, E., Nicole, M., & Blein, J. P. (2003). Cytological characterization of elicitin-induced protection in tobacco plants infected by Phytophthora parasitica or phytoplasma. *Phytopathology*, *93*(10), 1308-1319.

Lin, M. K., Lee, Y. J., Lough, T. J., Phinney, B. S., & Lucas, W. J. (2009). Analysis of the pumpkin phloem proteome provides insights into angiosperm sieve tube function. *Molecular & Cellular Proteomics*, *8*(2), 343-356.

Liu, D. D., Chao, W. M., & Turgeon, R. (2012). Transport of sucrose, not hexose, in the phloem. *Journal of experimental botany*, *63*(11), 4315-4320.

Loebenstein, G., Thottappilly, G., Fuentes, S., & Cohen, J. (2009). Virus and phytoplasma diseases. In *The sweetpotato* (pp. 105-134). Springer Netherlands.

Lough, T. J., & Lucas, W. J. (2006). Integrative plant biology: role of phloem long-distance macromolecular trafficking. *Annu. Rev. Plant Biol.*, *57*, 203-232.

Lu, Y. T., Li, M. Y., Cheng, K. T., Tan, C. M., Su, L. W., Lin, W. Y., ... & Yang, J. Y. (2014). Transgenic plants that express the phytoplasma effector SAP11 show altered phosphate starvation and defense responses. *Plant physiology*, *164*(3), 1456-1469.

Lucas, W. J., Groover, A., Lichtenberger, R., Furuta, K., Yadav, S. R., Helariutta, Y., ... & Patrick, J. W. (2013). The plant vascular system: evolution, development and FunctionsF. *Journal of Integrative Plant Biology*, *55*(4), 294-388.

Luge, T., Kube, M., Freiwald, A., Meierhofer, D., Seemüller, E., & Sauer, S. (2014). Transcriptomics assisted proteomic analysis of Nicotiana occidentalis infected by Candidatus Phytoplasma mali strain AT. *Proteomics*, *14*(16), 1882-1889.

MacLean, A. M., Orlovskis, Z., Kowitwanich, K., Zdziarska, A. M., Angenent, G. C., Immink, R. G., & Hogenhout, S. A. (2014). Phytoplasma effector SAP54 hijacks plant reproduction by degrading MADS-box proteins and promotes insect colonization in a RAD23-dependent manner. *PLoS Biol*, *12*(4), e1001835.

MacLean, A. M., Sugio, A., Makarova, O. V., Findlay, K. C., Grieve, V. M., Tóth, R., ... & Hogenhout, S. A. (2011). Phytoplasma effector SAP54 induces indeterminate leaf-like flower development in Arabidopsis plants. *Plant Physiology*, *157*(2), 831-841.

Marcone, C., Lee, I. M., Davis, R. E., Ragozzino, A., & Seemüller, E. (2000). Classification of aster yellows-group phytoplasmas based on combined analyses of rRNA and tuf gene sequences. *International Journal of Systematic and Evolutionary Microbiology*, *50*(5), 1703-1713.

Marcone, C., Neimark, H., Ragozzino, A., Lauer, U., & Seemüller, E. (1999). Chromosome sizes of phytoplasmas composing major phylogenetic groups and subgroups. *Phytopathology*, *89*(9), 805-810.

Marcone, C., Weintraub, P. G., & Jones, P. (2009). Movement of Phytoplasmas and the Development of Disease in the Plant. *Genomes, Plant Hosts and Vectors*, 114.

Margaria, P., Ferrandino, A., Caciagli, P., Kedrina, O., Schubert, A., & Palmano, S. (2014). Metabolic and transcript analysis of the flavonoid pathway in diseased and recovered Nebbiolo and Barbera grapevines (Vitis vinifera L.) following infection by Flavescence dorée phytoplasma. *Plant, cell & environment*, *37*(9), 2183-2200.

Margaria, P., & Palmano, S. (2011). Response of the Vitis vinifera L. cv.'Nebbiolo'proteome to Flavescence dorée phytoplasma infection. *Proteomics*, *11*(2), 212-224.

Martini, M., Musetti, R., Grisan, S., Polizzotto, R., Borselli, S., Pavan, F., & Osler, R. (2009). DNA-dependent detection of the grapevine fungal endophytes Aureobasidium pullulans and Epicoccum nigrum. *Plant Disease*, *93*(10), 993-998.

Matteoni, J. A., & Sinclair, W. A. (1983). Stomatal closure in plants infected with mycoplasmalike organisms. *Phytopathology*, *73*(3), 398-402.

Maust, B. E., Espadas, F., Talavera, C., Aguilar, M., Santamaría, J. M., & Oropeza, C. (2003). Changes in carbohydrate metabolism in coconut palms infected with the lethal yellowing phytoplasma. *Phytopathology*, *93*(8), 976-981.

McAinsh, M. R., & Pittman, J. K. (2009). Shaping the calcium signature. *New Phytologist*, *181*(2), 275-294.

Meinke, D. W., Cherry, J. M., Dean, C., Rounsley, S. D., & Koornneef, M. (1998). Arabidopsis thaliana: a model plant for genome analysis. *Science*, *282*(5389), 662-682.

Messiaen, J., Read, N. D. V., Cutsem, P. V., & Trewavas, A. J. (1993). Cell wall oligogalacturonides increase cytosolic free calcium in carrot protoplasts. *Journal of Cell Science*, *104*(2), 365-371.

Minato, N., Himeno, M., Hoshi, A., Maejima, K., Komatsu, K., Takebayashi, Y., ... & Kamiya, Y. (2014). The phytoplasmal virulence factor TENGU causes plant sterility by downregulating of the jasmonic acid and auxin pathways. *Scientific reports*, *4*, 1399.

Moghaddam, M. R. B., & van den Ende, W. (2012). Sugars and plant innate immunity. *Journal of experimental botany*, *63*, 3989–3998

Morton, A., Davies, D. L., Blomquist, C. L., & Barbara, D. J. (2003). Characterization of homologues of the apple proliferation immunodominant membrane protein gene from three related phytoplasmas. *Molecular Plant Pathology*, *4*(2), 109-114.

Murray, R. G. E., & Stackebrandt, E. (1995). Taxonomic note: implementation of the provisional status Candidatus for incompletely described procaryotes. *International Journal of Systematic and Evolutionary Microbiology*, *45*(1), 186-187.

Musetti, R. & Favali, M.A. (2003) Calcium localization and X-ray microanalysis in *Catharanthus roseus* L. infected with phytoplasmas. *Micron* 34, 387–393.

Musetti, R. (2010). Biochemical changes in plants infected by phytoplasmas. *Phytoplasmas: genomes, plant hosts and vectors*, 132-146.

Musetti, R., Buxa, S. V., De Marco, F., Loschi, A., Polizzotto, R., Kogel, K. H., & van Bel, A. J. (2013). Phytoplasma-triggered Ca2+ influx is involved in sieve-tube blockage. *Molecular Plant-Microbe Interactions*, *26*(4), 379-386.

Musetti, R., di Toppi, L. S., Ermacora, P., & Favali, M. A. (2004). Recovery in apple trees infected with the apple proliferation phytoplasma: an ultrastructural and biochemical study. *Phytopathology*, *94*(2), 203-208.

Musetti, R., Di Toppi, L. S., Martini, M., Ferrini, F., Loschi, A., Favali, M. A., & Osler, R. (2005). Hydrogen peroxide localization and antioxidant status in the recovery of apricot plants from European Stone Fruit Yellows. *European Journal of Plant Pathology*, *112*(1), 53-61.

Musetti, R., Favali, M. A., & Pressacco, L. (2000). Histopathology and polyphenol content in plants infected by phytoplasmas. *CYTOBIOS-CAMBRIDGE-*, 133-148.

Musetti, R., Marabottini, R., Badiani, M., Martini, M., di Toppi, L. S., Borselli, S., ... & Osler, R. (2007). On the role of H2O2 in the recovery of grapevine (Vitis vinifera cv. Prosecco) from Flavescence dorée disease. *Functional Plant Biology*, *34*(8), 750-758.

Musetti, R., Pagliari, L., Buxa, S. V., Degola, F., De Marco, F., Loschi, A., ... & van Bel, A. J. (2016). OHMS**: Phytoplasmas dictate changes in sieve-element ultrastructure to accommodate their requirements for nutrition, multiplication and translocation. *Plant signaling & behavior*, *11*(2), e1138191.

Musetti, R., Paolacci, A., Ciaffi, M., Tanzarella, O. A., Polizzotto, R., Tubaro, F., ... & Osler, R. (2010). Phloem cytochemical modification and gene expression following the recovery of apple plants from apple proliferation disease. *Phytopathology*, *100*(4), 390-399.

Nelson, R. S., & van Bel, A. J. (1998). The mystery of virus trafficking into, through and out of vascular tissue. In *Progress in Botany* (pp. 476-533). Springer Berlin Heidelberg.

Opalski, K. S., Schultheiss, H., Kogel, K. H., & Hückelhoven, R. (2005). The receptor-like MLO protein and the RAC/ROP family G-protein RACB modulate actin reorganization in barley attacked by the biotrophic powdery mildew fungus Blumeria graminis f. sp. hordei. *The Plant Journal*, *41*(2), 291-303.

Oparka, K. J., & Cruz, S. S. (2000). The great escape: phloem transport and unloading of macromolecules 1. *Annual review of plant biology*, *51*(1), 323-347.

Oshima, K., Ishii, Y., Kakizawa, S., Sugawara, K., Neriya, Y., Himeno, M., ... & Namba, S. (2011). Dramatic transcriptional changes in an intracellular parasite enable host switching between plant and insect. *PLoS One*, *6*(8), e23242.

Oshima, K., Shiomi, T., Kuboyama, T., Sawayanagi, T., Nishigawa, H., Kakizawa, S., ... & Namba, S. (2001). Isolation and characterization of derivative lines of the onion yellows phytoplasma that do not cause stunting or phloem hyperplasia. *Phytopathology*, *91*(11), 1024-1029.

Osler, R., Borselli, S., Ermacora, P., Ferrini, F., Loschi, A., Martini, M., ... & Loi, N. (2016). Transmissible tolerance to European stone fruit yellows (ESFY) in apricot: cross-protection or a plant mediated process?. *Phytoparasitica*, *44,* 203-211.

Osler, R., Borselli, S., Ermacora, P., Loschi, A., Martini, M., Musetti, R., & Loi, N. (2014). Acquired tolerance in apricot plants that stably recovered from European stone fruit yellows. *Plant Disease*, *98*(4), 492-496.

Osler, R., Carraro, L., Loi, N., Pavan, F., Firrao, G., Musetti, R., Ermacora, P., Loschi, A., Pertot, I. & Refatti, E. (1996). *Le più importanti malattie da fitoplasmi nel Friuli-Venezia Giulia: atlante*. Edito da Ente regionale per la promozione e lo sviluppo dell'agricoltura del Friuli-Venezia Giulia.

Pagliari, L., Martini, M., Loschi, A., & Musetti, R. (2016). Looking inside phytoplasma-infected sieve elements: A combined microscopy approach using Arabidopsis thaliana as a model plant. *Micron*, *89*, 87-97.

Palermo, S., Arzone, A., & Bosco, D. (2001). Vector-pathogen-host plant relationships of chrysanthemum yellows (CY) phytoplasma and the vector leafhoppers Macrosteles quadripunctulatus and Euscelidius variegatus. *Entomologia experimentalis et applicata*, *99*(3), 347-354.

Patrick, J. W., Zhang, W., Tyerman, S. D., Offler, C. E., & Walker, N. A. (2001). Role of membrane transport in phloem translocation of assimilates and water. *Functional Plant Biology*, *28*(7), 697-709.

Patui, S., Bertolini, A., Clincon, L., Ermacora, P., Braidot, E., Vianello, A., & Zancani, M. (2013). Involvement of plasma membrane peroxidases and oxylipin pathway in the recovery from phytoplasma disease in apple (Malus domestica). *Physiologia plantarum*, *148*(2), 200-213.

Pelissier, H. C., Peters, W. S., Collier, R., van Bel, A. J., & Knoblauch, M. (2008). GFP tagging of sieve element occlusion (SEO) proteins results in green fluorescent forisomes. *Plant and Cell Physiology*, *49*(11), 1699-1710.

Peters, W. S., van Bel, A. J., & Knoblauch, M. (2006). The geometry of the forisome–sieve element–sieve plate complex in the phloem of Vicia faba L. leaflets. *Journal of Experimental Botany*, *57*(12), 3091-3098.

Pieterse, C. M., Leon-Reyes, A., van der Ent, S., & van Wees, S. C. (2009). Networking by small-molecule hormones in plant immunity. *Nature chemical biology*, *5*(5), 308-316.

Pritchard, L., & Birch, P. R. (2014). The zigzag model of plant–microbe interactions: is it time to move on?. *Molecular plant pathology*, *15*(9), 865-870.

Punelli, F., Al Hassan, M., Fileccia, V., Uva, P., Pasquini, G., & Martinelli, F. (2016). A microarray analysis highlights the role of tetrapyrrole pathways in grapevine responses to "stolbur" phytoplasma, phloem virus infections and recovered status. *Physiological and Molecular Plant Pathology*, *93*, 129-137.

Read, S. M., & Northcote, D. H. (1983). Subunit structure and interactions of the phloem proteins of Cucurbita maxima (pumpkin). *European Journal of Biochemistry*, *134*(3), 561-569.

Robert-Seilaniantz, A., Grant, M., & Jones, J. D. (2011). Hormone crosstalk in plant disease and defense: more than just jasmonate-salicylate antagonism. *Annual review of phytopathology*, *49*, 317-343.

Rüping, B., Ernst, A. M., Jekat, S. B., Nordzieke, S., Reineke, A. R., Müller, B., ... & Noll, G. A. (2010). Molecular and phylogenetic characterization of the sieve element occlusion gene family in Fabaceae and non-Fabaceae plants. *BMC plant biology*, *10*(1), 219.

Sabnis, D. D., & Hart, J. W. (1978). The isolation and some properties of a lectin (haemagglutinin) from Cucurbita phloem exudate. *Planta*, *142*(1), 97-101.

Saigo, M., Golic, A., Alvarez, C. E., Andreo, C. S., Hogenhout, S. A., Mussi, M. A., & Drincovich, M. F. (2014). Metabolic regulation of phytoplasma malic enzyme and phosphotransacetylase supports the use of malate as an energy source in these plant pathogens. *Microbiology*, *160*(12), 2794-2806.

Sánchez-Rojo, S., López-Delgado, H. A., Mora-Herrera, M. E., Almeyda-León, H. I., Zavaleta-Mancera, H. A., & Espinosa-Victoria, D. (2011). Salicylic acid protects potato plants-from phytoplasma-associated stress and improves tuber photosynthate assimilation. *American journal of potato research*, *88*(2), 175-183.

Santi, S., Grisan, S., Pierasco, A., De Marco, F., & Musetti, R. (2013). Laser microdissection of grapevine leaf phloem infected by stolbur reveals site-specific gene responses associated to sucrose transport and metabolism. *Plant, cell & environment*, *36*(2), 343-355.

Scharte, J., Schön, H., & Weis, E. (2005). Photosynthesis and carbohydrate metabolism in tobacco leaves during an incompatible interaction with Phytophthora nicotianae. *Plant, Cell & Environment*, *28*(11), 1421-1435.

Scheler, C., Durner, J., & Astier, J. (2013). Nitric oxide and reactive oxygen species in plant biotic interactions. *Current opinion in plant biology*, *16*(4), 534-539.

Schwessinger, B., & Zipfel, C. (2008). News from the frontline: recent insights into PAMP-triggered immunity in plants. *Current opinion in plant biology*, *11*(4), 389-395.

Seemüller, E., Garnier, M., & Schneider, B. (2002). Mycoplasmas of plants and insects. In *Molecular Biology and Pathogenicity of Mycoplasmas* (pp. 91-115). Springer US.

Sels, J., Mathys, J., De Coninck, B. M., Cammue, B. P., & De Bolle, M. F. (2008). Plant pathogenesis-related (PR) proteins: a focus on PR peptides. *Plant Physiology and Biochemistry*, *46*(11), 941-950.

Siewert, C., Luge, T., Duduk, B., Seemüller, E., Büttner, C., Sauer, S., & Kube, M. (2014). Analysis of expressed genes of the bacterium 'Candidatus Phytoplasma mali'highlights key features of virulence and metabolism. *PloS one*, *9*(4), e94391.

Sinclair, W. A., Braun, E. J., & Larsen, A. O. (1976). Update on phloem necrosis of Elms. *Journal of Arboriculture*, *2*(6), 106-113.

Sjolund, R. D. (1997). The phloem sieve element: a river runs through it. *The Plant Cell*, *9*(7), 1137.

Srivastava, V. K., Tuteja, R., & Tuteja, N. (2015). Calcium-energized motor protein forisome controls damage in phloem: potential applications as biomimetic "smart" material. *Critical reviews in biotechnology*, *35*(2), 173-183.

Steer, M. W., & Newcomb, E. H. (1969). Development and dispersal of P-protein in the phloem of Coleus blumei Benth. *Journal of cell science*, *4*(1), 155-169.

Stintzi, A., & Browse, J. (2000). The Arabidopsis male-sterile mutant, opr3, lacks the 12-oxophytodienoic acid reductase required for jasmonate synthesis. *Proceedings of the National Academy of Sciences*, *97*(19), 10625-10630.

Sugio, A., MacLean, A. M., Grieve, V. M., & Hogenhout, S. A. (2011). Phytoplasma protein effector SAP11 enhances insect vector reproduction by manipulating plant development and defense hormone biosynthesis. *Proceedings of the National Academy of Sciences*, *108*(48), E1254-E1263.

Swanson, M. S., & Isberg, R. R. (1995). Association of Legionella pneumophila with the macrophage endoplasmic reticulum. *Infection and immunity*, *63*(9), 3609-3620.

Taheri, F., Nematzadeh, G., Zamharir, M. G., Nekouei, M. K., Naghavi, M., Mardi, M., & Salekdeh, G. H. (2011). Proteomic analysis of the Mexican lime tree response to "Candidatus Phytoplasma aurantifolia" infection. *Molecular BioSystems*, *7*(11), 3028-3035.

Taiz, L., & Zeiger, E. (1998). Translocation in the phloem. *Plant Physiology. Sinauer Associates, Sunderland, MA*, 251-285.

Thakur, M., & Sohal, B. S. (2013). Role of elicitors in inducing resistance in plants against pathogen infection: a review. *ISRN biochemistry*, *2013*.

Thomma, B. P., Nürnberger, T., & Joosten, M. H. (2011). Of PAMPs and effectors: the blurred PTI-ETI dichotomy. *The plant cell*, *23*(1), 4-15.

Turgeon, R., & Oparka, K. (2010). The secret phloem of pumpkins. *Proceedings of the National Academy of Sciences*, *107*(30), 13201-13202.

Valiunas, V., Wang, H. Z., Li, L., Gordon, C., Valiuniene, L., Cohen, I. S., & Brink, P. R. (2015). A comparison of two cellular delivery mechanisms for small interfering RNA. *Physiological reports*, *3*(2), e12286.

van Bel, A. J. (2003). The phloem, a miracle of ingenuity. *Plant, Cell & Environment*, *26*(1), 125-149.

van Bel, A. J., & Hess, P. (2003). Kollektiver Kraftakt zweier Exzentriker: Phloemtransport. *Biologie in unserer Zeit*, *33*(4), 220-230.

Van Bel, A. J., Helariutta, Y., Thompson, G. A., Ton, J., Dinant, S., Ding, B., & Patrick, J. W. (2013). Phloem: the integrative avenue for resource distribution, signaling, and defense. *Frontiers in plant science*, *4*, 471.

van Bel, A. J., Ehlers, K., & Knoblauch, M. (2002). Sieve elements caught in the act. *Trends in plant science*, *7*(3), 126-132.

van Bel, A. J., Furch, A. C., Will, T., Buxa, S. V., Musetti, R., & Hafke, J. B. (2014). Spread the news: systemic dissemination and local impact of Ca2+ signals along the phloem pathway. *Journal of experimental botany*, *65*, 1761-1787.

van Loon, L. C., & van Strien, E. A. (1999). The families of pathogenesis-related proteins, their activities, and comparative analysis of PR-1 type proteins. *Physiological and molecular plant pathology*, *55*(2), 85-97.

Vitali, M., Chitarra, W., Galetto, L., Bosco, D., Marzachì, C., Gullino, M. L., ... & Lovisolo, C. (2013). Flavescence dorée phytoplasma deregulates stomatal control of photosynthesis in Vitis vinifera. *Annals of applied biology*, *162*(3), 335-346.

Wani, S. H., Kumar, V., Shriram, V., & Sah, S. K. (2016). Phytohormones and their metabolic engineering for abiotic stress tolerance in crop plants. *The Crop Journal*, *4*(3), 162-176.

Wei, W., Cai, H., Jiang, Y., Lee, I. M., Davis, R. E., Ding, Y., ... & Zhao, Y. (2011). A new phytoplasma associated with little leaf disease in azalea: multilocus sequence characterization reveals a distinct lineage within the aster yellows phytoplasma group. *Annals of Applied Biology*, *158*(3), 318-330.

Wei, W., Kakizawa, S., Suzuki, S., Jung, H. Y., Nishigawa, H., Miyata, S. I., ... & Namba, S. (2004). In planta dynamic analysis of onion yellows phytoplasma using localized inoculation by insect transmission. *Phytopathology*, *94*(3), 244-250.

Weintraub, P. G., & Beanland, L. (2006). Insect vectors of phytoplasmas. *Annu. Rev. Entomol.*, *51*, 91-111.

Weisburg, W. G., Tully, J. G., Rose, D. L., Petzel, J. P., Oyaizu, H., Yang, D., ... & Van Etten, J. (1989). A phylogenetic analysis of the mycoplasmas: basis for their classification. *Journal of bacteriology*, *171*(12), 6455-6467.

Wergin, W. P., & Newcomb, E. H. (1970). Formation and dispersal of crystalline P-protein in sieve elements of soybean (Glycine max L.). *Protoplasma*, *71*(4), 365-388.

Xie, B., Wang, X., Zhu, M., Zhang, Z., & Hong, Z. (2011). CalS7 encodes a callose synthase responsible for callose deposition in the phloem. *The Plant Journal*, *65*(1), 1-14.

Yoo, S. C., Chen, C., Rojas, M., Daimon, Y., Ham, B. K., Araki, T., & Lucas, W. J. (2013). Phloem long-distance delivery of FLOWERING LOCUS T (FT) to the apex. *The Plant Journal*, *75*(3), 456-468.

Zafari, S., Niknam, V., Musetti, R., & Noorbakhsh, S. N. (2012). Effect of phytoplasma infection on metabolite content and antioxidant enzyme activity in lime (Citrus aurantifolia). *Acta physiologiae plantarum*, *34*(2), 561-568.

Zhang, B., Tolstikov, V., Turnbull, C., Hicks, L. M., & Fiehn, O. (2010). Divergent metabolome and proteome suggest functional independence of dual phloem transport systems in cucurbits. *Proceedings of the National Academy of Sciences*, *107*(30), 13532-13537.

Zhang, C., Shi, H., Chen, L., Wang, X., Lü, B., Zhang, S., ... & You, Z. (2011). Harpin-induced expression and transgenic overexpression of the phloem protein gene AtPP2-A1 in Arabidopsis repress phloem feeding of the green peach aphid Myzus persicae. *BMC plant biology*, *11*(1), 1.

Zhao, Y., & Davis, R. E. (2016). Criteria for phytoplasma 16Sr group/subgroup delineation and the need of a platform for proper registration of new groups and subgroups. *International journal of systematic and evolutionary microbiology*, *66*(5), 2121-2123.

Zhong, B. X., & Shen, Y. W. (2004). Accumulation of Pathogenesis-related Type-5 Like Proteins in Phytoplasmainfected Garland Chrysanthemum Chrysanthemum coronarium. *Acta biochimica et biophysica Sinica*, *36*(11), 773-779.

Zimmermann, M. R., Schneider, B., Mithöfer, A., Reichelt, M., Seemüller, E., & Furch, A. C. (2015). Implications of Candidatus Phytoplasma mali infection on phloem function of apple trees. *Endocytobiosis and cell research: journal of the International Society of Endocytobiology*, *26*, 67-75.

8. Publications.

8.1. Papers.

Paper 1.

Title: OHMS: phytoplasmas dictate changes in sieve-element ultrastructure to accommodate their requirements for nutrition, multiplication and translocation**

Authors: Musetti, R., Pagliari, L., Buxa, S. V., Degola, F., De Marco, F., Loschi, A., ... & van Bel, A. J.

Year of publication: 2016

Journal: Plant signaling & behavior, 11(2), e1138191

Abstract: Phytoplasmas are among the most recently discovered plant pathogenic microorganisms so, many traits of the interactions with host plants and insect vectors are still unclear and need to be investigated. At now, it is impossible to determine the precise sequences leading to the onset of the relationship with the plant host cell. It is still unclear how phytoplasmas, located in the phloem sieve elements, exploit host cell to draw nutrition for their metabolism, growth and multiplication.In this work, basing on microscopical observations, we give insight about the structural interactions established by phytoplasmas and the sieve element plasma membrane, cytoskeleton, sieve endoplasmic reticulum, speculating about a possible functional role.

Keywords: actin, plasma membrane, phytoplasma, phytoplasma adhesion, phytoplasma anchoring, sieve elements, sieve-element reticulum

Doi: 10.1080/15592324.2016.1138191

Paper 2.

Title: Epifluorescence microscopy imaging of phytoplasmas in embedded leaf tissues using DAPI and SYTO13 fluorochromes

Authors: Buxa S. V., Pagliari, L., & Musetti, R.

Year of publication: 2016

Journal: MICROSCOPIE

Abstract: The use of DNA-specific dyes, i. e. DAPI, is extensively reported for phytoplasma detection in fresh plant materials. However, fluorescence-based microscopy and imaging of fresh tissues often evidences technical limitations which are more significant in infected tissues, because phenolic and other defense-related compounds accumulate in the cell wall and in the vacuole making difficult sample preparation. In this paper, we describe a method based on the use of epifluorescence microscopy and the DNA probes DAPI and SYTO13® for phytoplasma visualization in resin-embedded plant tissues. The method allows detection of phytoplasmas and it is recommended for tissues that are recalcitrant to conventional imaging.

Keywords: DAPI, epifluorescence microscopy, phytoplasmas, stolbur, SYTO13®, tomato

Doi: 10.4081/microscopie.2016.5271

Paper 3.

Title: Looking inside phytoplasma-infected sieve elements: A combined microscopy approach using *Arabidopsis thaliana* as a model plant

Authors: Pagliari, L., Martini, M., Loschi, A., & Musetti, R.

Year of publication: 2016

Journal: Micron

Abstract: Phytoplasmas are phloem-inhabiting plant pathogens that affect over one thousand plant species, representing a severe threat to agriculture. The absence of an effective curative strategy and the economic importance of many affected crops make a priority of studying how plants respond to phytoplasma infection. Nevertheless, the study of phytoplasmas has been hindered by the extreme difficulty of culturing them in vitro and by impediments to natural host plant surveys such as low phytoplasma titre, long plant life cycle and poor knowledge of natural host-plant biology. Stating correspondence between macroscopic symptoms of phytoplasma infected *Arabidopsis thaliana* and those observed in natural host plants, over the last decade some authors have started to use this plant as a model for studying phytoplasma-plant interactions. Nevertheless, the morphological and ultrastructural modifications occurring in *A. thaliana* tissues following phytoplasma infection have never been described in detail. In this work, we adopted a combined-microscopy approach to verify if *A. thaliana* can be considered a reliable model for the study of phytoplasma-plant interactions at the microscopical level.

The consistent presence of phytoplasma in infected phloem allowed detailed study of the infection process and the relationship established by phytoplasmas with different components of the sieve elements. In infected A. thaliana, phytoplasmas induced strong disturbances of host plant development that were mainly due to phloem disorganization and impairment. Light microscopy showed collapse, necrosis and hyperplasia of phloem cells. TEM observations of sieve elements identified two common plant-responses to phytoplasma infection: phloem protein agglutination and callose deposition.

Keywords: Phytoplasma; Arabidopsis thaliana; Phloem; Combined microscopy

Doi: 10.1016/j.micron.2016.07.007

Paper 4.

Title: Combined microscopy and molecular analyses show phloem occlusions and cell wall modifications in tomato leaves in response to 'Candidatus Phytoplasma solani'

Authors: De Marco, F., Pagliari, L., Degola, F., Buxa, S. V., Loschi, A., Dinant, S., ... & Musetti, R.

Year of publication: 2016

Journal: Journal of microscopy

Abstract: Callose deposition, phloem-protein conformational changes and cell wall thickening are calcium-mediated occlusions occurring in the plant sieve elements in response to different biotic and abiotic stresses. However, the significance of these structures in plant–phytoplasma interactions requires in-depth investigations. We adopted a novel integrated approach, based on the combined use of microscopic and molecular analyses, to investigate the structural modifications induced in tomato leaf tissues in presence of phytoplasmas, focusing on vascular bundles and on the occlusion structures. Phloem hyperplasia and string-like arrangement of xylem vessels were found in infected vascular tissue. The diverse occlusion structures were differentially modulated in the phloem in response to phytoplasma infection. Callose amount was higher in midribs from infected plants than in healthy ones. Callose was observed at sieve plates but not at pore-plasmodesma units. A putative callose synthase gene encoding a protein with high similarity to Arabidopsis CalS7, responsible for callose deposition at sieve plates, was upregulated in symptomatic leaves, indicating a modulation in the response to stolbur infection. P-proteins showed configuration changes in infected sieve elements, exhibiting condensation of the filaments. The transcripts for a putative P-protein 2 and a sieve element

occlusion-related protein were localized in the phloem but only the first one was modulated in the infected tissues.

Keywords: Callose, phloem, phytoplasma, P-proteins, tomato.

Doi: 10.1111/jmi.12426

8.2. Abstracts.

Abstract 1

Title: A combined microscopy approach to study plant-phytoplasma interaction using *Arabidopsis thaliana*

Authors: Pagliari, L., & Musetti, R.

Year of publication: 2016

Congress: The 16th European Microscopy Congress 2016

Abstract: Phytoplasmas, obligate parasites of plants and phloem-feeding insects, belong to Mollicutes (Lee *et al.*, 2004) and are associated with several hundreds of diseases affecting over one thousand plant species, including many economically important crops (Marcone, 2014). There is no effective curative strategy available so far, so the sole ways to limit the infection outbreaks are the use of insecticides and the removal of symptomatic plants (Bertaccini *et al.*, 2014). Even if not all infections are necessarily deleterious, symptoms in infected plants suggest heavy disorders of phloem functions and growth-regulator balancing (Lee *et al.*, 2000). Upon their discovery (Doi *et al.*, 1967), the study of phytoplasmas has been hindered by the extreme difficulty to culture them in vitro, due to their lack of fundamental metabolic pathways (Bai *et al.*, 2006). Moreover, the study in natural plant hosts is often limited by environmental conditions, long plant life cycle and poor knowledge of host-plant biology. Therefore, in the last decade some authors suggested to use Arabidopsis thaliana as model plant for studying phytoplasma-plant interactions. This choice was supported by the correspondence between the macroscopic symptoms developed in infected *A. thaliana* and those observed in natural host plants (Bressan and Purcell, 2005; Hoshi *et al.*, 2009; Cettul and Firrao, 2011; MacLean *et al.*, 2011). Nevertheless, morphological and ultrastructural modifications occurring in infected *A. thaliana* tissues have never been described in detail. In this work, we adopted a combined microscopy approach to verify if this plant is a reliable model for the study of phytoplasma-plant interactions at microscopical level. Using DAPI and fluorescence microscopy (FM),

phytoplasma presence and localization were demonstrated in every infected plant. Transmission electron microscopy (TEM) observations confirmed phytoplasma massive presence into the sieve elements (SEs) (Figure 1). Phytoplasma appeared well preserved, with typical pleomorphic shape, free-floating and dividing in the lumen or adhered to SE membrane, probably connecting to the host (Marcone *et al.*, 2014; Buxa *et al.*, 2015). Phytoplasmas also established relationships with sieve element reticulum (SER). Pathogen presence, probably linked to nutrient uptake (Celli *et al.*, 2015; Musetti *et al.*, 2016), caused SER hyperproliferation, as observed in many other plant-phytoplasma interaction (Rudzinska-Langwald and Kaminska, 2001; Buxa *et al.*, 2015) (Figure 1). Pathogen spread was documented by the passage through sieve pores. As remarked above, phytoplasma presence affected host plant development (Lee *et al.*, 2000). In infected *A. thaliana* plants, light microscopy (LM) evidenced a profound disturbance in phloem morphology at histological level, mainly consisting in collapse, necrosis and hyperplasia of the phloem components. The relationship between necrosis and hyperplasia could be explained as a plant response to the impaired phloem functionality (Oshima *et al.*, 2001) or due to pathogen effectors (Bai *et al.*, 2009; Sugio *et al.*, 2011). At ultrastructural level, as previously observed in other phytoplasma hosts (Musetti *et al.*, 2000; 2013; Kaminska *et al.*, 2001; Santi *et al.*, 2013), phloem components showed plasmolysis or were collapsed or necrotized. Even in vital SEs, abnormalities of cell membrane profile and cell wall thickness were visible. TEM observations showed two typical plant responses to phytoplasma infection: phloem-protein agglutination and callose deposition at the sieve plates, which limited sieve-pore diameter (Figure 1). These phenomena have been interpreted as a plant reaction to physically limit pathogen spread (Lherminier *et al.*, 2003; Gamalero *et al.*, 2010; Luna *et al.*, 2011; Musetti *et al.*, 2010; 2013). Phloem functionality experiments using CFDA and confocal laser scanner microscopy (CLSM) suggested that sieve-pore obstruction leads to phloem impairment (Figure 2 A, C). This phenomenon is also associated to the accumulation of photo-assimilates, visible as chloroplast starch deposits under LM and TEM (Figure 2 B, D), as previously reported in other host plants (Maust *et al.*, 2003; Junqueira *et al.*, 2004; Musetti *et al.*, 2013). This study proved that phloem tissue of infected *A. thaliana* presented the main morphological and ultrastructural response to phytoplasma infection as reported in natural hosts. Moreover, analyses carried on *A. thaliana* were not affected by troubles linked to low phytoplasma titre and uneven distribution, typical of woody plants. Therefore, we can state that *A. thaliana* revealed a reliable model plant for phytoplasma-plant interactions, concerning both macroscopic symptoms and morphological and ultrastructural changes.

Keywords: combined microscopy, plant-pathogen interaction

Doi: 10.1002/9783527808465.EMC2016.6047

Abstract 2.

Title: SEO1 AND SEO2 GENES ARE INVOLVED IN THE RESPONSE OF ARABIDOPSIS TO PHYTOPLASMA INFECTION

Authors: Pagliari, L., Buxa, S.V., Martini, M., Musetti, R.

Year of publication: 2015

Congress: XXI SIPAV National Congress 2015

Journal: Journal of Plant Pathology

Abstract: Phytoplasmas are plant-pathogenic prokaryotes restricted to the sieve elements and transmitted from plant to plant by phloem feeding insects. Curative strategies are not available so far, therefore plant natural defence mechanisms, mainly those occurring in the sieve elements, should be studied more in depth. One of the first responses of the sieve elements undergoing pathogen attack (or abiotic stimuli) is the aggregation of the Phloem protein (P-protein) filaments. P-proteins are able to plug affected sieve elements likely to avoid pathogen diffusion, moreover they seem to have a role also in the systemic defence signalling. Nevertheless, the role of the P-proteins during plant-pathogen interactions is still matter of debate. Among the genes encoding for P-proteins, AtSEOR1 and AtSEOR2 are reported to be essentials for filament formation in Arabidopsis thaliana. To evaluate the effective role of P-proteins in the limitation of phytoplasma spread through the sieve elements, wild type and mutant (knockout for AtSEOR1 or AtSEOR2 or both) *A. thaliana* plants have been used and infected with '*Candidatus* Phytoplama asteris'. Lacking AtSEOR1 and AtSEOR2 in healthy plants caused the absence of P-protein filaments: this did not affect plant phenotype, tissue morphology nor sieve-element ultrastructure. Both wild type and knockout infected plants developed disease symptoms, but in knockout plants they were more severe. Surprisingly, infected knockout plants evidenced filaments in the sieve elements, morphologically identical to the ones observed in wild type plants. On the other hand, filaments should not be as effective as the ones in wild type plants. Experiments carried out using CFDA and confocal microscope demonstrated that sieve-element mass flow was significantly reduced only in infected wild type plants.